SEVENTH FRAMEWORK PROGRAMME

THEME [ENERGY.2012.7.1.1] Integration of Variable Distributed Resources in Distribution Networks

(Deliverable 3.4)

Description of Pre-prototype of the Multi-Temporal Operational Management Tool for the MV /LV Distribution Grid

Lead Beneficiary:

INESC Porto

AUTHORS:

Authors	Organization	Email
José Meirinhos	INESC	jose.l.meirinhos@inescporto.pt
Clara Gouveia	INESC	clara.s.gouveia@inescporto.pt
Hélder Costa	INESC	helder.m.costa@inescporto.pt
André Madureira	INESC	andre.g.madureira@inescporto.pt
Panagiotis Anagnostopoulos	ICCS	pan-agniou85@hotmail.com
Stavros Papathanassiou	ICCS	st@power.ece.ntua.gr
Nikos Hatziargyriou	ICCS	nh@power.ece.ntua.gr
Luís González Sotres	COMILLAS	Luis.Gonzalez@iit.upcomillas.es
Javier Matanza	COMILLAS	jmatanza@upcomillas.es
Nuno Silva	EFACEC	nuno.silva@efacec.com
Paulo Rodrigues	EFACEC	pdr@efacec.com
Paulo Viegas	EFACEC	paulo.seixas.viegas@efacec.com

Access:

Project Consortium	
European Commission	**X**
Public	

Status:

Draft version	
Submission for Approval	**X**
Final Version	

Executive Summary

This document corresponds to the work developed within WP3 “Design of New Tools for Smart Distribution System Operation”, where a set of advanced functionalities are developed to enable maximizing the integration of Renewable Energy Sources (RES) in distribution networks, as included in the Description of Work (DoW) [1]. In particular, the development of Task T3.4 “Advanced Coordinated Voltage Control” is addressed where the main objective is to maximize the integration of renewable energy in distribution networks using advanced operation strategies implemented at the level of the HV/MV primary substation to control voltage magnitudes and real power injections working at the Low Voltage (LV) level and the Medium Voltage (MV) levels.

In fact, large-scale integration of Distributed Energy Resources (DER), and especially variable RES, brings significant challenges to grid operation that require new approaches and tools for distribution system management with voltage control being one of the most demanding tasks. Within the SuSTAINABLE concept, advanced voltage control involves a coordinated management of the several DER connected at the MV and LV levels in order to ensure a smooth and efficient operation of the distribution system as a whole. The proposed approach is developed in accordance to the technical reference architecture defined in Task 2.2 of WP2, where the main focus is put at the MV network level. Furthermore, the database specification and data communication requirements for both the MV and LV control are identified in appendix to this document.

Therefore, two innovative approaches for voltage control at the MV level are proposed. These approaches are based on a preventive day-ahead analysis using data from forecasting tools for load and RES to establish a plan for operation for the different DER for the next day and a corrective intraday analysis aimed at minimizing the deviations from the day-ahead plan. INESC developed an approach for advanced voltage control using a multi-temporal Optimal Power Flow (OPF) solved by a meta-heuristic in order to tackle large dimension systems. The performance of the algorithm is tested in a real, large dimension test network with good results. This algorithm will also be tested through simulation for a part of the Évora network using real forecasting data in WP6. ICCS has also developed an algorithm for advanced voltage control in MV networks using multi-objective optimization. A small scale demo network is used to show indicative results obtained from the application of the algorithm aimed at highlighting the variety of problems that can be addressed, as well as the potential solutions and the effectiveness of the algorithm. The resulting algorithm is going to be implemented on the real study-case network of Rhodes in Sub-task 5.2.2 within WP5.

At the LV level, two distinct yet complementary approaches are proposed and developed by INESC. First, a local control scheme based on active power / voltage droop functions installed at the inverter levels of DER is presented. This action is able to quickly mitigate eventual voltage problems that may arise in grid operation resulting from the variability of RES. Validation of the proposed methodology was achieved through some preliminary tests in a laboratory environment. Another level of control is proposed,

where a centralized scheme is able to ensure a more optimized operation of the LV grid. In this case, a set of rules embedded in the Distribution Transformer Controller (DTC) implements a merit order aimed at mobilizing the most adequate resources to correct a specific voltage problem while trying to maximize the integration of energy from RES. This approach has been tested for a real LV test network with large-scale integration of DER. Both these approaches will be tested in a laboratory environment of INESC in Sub-task 5.2.2 within WP5. The centralized control scheme will also be evaluated in real field tests to be conducted in the main site of Évora within WP6. Moreover, the impact of the communication infrastructure on the performance of the algorithm is evaluated, which allows assessing the minimum requirements for the performance of the chosen communication system.

Details on the implementation of the voltage control algorithms developed for MV and LV in the SSC and DTC, respectively, are also given, including the interfaces and communication protocols required.

This document is structured as follows. In Chapter 2, the proposed approach for the advanced coordinated voltage control in SuSTAINABLE is described. Chapter 3 describes the two methodologies developed for the multi-temporal OPF for MV network control. In Chapter 4, the voltage control scheme for LV networks is presented, including the centralized and local control schemes. Chapter 5 includes some details on the implementation of the voltage control modules. Finally, in Chapter 6, the main conclusions are drawn from all the studies that have been produced.

Table of Contents

List of Figures

List of Tables

List of Acronyms and Abbreviations

4Q	Four Quadrant
μG	Microgeneration
AMI	Advanced Metering Infrastructure
AVR	Automatic Voltage Regulator
BER	Bit Error Rate
CB	Capacitor Bank
CHP	Combined Heat and Power
COSEM	Companion Specification for Energy Metering
CSMA	Carrier Sense Multiple Access
DEEPSO	Differential Evolution – Evolutionary Particle Swarm Optimization
DER	Distributed Energy Resources
DFIG	Doubly-fed Induction Generator
DG	Distributed Generation
DLMS	Device Language Message Specification
DoW	Description of Work
DSM	Demand Side Management
DSO	Distribution System Operator
DTC	Distribution Transformer Controller
EB	Smart Meter
FE	Frontend
FEC	Forward Error Correction
GPRS	General Packet Radio Service
HV	High Voltage
KPI	Key Performance Indicator
LAN	Local Area Network
LLC	Logical Link Control
LV	Low Voltage
MAC	Media Access Control

MGCC	MicroGrid Central Controller
MV	Medium Voltage
MIQCQP	Mixed Integer Quadratically Constrained Quadratic problem
OLTC	On-Load Tap Changer
OPF	Optimal Power Flow
OWL	One-Way Latency
PLC	Power Line Communication
PV	Photovoltaic
RES	Renewable Energy Sources
RF	Radio-Frequency
RTU	Remote Terminal Unit
SC	Switchable Capacitor
SCADA/DMS	Supervisory Control and Data Acquisition / Distribution Management System
SNR	Signal to Noise Ratio
SOC	State of Charge
SSC	Smart Substation Controller
SVR	Step Voltage Regulator
TAN	Transformer Area Netowrk
WAN	Wide Area Network
WP	Work Package
WT	Wind Turbine

1 Introduction

It is an obligation of the Distribution System Operator (DSO) to ensure that customers are supplied power at adequate levels of voltage, *i.e.* within certain pre-specified limits [2]. Evidently, this must be taken into account in the design and planning of the distribution system, which has obvious implications on the costs of the electrical circuits used. This means that it is of the DSO's best interest to make the maximum use of existing circuits while ensuring the required voltage levels.

The advent of Distributed Generation (DG) in particular changed considerably the way in which distribution systems were planned and operated since distribution grids used to be strictly passive networks, with no power injections at the lower voltage levels, and have now become fully active networks with multiple power injections and bidirectional flows. Furthermore, the variability of the power produced by DG based on Renewable Energy Sources (RES) such as solar PV or wind generation has also a significant impact on the network that must be effectively addressed in order not to compromise system security and quality of supply. One of the main effects of a large scale integration of non-controllable DG in weak distribution networks is the so-called voltage rise effect [3].

In a scenario without DG, there would be a voltage drop across the distribution transformer and the feeders downstream so that voltage at the customer side would be less than the voltage at primary side of the transformer. The presence of the DG introduces a reverse power flow to counteract this normal voltage drop, sometimes even raising voltage, and the voltage may actually be higher at the customer side than on the primary side of the distribution transformer, exceeding the maximum limit allowed.

Figure 1 shows the effect of DG in an LV given several scenarios of DG penetration. It can be observed that voltage may rise above admissible limits if there is high DG penetration, where DG is forced to export its power to the upstream MV network.

In this context, traditional voltage regulation methods often based on Automatic Voltage Regulators (AVRs) or On-Load Tap Changing (OLTC) transformers are inadequate. On one hand, this is due to the fact that voltage profiles in an active network can be much more irregular; on the other hand, there can be a significant lack of coordination between the voltage regulation devices, which may reduce the effectiveness of the control strategy.

Consequently, the voltage rise effect can be a major concern when connecting DG, particularly based on RES, to the distribution system. Due to operational issues, most DSOs require that DG operate at zero reactive power or at a fixed power factor, which limits the amount of DG installed capacity in order to guarantee admissible voltage profiles in the worst case scenario.

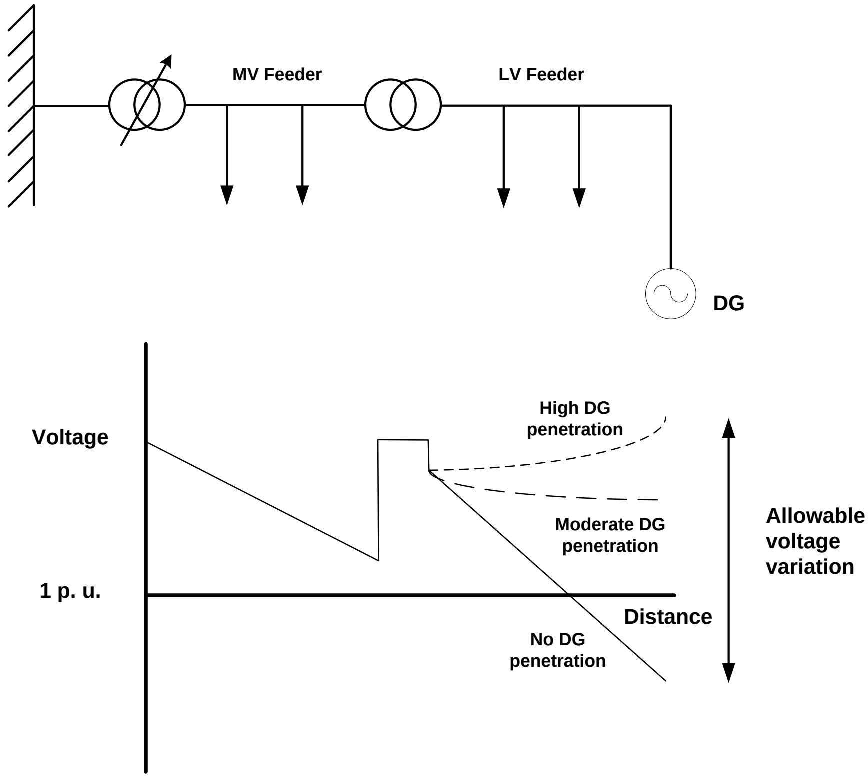

Figure 1 – Voltage Variation down a Radial Feeder for several DG Penetration Scenarios [4]

In order to increase the maximum allowable DG connection capacity, strategies able to control the voltage rise effect must be employed [5]. Basically, three main approaches can be found in the available technical literature: local distributed voltage control, centralized voltage control (active network management) and generation curtailment [6, 7].

Distributed control can be achieved by not enforcing unity power factor and allowing DG to manage its reactive power output (either injecting or absorbing). This voltage control mode may be employed when voltage limits are overstepped and can help reducing the voltage rise effect, thus allowing more DG to be connected to the network. For instance, power electronic interfaces are capable of controlling their active and reactive power independently as long as their operational limits are not exceeded [7].

On the other hand, centralized voltage control is based on information about a large part or even the whole distribution network in order to determine the control actions to be performed. Typically, these methods regulate not only substation voltage and DG reactive power but also other components with voltage control capability such as capacitor banks, static VAR compensators, static synchronous compensators, *etc.* Usually, network voltages either measured or estimated are required as well as precise information on the state of the network.

Within the SuSTAINABLE concept, an increased knowledge of the distribution network based on network sensing, together with the new information available from an

Advanced Metering Infrastructure (AMI), will allow developing new advanced functionalities designed for supporting network operation. These functionalities will be able to exploit in a coordinated way the different DER located at the MV and LV levels, namely DG, distributed storage systems, controllable loads under Demand Side Management (DSM) actions, as well as transformers with OLTC capability and other reactive power regulation devices. This will enable moving towards the paradigm of a Smart Distribution Grid.

As a result, new advanced voltage control schemes, taking advantage of smart grid technologies (including smart meters, enhanced power electronic interfaces and other intelligent electronic devices), are necessary. These new control schemes should ensure that the different Distributed Energy Resources (DER) are operated in a coordinated way in order to enable a safe and efficient operation of the distribution systems. It must be stressed that the definition of DER used here includes not only DG units but also controllable loads and storage systems.

Some approaches can be found in the scientific literature regarding the state-of-the-art on the voltage control. For instance, authors in [8, 9] present interesting contributions on the coordinated use of DG and other voltage regulation devices in order to ensure that voltage profiles are kept within admissible limits in distribution networks. However, current available methodologies usually do not address the coordinated operation of traditional voltage regulation devices such as Capacitor Banks (CBs) or OLTC transformers with DG units and demand with interruptibility contracts. Moreover, most of these solutions do not address the distribution system as a whole and are not designed for preventive operation but rather react to the present conditions of the distribution grid. The approach developed in SuSTAINABLE is much more advanced since it is able to ensure a preventive control by relying on both load and RES forecasts, as well as on results obtained from state estimation.

In SuSTAINABLE, a novel strategy for advanced coordinated voltage control is proposed aimed at taking advantage of the DER connected at the MV and LV levels. This approach is described in detail in Chapter 2.

2 Advanced Coordinated Voltage Control

The proposed scheme for voltage control was defined in accordance to the overall SuSTAINABLE architecture presented in Deliverable D2.3 [10] and resulted from a discussion between the partners of the consortium about the foreseen future for grid operation and automation at the different voltage levels.

As defined in [10], the main objective of the SuSTAINABLE concept is related to the maximization of the integration of energy from variable RES in the distribution system. In order to achieve this, it is necessary to develop a methodology that will effectively be able to control voltage throughout the network by coordinating all available regulation devices, DG active and reactive output power, storage and controllable loads. This strategy will be implemented at the level of the HV/MV primary substation (Smart Substation Controller – SSC), while a secondary control level will also exist at the level of the MV/LV secondary substations (Distribution Transformer Controller – DTC).

As a result, the proposed methodology will exploit two different levels of control, as follows:

- **At the MV level** – using a multi-temporal Optimal Power Flow (OPF) at the functional level of the SSC to coordinate the several MV voltage control resources (DG, storage devices, controllable loads, OLTC transformers, CBs, *etc.*) in order to avoid technical problems by satisfying the constraints and minimizing a single or a multi-objective function; this functionality should be fed with the results from the state estimation module and with forecasts from the RES and load forecasting systems.
- **At the LV level** – centralized controller housed in the DTC, which will send set-points to DER (*i.e.* controllable loads, microgeneration (μG), storage devices) located within the corresponding LV network in order to follow the requests from the SSC or by responding autonomously to voltage violations that may be identified; in addition, local droop functionalities are implemented in some inverters interfacing the DER available with the centralized voltage control algorithm being able to remotely update the parameters of these droops.

Figure 2 illustrates the proposed concept for the voltage control approach encompassing both the MV and LV levels.

In Chapter 3, the MV control strategy based on the multi-temporal OPF is presented. Concerning the LV control scheme, the proposed approach is detailed in Chapter 4. Furthermore, in Appendix B, the database specification and data communication requirements for the MV multi-temporal OPF and for the LV centralized control are presented.

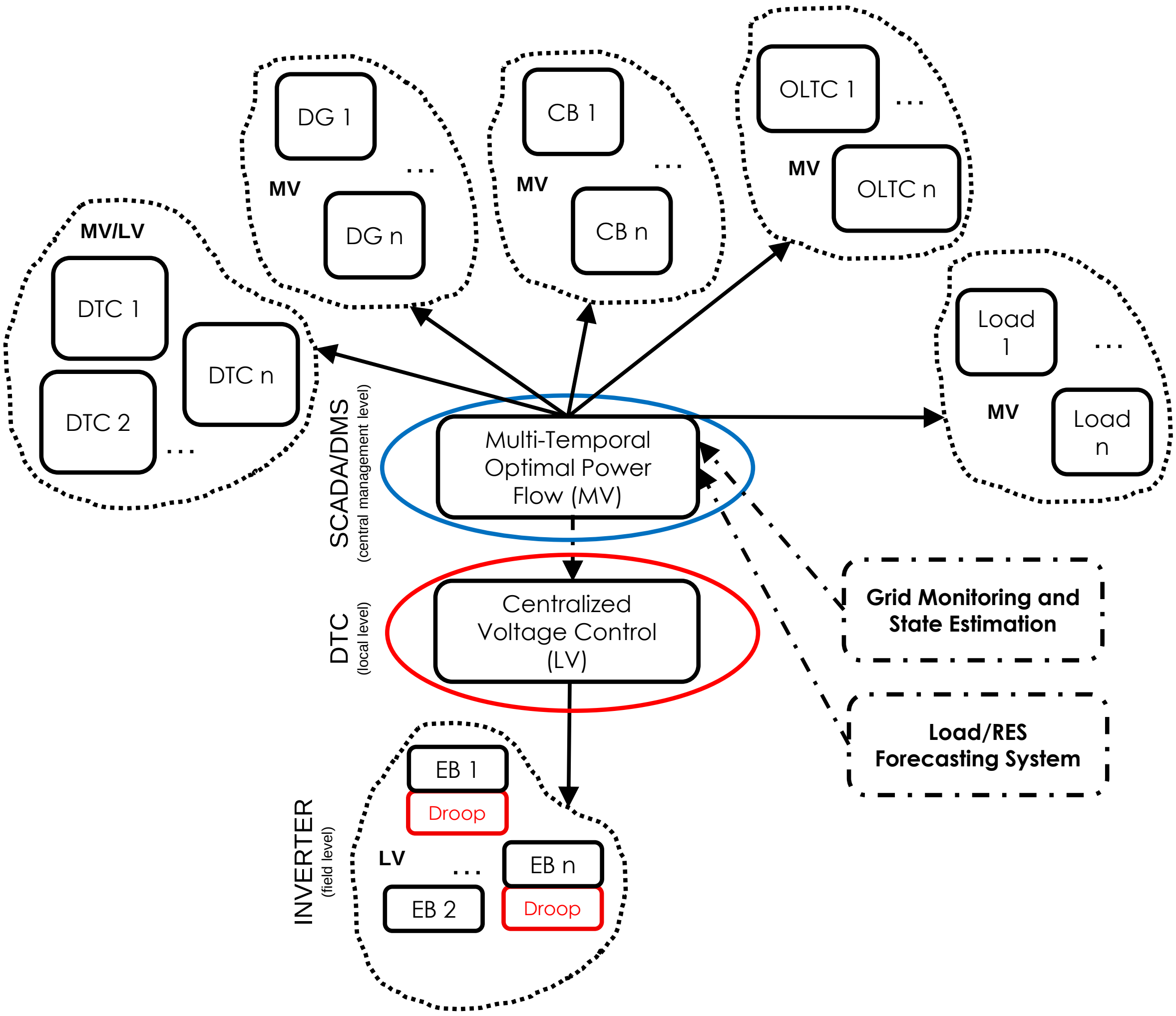

Figure 2 – Framework of the Voltage Control System

3 Multi-Temporal Optimal Power Flow for MV Grids

A multi-temporal OPF that will operate at the level of the HV/MV primary substation, *i.e.* at the functional level of the SSC, will be responsible for controlling MV network operation. Nevertheless, since the load / RES forecasting systems are located at the central systems' level of the Supervisory Control and Data Acquisition / Distribution Management System (SCADA/DMS), the multi-temporal OPF will also be physically at the SCADA/DMS. An overview of the proposed approach is given in Figure 3.

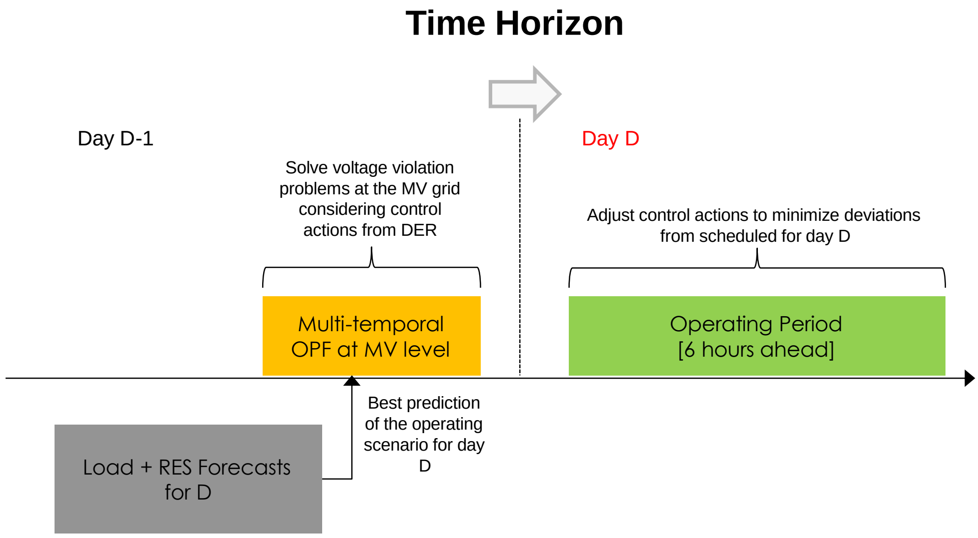

Figure 3 – Proposed Approach for the Voltage Control at the MV Level

As can be observed, the approach developed is expected to work in 2 time-frames:

- <u>Day-ahead (D-1 Analysis)</u> → Taking as inputs load and generation bids from the market agents as well as results from state estimation, the multi-temporal OPF will produce a set of control actions for the next day by MV network node (*i.e.* by DTC). The main goal, in line with the SuSTAINABLE concept, will be to maximize the integration of energy coming from variable RES subject to a set of technical and operational constraints, namely node voltage limits and branch thermal limits. In this algorithm, the available DER will be utilized, including not only the resources owned by the DSO but also resources from customers providing ancillary services to the system. The resulting actions will allow defining the operation plan for the next day and close both the energy and ancillary services market.
- <u>N-hours ahead (6-hours Ahead Analysis)</u> → The same multi-temporal OPF developed for the day-ahead analysis will be used n-hours ahead in order to adjust the control actions previously identified feeding from more recent and accurate data regarding load and RES forecast (generated by the DSO forecasting system). The main objective will now be to minimize the deviations in a sliding window of 6-hours ahead (with hourly updates) regarding the scheduled scenario in D-1

analysis. This will enable correcting the deviations that occur and solve technical problems that may arise close to real-time.

Two different approaches for the multi-temporal OPF are presented here. In Section 3.1 the problem is formulated as a single-objective optimization problem that is solved using a meta-heuristic approach developed by INESC. In Section 3.2, by ICCS, the problem has a multi-objective formulation and is solved by an algorithm for mixed integer quadratically constrained quadratic problems.

3.1 Single-objective Formulation

The approach presented in this section was developed aiming at maximizing the integration of energy generated by RES, according to the SuSTAINABLE concept, taking into account the physical and technical constraints of the MV network and its elements.

Therefore, in order to cope with high DG penetration due to increase of generation units connected directly to the distribution system, in addition to the existence of responsive loads and dispersed storage solutions, an effective voltage control scheme must be based both on active and reactive power control. In order to allow a large-scale deployment of these devices, the implementation of some type of hierarchical coordinated management scheme is required. This approach will enable taking full profit of the benefits that all these resources can bring to system operation. Although local control approaches may also be employed, a pure decentralized control approach will not be able to achieve an optimum and global solution.

Nevertheless, distribution systems have specific characteristics that may affect traditional voltage control schemes. For instance, the decoupling between active power and voltage magnitude that can be observed at the transmission level does not hold at the lower voltage levels of the distribution system given the X/R ratio of many of the distribution lines. As a result, reactive power control is not sufficient to maintain efficient system operation.

The proposed control functionality is intended to aid the DSO in real-time to optimize the operation of the distribution system in terms of voltage control based on data from generation scheduling and forecasting for loads and RES for the next operation period, in a sort of predictive mode. In this work, it was considered that hourly intervals for the day-ahead and a sliding window of 6 hours-ahead were adequate in order to maintain voltage profiles within admissible limits.

The approach was formulated as an optimization problem to be solved by a multi-temporal OPF using a new meta-heuristic approach developed in INESC that is a variant of Evolutionary Particle Swarm Optimization borrowing concepts from Differential Evolution (DEEPSO) [11]. This approach involves a coordinated action between all DER available, such as microgrids, DG units, and storage devices, as well as OLTC transformers, CBs and controllable loads directly connected at the MV level.

3.1.1 Proposed Approach

As previously explained, the approach for voltage control at the MV level will work in two different time-frames. First, a day-ahead analysis will be conducted based on forecasting data for the next day in order to define a set of control actions for each hour of the day (Section 3.1.1.1). Then, an intraday analysis will be performed based on updated information from forecasting in order to adjust the control actions previously identified for a 6-hours sliding window (Section 3.1.1.2).

3.1.1.1 Day-ahead (D-1) Analysis

The approach for optimization for the day-ahead (D-1) involves analysing a 24 hour time horizon with hourly steps based on the load forecasting and RES forecasting results. The best solution is a set of set-points for the several DER for each of the 24 hours of the day that is achieved taking into account time interdependencies for all control variables.

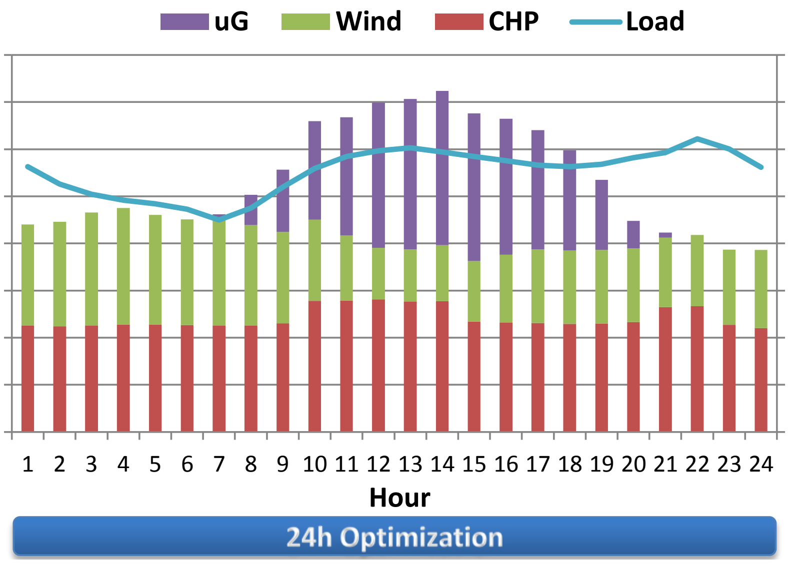

Figure 4 – Optimization Window for D-1 Analysis

As shown in Figure 4, the blue bar represents the number of hours or the window for which the optimization is performed and the best global solution obtained.

3.1.1.2 Intraday (6 hours-ahead) Analysis

On day analyses, the solution found on day D-1 is taken into account as a starting point for the optimization. In this case, the time horizon is a sliding window of 6 hours-ahead. The algorithm will run the optimization for this period based on updated information from the forecasting modules (for load and RES) trying to minimize the deviations from the plan that was defined in the day-ahead optimization.

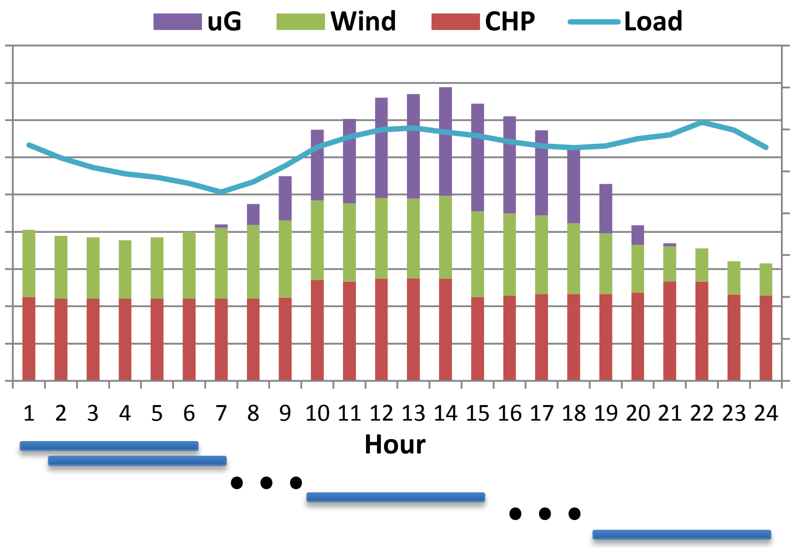

Figure 5 – Sliding Window for Optimization on D Analysis

In Figure 5, the blue bars represent the sliding window of 6 hours that is recalculated at each hour whenever new forecasts are available for both RES and load for the whole day.

3.1.2 Mathematical Formulation

3.1.2.1 Day-ahead Analysis

The approach developed for advanced coordinated voltage control in MV distribution grids with maximization the integration of energy from variable RES, taking into account the power flow constraints in distribution systems can be formulated as an optimization problem.

The voltage control algorithm exploits the control capabilities available for the DSO. The main control variables considered here are the following:

- Reactive power (Q) from DG units – Continuous variable;
- Active power curtailment (P) from from DG units – Continuous variable;
- Active power injection / absorption from dispersed storage devices – Continuous variable;
- Power consumption (P) from controllable loads – Continuous variable;
- Tap positions of OLTC transformers – Discrete variable;
- Tap positions of CBs – Discrete variable.

These control variables are regarded as set-points that are sent to each device connected to the MV level, exploiting the communication infrastructure available through the hierarchical control structure defined by the SuSTAINABLE architecture. As mentioned above, some of these control variables such as the power from generators, storage and loads, can be modelled as continuous variables while others, such as the OLTC settings and CBs steps, are of a discrete nature.

3.1.2.1.1 Objective Function

In the optimization problem, the definition of the objective function to be used by the algorithm is very important. For the D-1 analysis the main goal reflects the need to minimize the amount of active power curtailment required for voltage control purposes. As a result, the following two objectives are pursued:

- Minimize the curtailment of DG (thus maximizing the integration of energy from RES);
- Minimize the shedding of controllable loads.

The resulting objective function combines these two terms using a type of trade-off approach, as shown in the objective function below.

$$\min F = \min \sum_{h=1}^{24} \left(\omega_1 \cdot f_1^h + \omega_2 \cdot f_2^h\right) \tag{3.1}$$

In order to ensure a hierarchy in the use of DER mentioned above, the values of the weights (ω_i) define the relation between a variation in one objective (in this case DG curtailment) and the other objective (in this case load shedding). These decision parameters should reflect the preferences of the decision-maker, which in this case should be the DSO. This means that the DSO must decide which objective should be favoured (DG curtailment or shedding of controllable loads) by defining the appropriate values for ω_1 and ω_2.

The expression for f_1 concerning DG curtailment is shown below.

$$f_1 = \sum_{i=1}^{n} (P_{DG_i}^{max} - P_{DG_i}) \tag{3.2}$$

The other control measure considered is the shedding of controllable loads. Note that this control only concerns certain loads assigned as non-priority that are assumed to be controlled according to a flexibility contract with the DSO.

$$f_2 = \sum_{i=1}^{n} \left[(P_{l_i}^{initial} - P_{l_i}^{final}) + (Q_{l_i}^{initial} - Q_{l_i}^{final}) \right] \tag{3.3}$$

Where

ω_1 and ω_2 are the weights associated to functions f_1 and f_2, respectively.

$P_{DG_i}^{max}$ is the maximum active power generation from DG at bus i.

$P_{DG_i}$is the current active power generation from DG at bus i.

$P_{l_i}^{initial}$ and $Q_{l_i}^{initial}$ are the current active and reactive power of the controllable load at bus i, respectively.

$P_{l_i}^{final}$ and $Q_{l_i}^{final}$ are the active and reactive power of the controllable load at bus i after the activation of the flexibility contract, respectively.

3.1.2.1.2 Constraints

The constraints used in formulation approach can be separated into equality constraints and inequality constraints. The equality constraints include the traditional power flow equations considering a full AC model.

$$P_{inj_i} + P_{DG_i} + P_{D_i} - P_{C_i} - P_{L_i} = P\,(V, \theta,\, T_t, T_{CB}) \tag{3.4}$$

$$Q_{inj_i} + Q_{DG_i} + Q_{CB_i} - Q_{L_i} = Q\,(V, \theta,\, T_t, T_{CB}) \tag{3.5}$$

Where

P_{inj_i} and Q_{inj_i} are the active and reactive power injections at bus i, respectively.

Q_{DG_i} is the reactive power generation from DG at bus i, respectively.

P_{D_i} is the active power provided from the discharging of the storage at bus i.

P_{C_i} is the active power consumed from the charging of the storage unit at bus i.

P_{L_i} and Q_{L_i} are the active and reactive power of the controllable load at bus i, respectively.

Q_{CB_i} is the reactive power generated from CBs at bus i.

V is the voltage magnitude.

θ is the voltage angle.

T_t and T_{CB} are the tap positions from OLTC transformers and CBs, respectively.

The inequality constraints are mostly related to operation limits or to physical limits of devices. Therefore, the main inequality constraints considered are presented below.

$$P_{DG_i}^{min} \leq P_{DG_i} \leq P_{DG_i}^{max} \tag{3.6}$$

$$Q_{DG_i}^{min} \leq Q_{DG_i} \leq Q_{DG_i}^{max} \tag{3.7}$$

$$V_i^{min} \leq V_i \leq V_i^{max} \tag{3.8}$$

$$S_{ik} \leq S_{ik}^{max} \tag{3.9}$$

Where

$P_{DG_i}^{min}$ and $P_{DG_i}^{max}$ are the minimum and maximum active power generation from DG at bus i, respectively.

$Q_{DG_i}^{min}$ and $Q_{DG_i}^{max}$ are the minimum and maximum reactive power generation from DG at bus i, respectively (+ if generating reactive power and – if consuming reactive power).

V_i is the voltage at bus i.

V_i^{min} and V_i^{max} are the minimum and maximum voltage at bus i, respectively.

S_{ik} is the apparent power flow in branch ik.

S_{ik}^{max} is the maximum apparent power flow in branch ik.

In the management of storage systems, it is necessary to limit the maximum storage capacity of each unit operating in the network as shown in expression (3.10).

$$E_{st_i}^{min} \leq \sum_{h=1}^{24} E_{st_i}^{h} \leq E_{st_i}^{max} \tag{3.10}$$

In addition are considered the charge and discharge energy limits in each hour, as shown in the next expressions:

$$\eta_{C_i} \cdot E_{C_i}^{h} \leq E_{max\_C_i}^{h} \tag{3.11}$$

$$\frac{E_{D_i}^{h}}{\eta_{D_i}} \leq E_{max\_D_i}^{h} \tag{3.12}$$

Taking into account these limits, the storage systems cannot operate with a charge rate which exceeds the maximum storage capacity and do not operate with a discharge rate that exceeds the energy that is stored in batteries. Therefore, the State of Charge (SOC) of the storage unit can be expressed as follows:

$$SOC_i^{h} = SOC_i^{h-1} + \left(\eta_{C_i} \cdot E_{C_i}^{h} - \frac{E_{D_i}^{h}}{\eta_{D_i}}\right) \tag{3.13}$$

Where

$E_{st_i}^{h}$ is the energy stored in the battery in hour h at bus i.

$E_{st_i}^{min}$ and $E_{st_i}^{max}$ are the minimum and maximum energy stored in the battery at bus i, respectively.

$E_{C_i}^{h}$ and $E_{D_i}^{h}$ are the energy stored from charge and discharge in hour h at bus i, respectively.

η_{C_i} and η_{D_i} are efficiency from charge and discharge in the battery at bus i, respectively.

$E_{max\_C_i}^{h}$ is the maximum energy from charge in hour h at bus i.

$E_{max\_D_i}^{h}$ is the maximum energy from discharge in hour h at bus i.

SOC_i^h is the state of charge in hour h at bus i.

SOC_i^{h-1} is the state of charge in hour $h-1$ at bus i.

The OLTC in transformers and the voltage regulators in CBs are modelled as tap-changing for monitoring and regulate the voltage in feeders to the defined limits by changing the turn ratio of the transformers and switching steps of the CBs. The approach implemented restricts the number of tap position changes in two consecutive 1-hour periods, according to (3.14), in order to prevent OLTC transformer taps from deteriorating due to intensive use. The number of maximum tap changes allowed can be adjusted to reflect the policy of the decision-maker. To limit the range of switching actions because the physical limits of equipment, the minimum and maximum additional constraint for transformers (3.15) and CBs (3.16) was included.

$$\left|T_{t_i}^{\,h} - T_{t_i}^{\,h-1}\right| \le \delta_i \tag{3.14}$$

$$T_{t_i} \in \left\{T_{t_i}^{\,min}, \cdots, T_{t_i}^{\,max}\right\} \tag{3.15}$$

$$T_{CB_i} \in \left\{T_{CB_i}^{\,min}, \cdots, T_{CB_i}^{\,max}\right\} \tag{3.16}$$

Where

T_{t_i} is the tap for the OLTC transformer i.

$T_{t_i}^{\,h}$ and $T_{t_i}^{\,h-1}$ is the tap for the OLTC transformer i in hour h and $h-1$, respectively.

δ_i is the step size allowed for OLTC transformer i.

$T_{t_i}^{\,min}$ and $T_{t_i}^{\,max}$ are the minimum and maximum of the range for the OLTC in transformer i, respectively.

T_{CB_i} is the tap for the CB i.

$T_{CB_i}^{\,min}$ is the minimum of the range for the tap in CB i.

${T_{CB}}_i^{max}$ is the maximum of the range for the tap in CB i.

3.1.2.2 Intraday Analysis

3.1.2.2.1 Objective Function

The intraday analysis performs the optimization for a sliding window of 6 hours and has a formulation similar to the day-ahead problem with the difference being the objective function. In this case, new factors are added in order to reflect the differences between what was planned in D-1 and the current solution. Therefore, the objective function becomes:

$$\min F = \sum_{h=1}^{6} \left(\omega_1 \cdot f_1^h + \omega_2 \cdot f_2^h + \Delta_{E_{st}}^h + \Delta_{T_i}^h + \Delta_{T_{CB}}^h\right) \tag{3.17}$$

The additional expressions for $\Delta_{P_{stor}}^h$, $\Delta_{T_i}^h$ and $\Delta_{T_{CB}}^h$ correspond to the difference for the optimized variables on the day-ahead analysis and the optimized variables on intraday analyses as shown below. It should be stressed that these terms have been normalized in the objective function since they are expressed in different units.

$$\Delta_{E_{st}}^h = \sum_{i}^{n} \left\| E_{st_i}^{D-1}(h) - E_{st_i}^{D}(h) \right\| \tag{3.18}$$

$$\Delta_{T_i}^h = \sum_{i}^{n} \left\| T_{t_i}^{D-1}(h) - T_{t_i}^{D}(h) \right\| \tag{3.19}$$

$$\Delta_{T_{CB}}^h = \sum_{i}^{n} \left\| T_{CB_i}^{D-1}(h) - T_{CB_i}^{D}(h) \right\| \tag{3.20}$$

Where

$E_{st_i}^{D-1}(h)$ and $E_{st_i}^{D}(h)$ are the energy stored in hour h at bus i in Day-ahead (D-1) and in Intraday (D), respectively.

$T_{t_i}^{D-1}(h)$ and $T_{t_i}^{D}(h)$ are the tap positions from OLTC transformers in hour h at bus i in Day-ahead (D-1) and in Intraday (D), respectively.

$T_{CB_i}^{D-1}(h)$ and $T_{CB_i}^{D}(h)$ are the tap positions from CBs in hour h at bus i in Day-ahead (D-1) and in Intraday (D), respectively.

3.1.2.2.2 Constraints

The constraints are the same as for the day-ahead analysis presented in Section 3.1.2.1.2.

3.1.3 Implementation of the Algorithm

As previously described, the approach for voltage control in distribution networks integrating RES was built by formulating an optimization problem. The main characteristics of this formulation are presented in this section, with emphasis on the optimization method and on the implementation of the voltage control algorithm as a tool to be made available for support the network operation.

The optimization problem as presented in this work may be formulated as a mixed, nonlinear optimization problem. This means that both continuous and discrete variables are considered. This type of algorithms (meta-heuristic) is intended find the global optimum or, at least, a good local optimum without requiring many previous assumptions on the problem.

In this work, the meta-heuristic approach chosen was DEEPSO, a method developed in INESC Porto[1], described as EPSO (Evolutionary Particle Swarm Optimization) with a touch of DE (Differential Evolution). EPSO itself is already a hybrid between Particle Swarm Optimization (PSO) and Evolutionary Programming.

The method consists in moving a set of particles that exploit the space of solutions with n dimensions, according to the number of problem variables. Each particle corresponds to an alternative solution of the optimization problem with the following composition:

- X_i – position of the particle
- V_i – velocity of the particle
- b_i – best solution of each particle
- b_g – global optimum of all particles

In DEEPSO, each particle is defined by its position X_i and velocity V_i for the coordinate position i, and the particle movement rule (shown in Figure 6) is explained in the following equation:

$$X_i^{new} = X_i \cdot V_i^{new} \tag{3.21}$$

[1] EPSO – Evolutionary Particle Swarm Optimization
For more information see http://epso.inescporto.pt

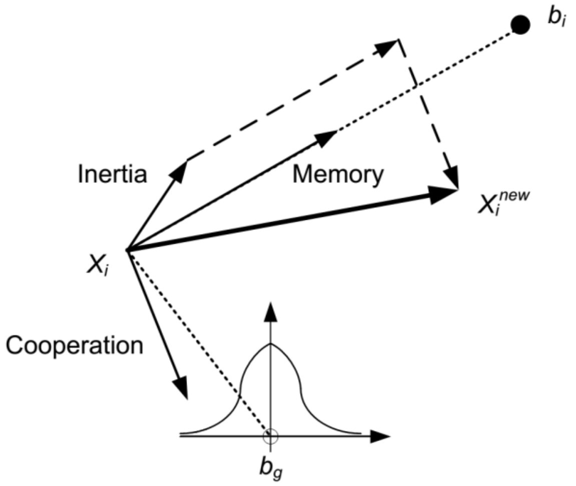

Figure 6 – Movement of a Particle in EPSO

As previously explained, the proposed algorithm aims at identifying a set of control actions exploiting the available DER and other controllable devices for voltage control purposes in a period of 24 hours. The scheme of the population with 30 individuals (solutions to the problem or "particles" in the context of PSO problems) in DEEPSO for all 24 hours is shown in Figure 7.

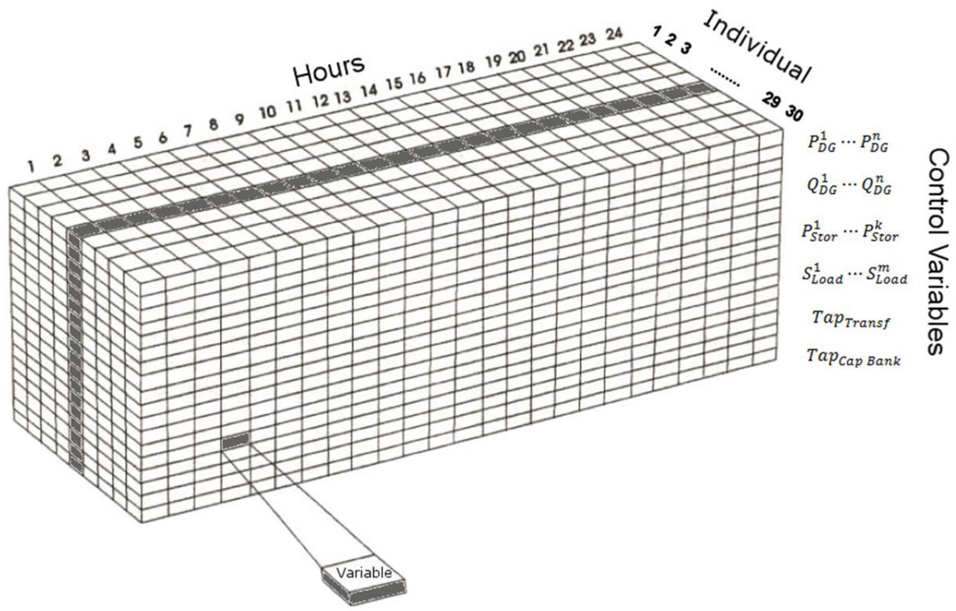

Figure 7 – Dimension of the Population in the DEEPSO

Given a population with a set of particles, the general scheme of the DEEPSO algorithm used in this work, becomes:

- **REPLICATION** – each particle is replicated (cloned) r times
- **MUTATION** – each particle has its strategic parameters mutated

- **REPRODUCTION** – each mutated particle generates an offspring through recombination, according to the particle movement rule
- **EVALUATION** – the offspring have their fitness evaluated
- **SELECTION** – the best particles survive to form a new generation, composed of a selected descendant from every individual in the previous generation

Concerning the constraints, these are usually allocated in the traditional evolutionary strategies way, *i.e.* by adding penalties to the objective function. Several penalty functions can be used such as linear penalty or quadratic penalty. In the optimization problem, operational limits were modelled as “hard constraints” with high penalization and voltage deviations and branch overloads where modelled as “soft constraints” implemented through quadratic penalty functions, as shown in Figure 8, included in the objective-function.

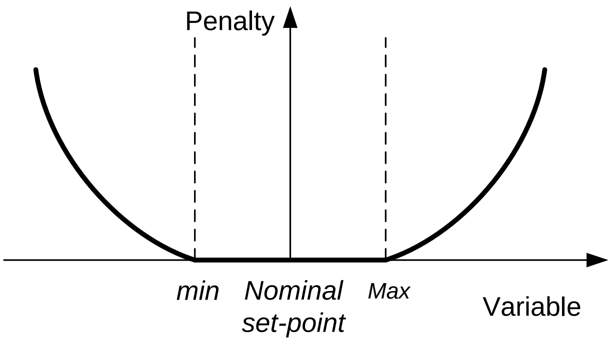

Figure 8 – Quadratic Penalty Function

The global algorithm for the control voltage is presented in Figure 9. The algorithm structure can be divided into two main parts. The first consists in obtaining a base scenario by performing hourly power flow simulations for a period of 24 hours, with a given load and generation profiles in order to check if the voltage values at all buses of the network are inside the technical limits.

The second part of the algorithm is performed using the DEEPSO optimization process in order to identify the control actions required to solve the voltage violations that were identified in the previous step.

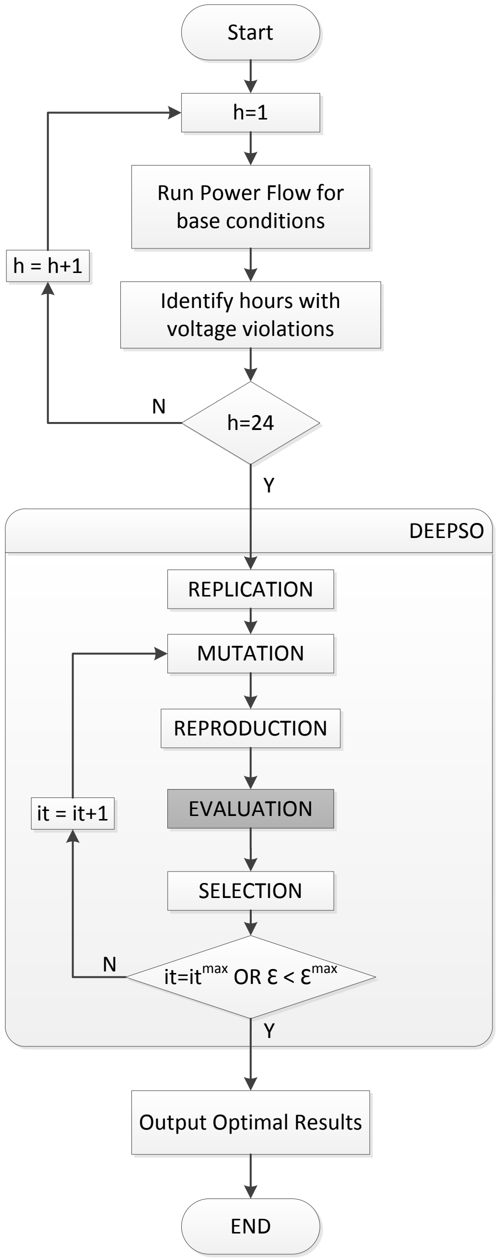

Figure 9 – DEEPSO Algorithm

One of the most important steps in the whole algorithm is the evaluation process within the DEEPSO. Since each particle is composed by the control variables for 24 hours, the evaluation step is performed by running a power flow for each of the 24 hours for each particle in order to evaluate the fitness function, as shown in Figure 10.

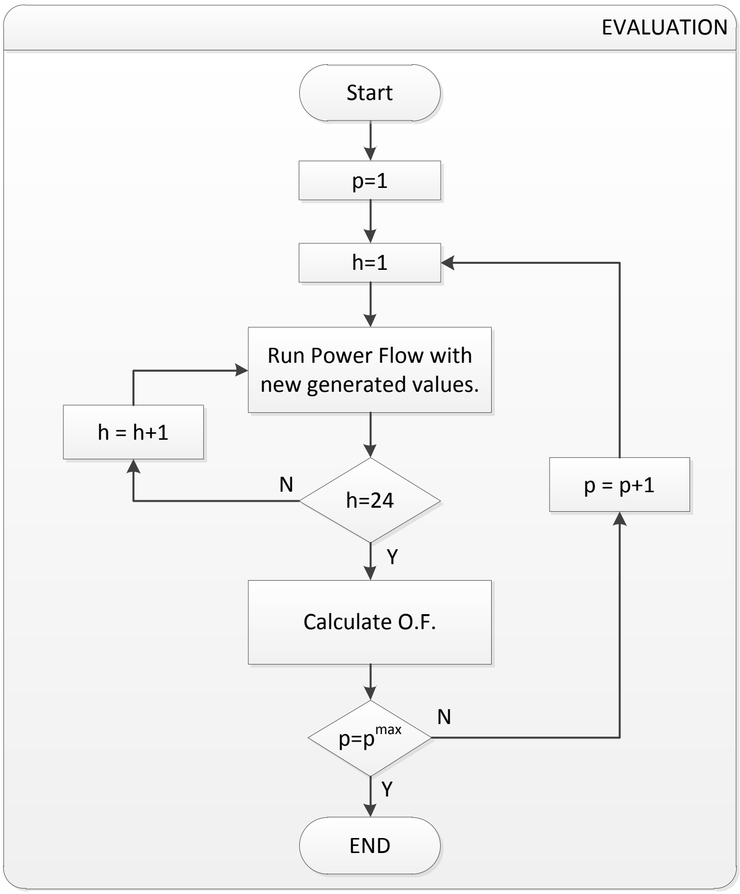

Figure 10 – Evaluation Process

The formulation of the optimization problem described above has been implemented in the simulation platform MATLAB and power flow solver from MATPOWER[2].

3.1.4 Application Results

This section presents some of the simulation results that have been obtained with the tool developed for the multi-temporal OPF developed by INESC. The proposed methodology was tested on a large scale test network characterized by high DG penetration using as a reference a scenario with no control actions.

The MV network is based on a real Portuguese MV distribution network, and the diagram is presented in Figure 11. This network is typically rural, with a radial structure that includes two distinct areas with different voltage levels: 30 kV before the OLTC transformer (shown on the top of Figure 11) and 15 kV after the OLTC transformer (middle of Figure 11). The OLTC transformer is a 30/15 kV transformer with taps on the secondary side. The network has a total of 210 nodes and 212 branches.

[2] MATPOWER – A MATLAB Power System Simulation Package.
For more information see http://www.pserc.cornell.edu/matpower

This network includes several DER such as DG units (one CHP unit and two wind generators with doubly-fed induction generator – DFIG) and six microgrids directly connected to MV network. From the MV point of view, each microgrid was considered as a single bus with an equivalent generator (corresponding to the sum of all µG) and equivalent load (corresponding to the sum of all LV loads). The µG technology considered here is based on solar PV. Furthermore, two storage devices (batteries) were considered, as well as a capacitor bank and two controllable loads.

The network data for the test network used here is included in Appendix A.

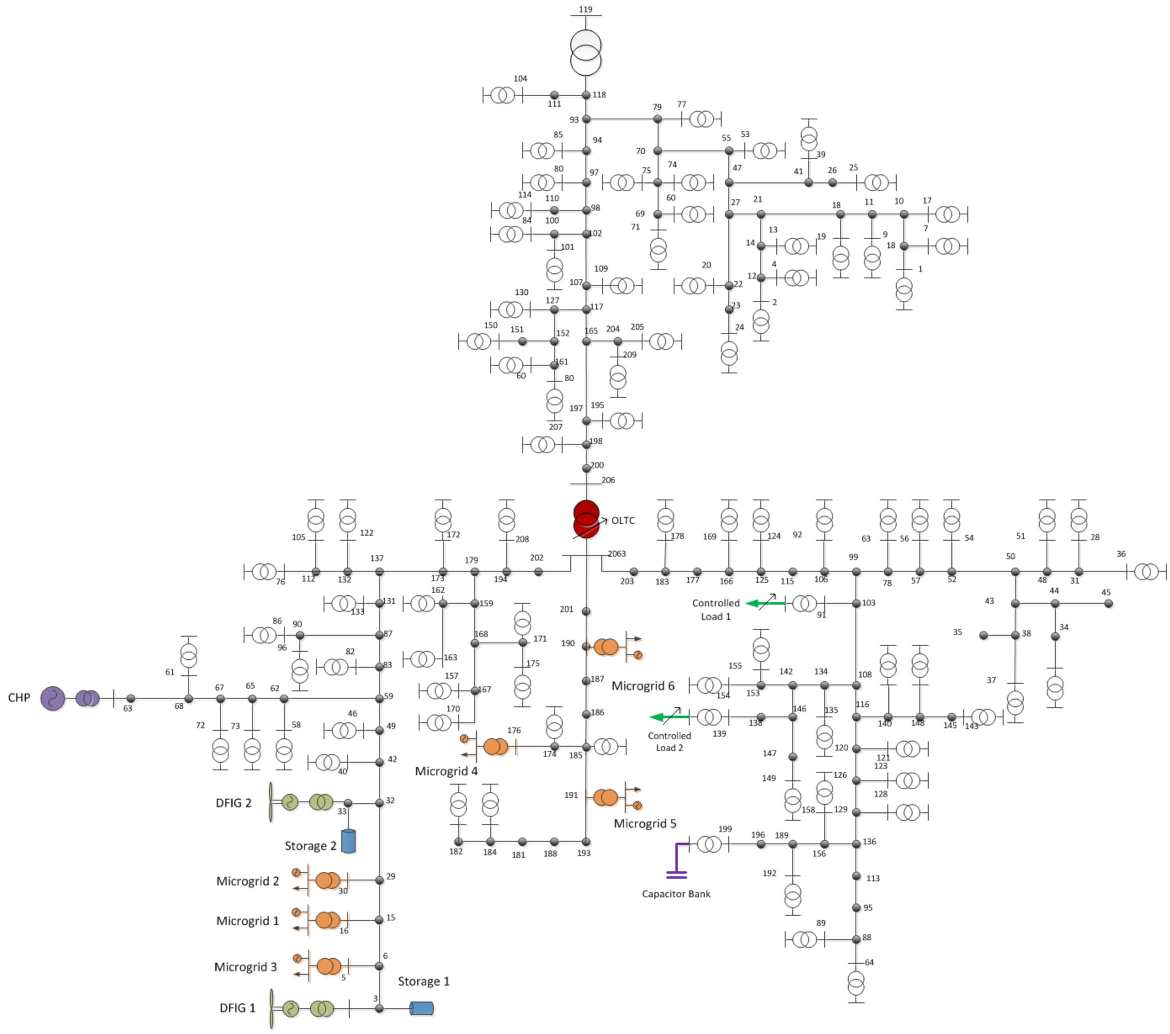

Figure 11 – MV Test Network

3.1.4.1 Day-ahead (D-1) Analysis

In order to run the algorithm for the day-ahead analysis, real forecast data is necessary. This will be done for validation in WP6 using the data from the Évora site as previously stated. Here, since the main objective is merely to test the performance of proposed approach, daily profiles for both load and generation are used to build the scenarios for simulation.

The scenarios used in the simulation were obtained by applying the load and generation profiles to the total load installed capacity and total generation capacity, respectively. The profile used for 24 hours is provided by Portuguese Transmission System Operator (REN) and is referred to May 31st, 2014 [12]. This profile is presented in Figure 12.

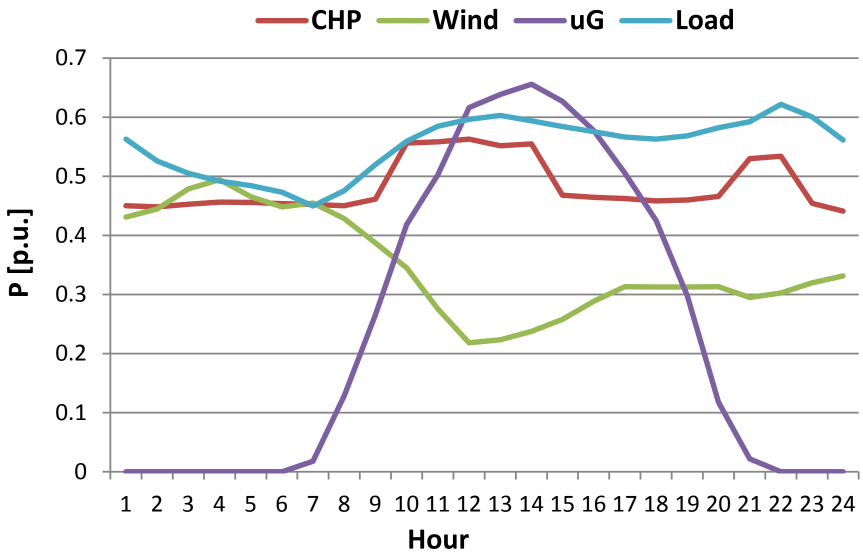

Figure 12 – Load and Generation Profiles used for Day-ahead Analysis

3.1.4.1.1 Scenario 1 (Moderate DG Penetration)

This first scenario is characterized by a large production of DG and a moderate consumption, which creates a situation with some voltage deviations in some buses.

The profiles for load and DG for this scenario are shown in Figure 13.

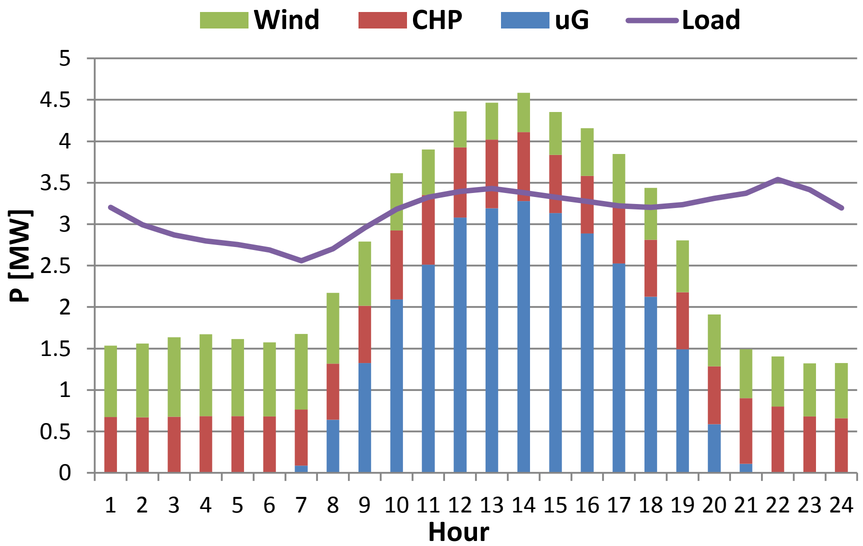

Figure 13 – Load and Generation for 24 hours (Scenario 1)

Figure 14 shows the maximum and minimum values for voltage for each hour of the day considering that no control actions are undertaken (base case), *i.e.* without running the optimization algorithm.

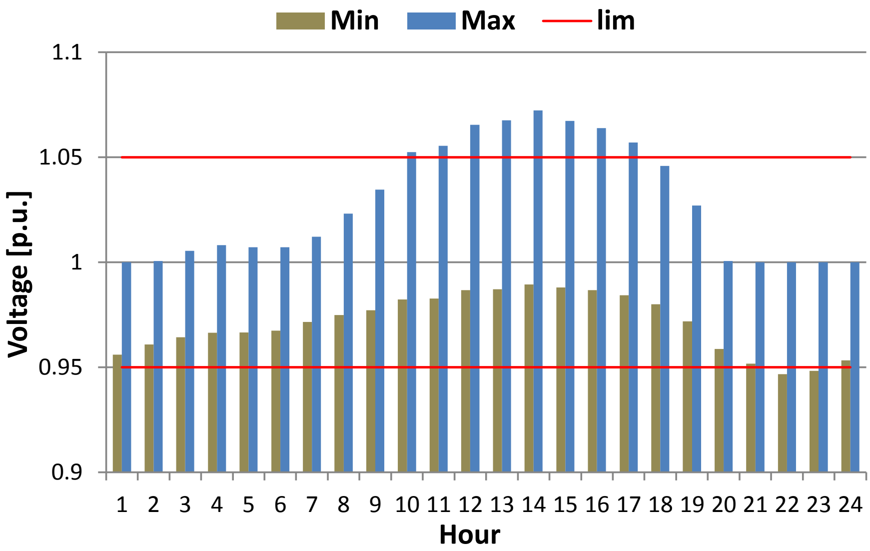

Figure 14 – Maximum and Minimum Voltage Values for 24 hours (Scenario 1)

As can be observed from Figure 14, without the voltage control algorithm, voltage values are above the admissible range of ±5% due to large penetration of DG, especially PV-based µG.

In this case, the PV units have their peak generation at 14:00, which is outside the hours of peak demand. Therefore, there is excess of generation in the MV that is exported to the HV network. This fact causes overvoltages around 14:00. On the other hand, around 21:00 (corresponding to the peak load hour), the amount of power provided by the DG units is smaller than the load, which causes undervoltages.

After running the optimization algorithm, all voltage violations were corrected as can be seen in the Figure 15 and Figure 16 (green bars).

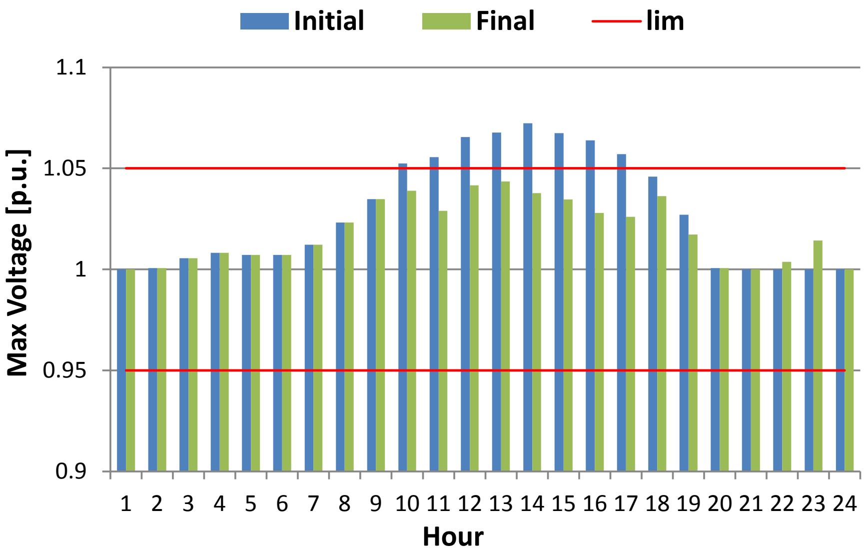

Figure 15 – Maximum Voltage Values for 24 hours (Scenario 1)

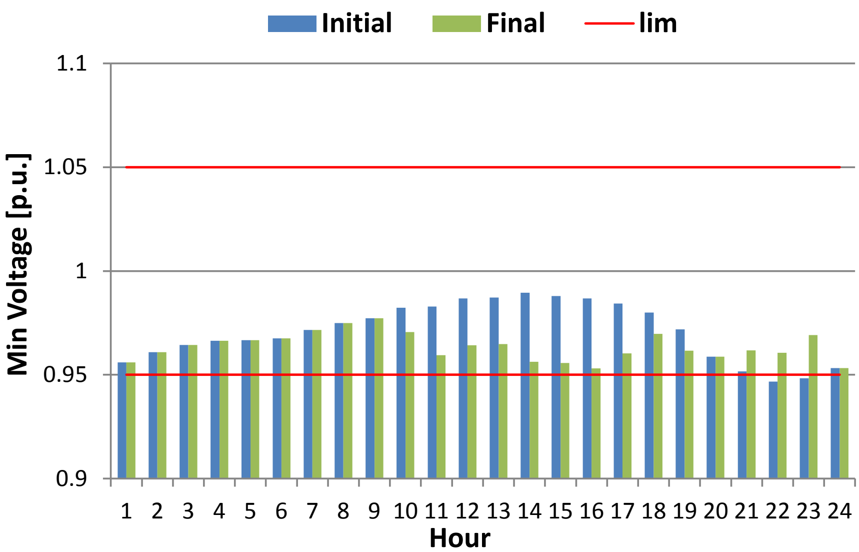

Figure 16 – Minimum Voltage Values for 24 hours (Scenario 1)

In order to ensure that the voltage values were brought inside admissible limits, the DER available, namely batteries, CBs and the OLTC transformer were used. It must be stressed that, in this scenario, no load shedding or DG curtailment was required in order to control the voltage profiles.

As can be seen in Figure 17, the two batteries have a good contribution to voltage control by storing energy (negative values) at hours when there is excess DG and provide the stored energy (positive values) in peak load hours.

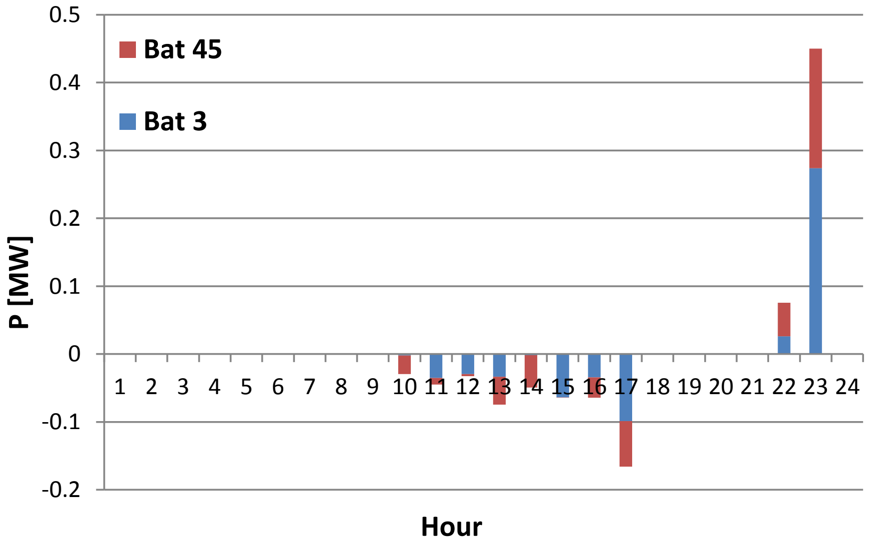

Figure 17 – Charging / Discharging of Batteries (Scenario 1)

Also, the reactive power by provided by the DG units (positive when injecting and negative when absorbing), shown in Figure 18, assists in the voltage control.

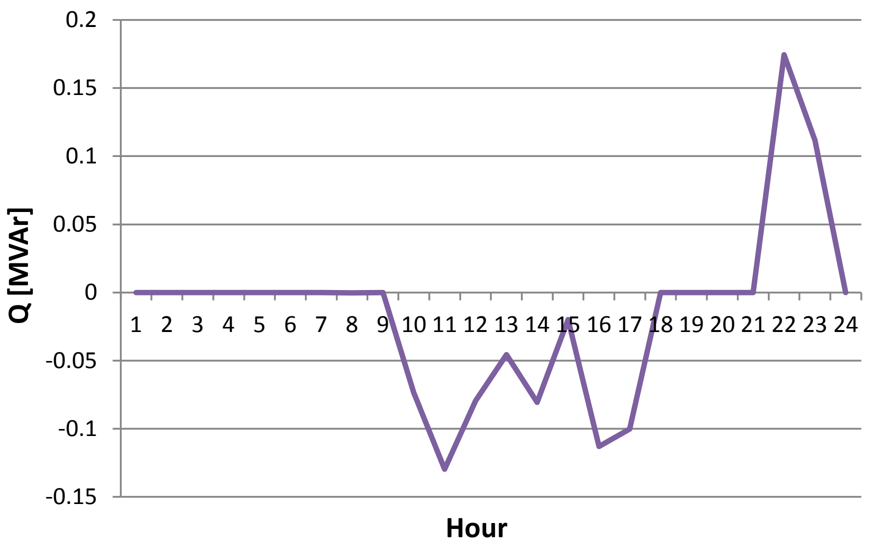

Figure 18 – Total Reactive Power provided by DG (Scenario 1)

In hours of peak load, the CBs have also contributed to increase the voltage in peak load as shown in Figure 19.

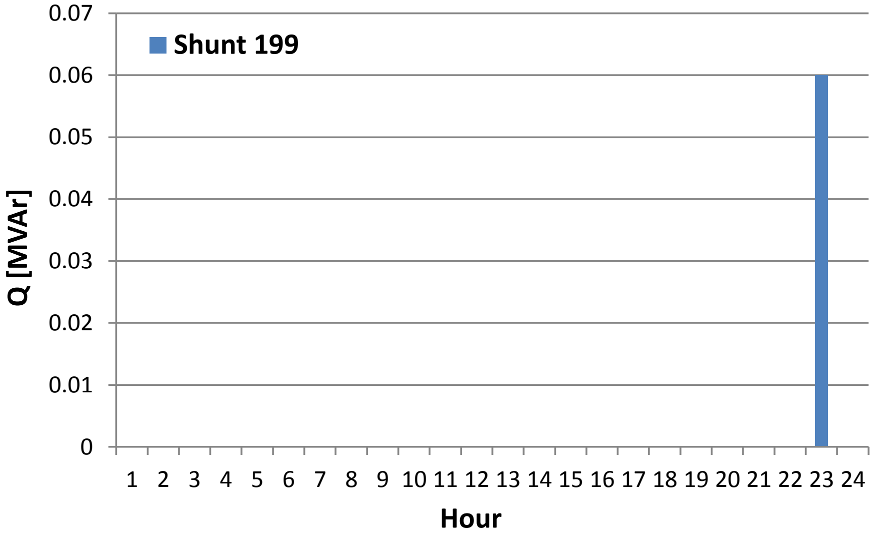

Figure 19 – Reactive Power provided by capacitor Bank (Scenario 1)

The Figure 20 shows the tap values at the OLTC transformer. According to the modelling of the transformer with taps on the secondary side, tap values above 1 raise the voltage on the secondary of the transformer. Consequently, lower tap values are used when voltage profiles are typically high and higher tap values are used when voltage profiles are low. As can be observed, the constraint used for limiting the number of switching actions of the OLTC transformer was able to limit the number of tap changes in consecutive one-hour periods. In fact, only one tap change was necessary from one period to the other.

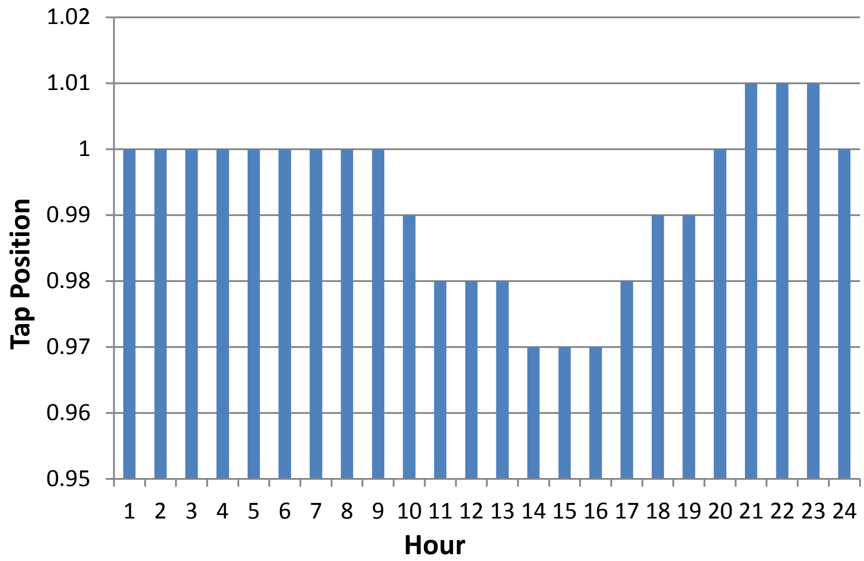

Figure 20 – Tap Position of the OLTC Transformer (Scenario 1)

In order to assess the performance of the optimization algorithm used for voltage control, the fitness function (shown in Figure 21) was used to illustrate the evolution of the best solution, *i.e.* to evaluate the convergence of the algorithm. As can be seen, the algorithm reached convergence (with the fitness function reaching 0, which means that, as previously stated, no load shedding or DG curtailment occurred) in less than 1000 iterations.

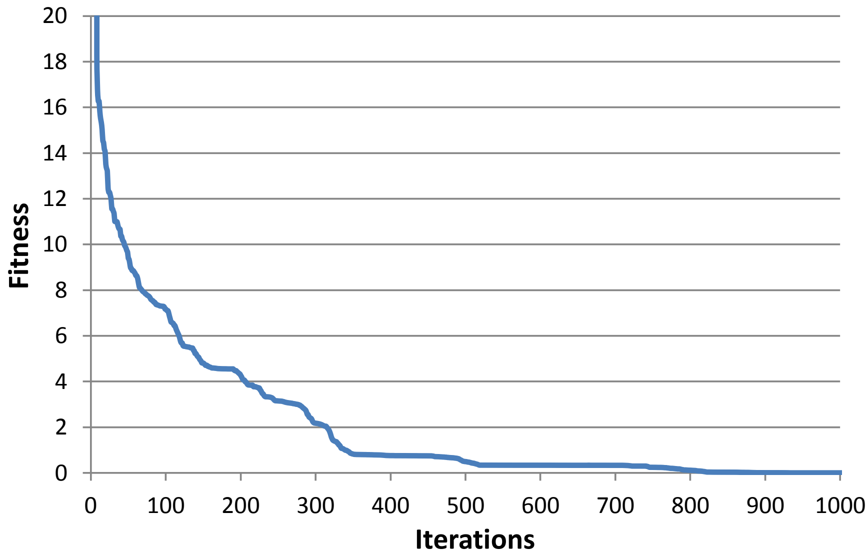

Figure 21 – Evolution of the Algorithm (Scenario 1)

3.1.4.1.2 Scenario 2 (Extreme DG Penetration)

This second scenario is characterized by an extreme integration of DG and a moderate consumption, which creates a situation with multiple voltage violations.

The profiles for load and DG for this scenario are shown in Figure 22.

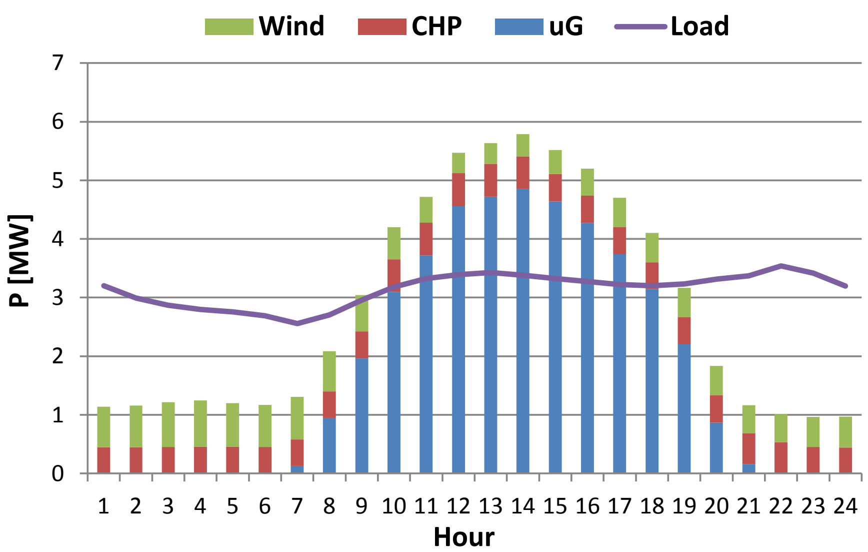

Figure 22 – Load and Generation for 24 hours (Scenario 2)

Figure 23 shows the maximum and minimum values for voltage for each hour of the day considering that no control actions are undertaken (base case), *i.e.* without running the optimization algorithm.

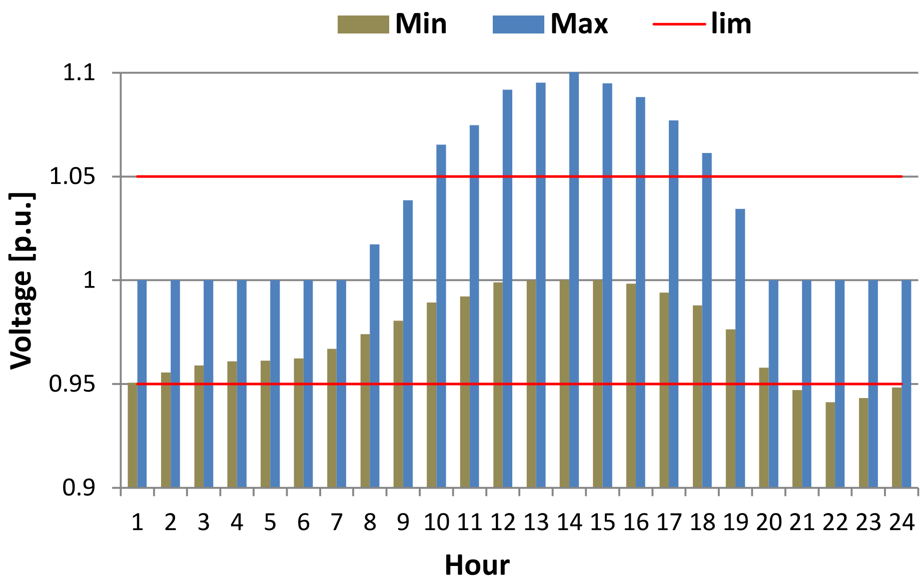

Figure 23 – Maximum and Minimum Voltage Values for 24 hours (Scenario 2)

As can be observed from Figure 23, without the voltage control algorithm, voltage values are outside the admissible range of ±5% (even reaching around 1.1 p.u.) due to large penetration of DG, especially PV-based µG.

Similarly to what happens in scenario 1, the PV units have their peak generation at 14:00, which is outside the hours of peak demand. Therefore, there is excess of generation in the MV that is exported to the HV network. This fact causes hard overvoltages around 14:00. On the other hand, around 21:00 (corresponding to the peak load hour), the amount of power provided by the DG units is smaller than the load, which causes undervoltages.

After running the optimization algorithm, all voltage violations were corrected as can be seen in the Figure 24 and Figure 25 (green bars).

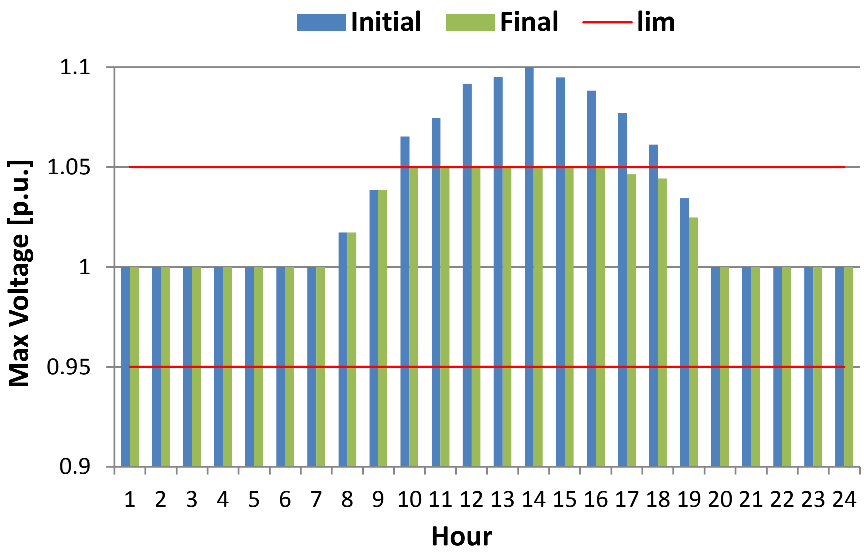

Figure 24 – Maximum Voltage Values for 24 hours (Scenario 2)

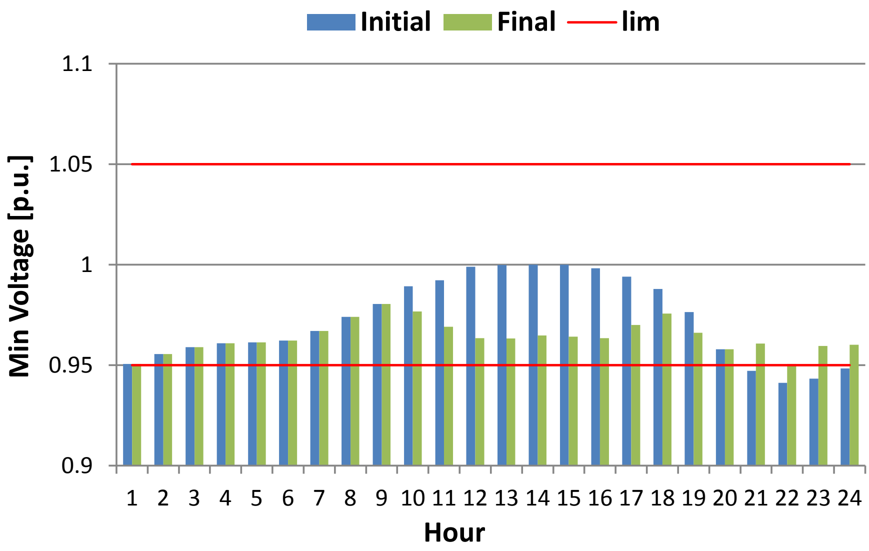

Figure 25 – Minimum Voltage Values for 24 hours (Scenario 2)

In order to ensure that the voltage values were brought inside admissible limits, the DER available were used, and the results for these control variables are shown below.

As in scenario 1, no load shedding was required in order to control the voltage profiles. Nevertheless, it was necessary to curtail some renewable generation in order to bring voltage values back inside admissible limits since here it was assumed that the CHP unit was unavailable for active power curtailment. In Figure 26, the generation curtailment that was required is shown. The worst hour is at 14:00, where there is a greater penetration of renewable generation that leads to the most extreme voltage deviations.

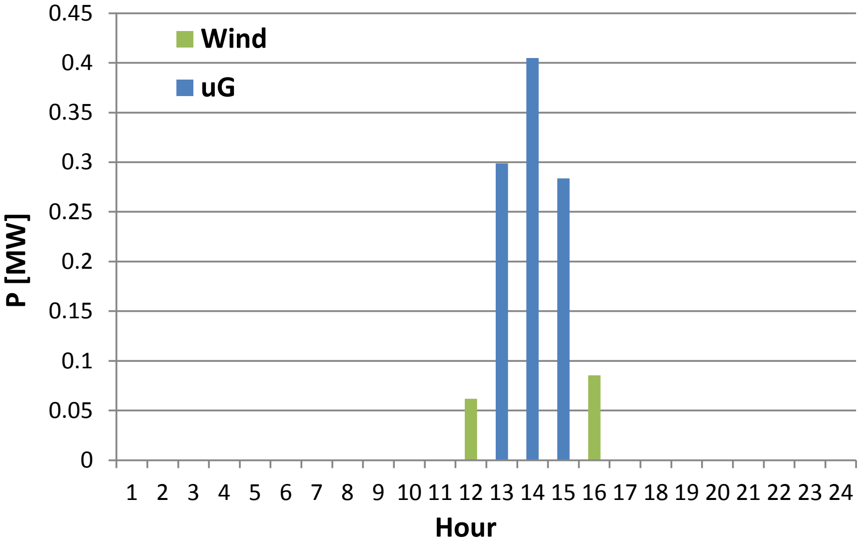

Figure 26 – Active Power Curtailment from DG (Scenario 2)

The contribution of other control variables such as the two batteries, shown in Figure 27, have an important role to voltage control by storing energy (negative values) at hours when there is excess DG and provide the stored energy (positive values) in peak load hours. In this case, the maximum SoC of the batteries is achieved during the day in order to avoid voltage violations.

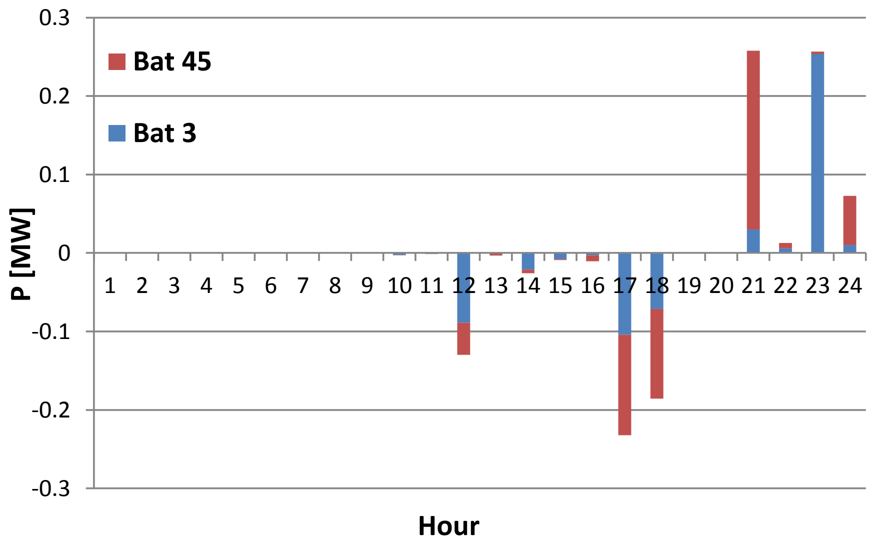

Figure 27 – Charging / Discharging of Batteries (Scenario 2)

Also, the reactive power by provided by the DG units (positive when injecting and negative when absorbing), shown in Figure 28, assists in the voltage control.

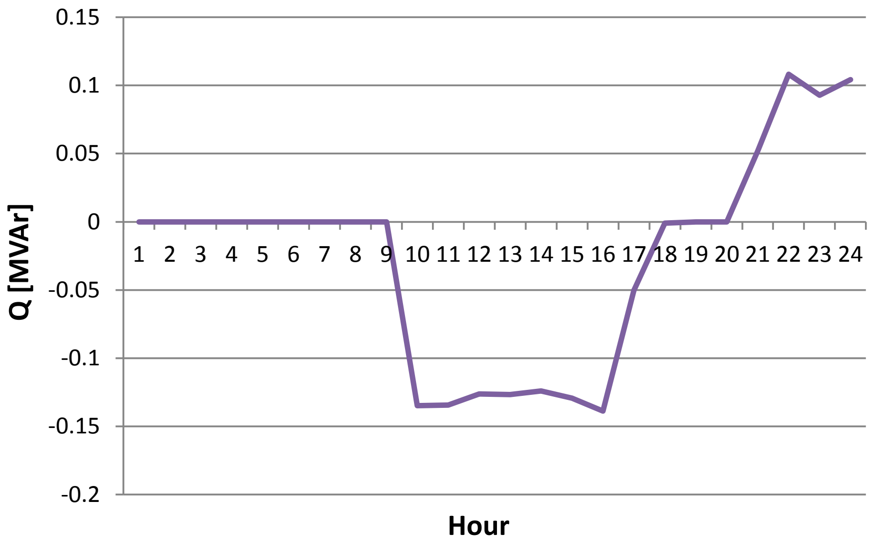

Figure 28 – Total Reactive Power provided by DG (Scenario 2)

In hours of peak load, the CBs have also contributed to increase the voltage in peak load as shown in Figure 29.

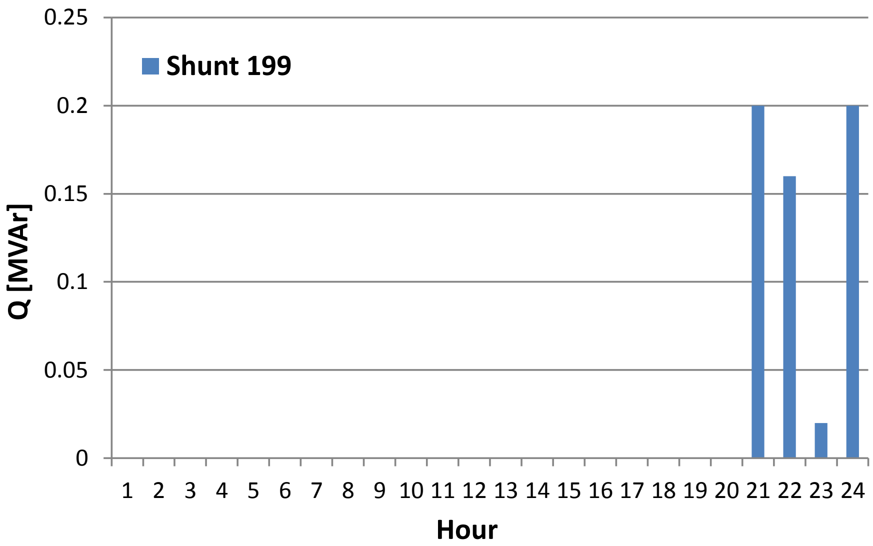

Figure 29 – Reactive Power provided by capacitor Bank (Scenario 2)

Similar to the scenario 1, the constraint used for limiting the number of switching actions of the OLTC transformer was able to limit the number of tap changes in consecutive one-hour periods. In fact, only one tap change was necessary from one period to the other. Figure 30 shows the tap values at the OLTC transformer.

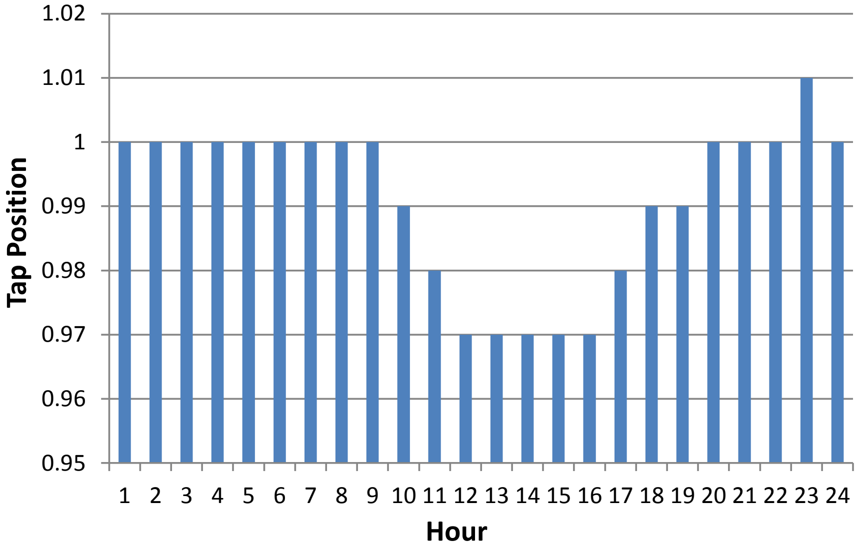

Figure 30 – Tap Position of the OLTC Transformer (Scenario 2)

Again, in order to assess the performance of the optimization algorithm used for voltage control, the fitness function (shown in Figure 31) to illustrate the evolution of the best solution, *i.e.* to evaluate the convergence of the algorithm.

In this scenario the algorithm converges not so quickly as in scenario 1 due to the magnitude of the voltage violations that required more control actions to be solved. Nevertheless, a good approximate solution is found in fewer than 4000 iterations. In this scenario, the fitness function stabilizes at a value of around 1.13, which corresponds only to the active power curtailment of DG meaning that all constraints have been satisfied.

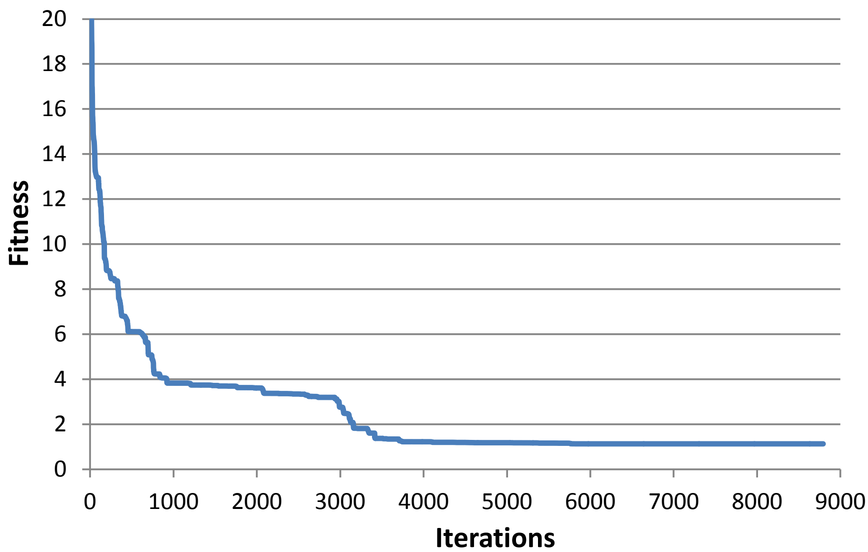

Figure 31 – Evolution of the Algorithm (Scenario 2)

3.1.4.2 Intraday (6 hours-ahead) Analysis

As previously explained, for the intraday analysis, a sliding window of 6 hours-ahead is computed for each hour. In order to show the performance of the algorithm in the intraday analysis, since no forecasting data is available, the data for the next week (same week day) was used corresponding to the date of June, 7th as provided by the Portuguese Transmission System Operator. The corresponding profile for both generation and load is presented in Figure 32.

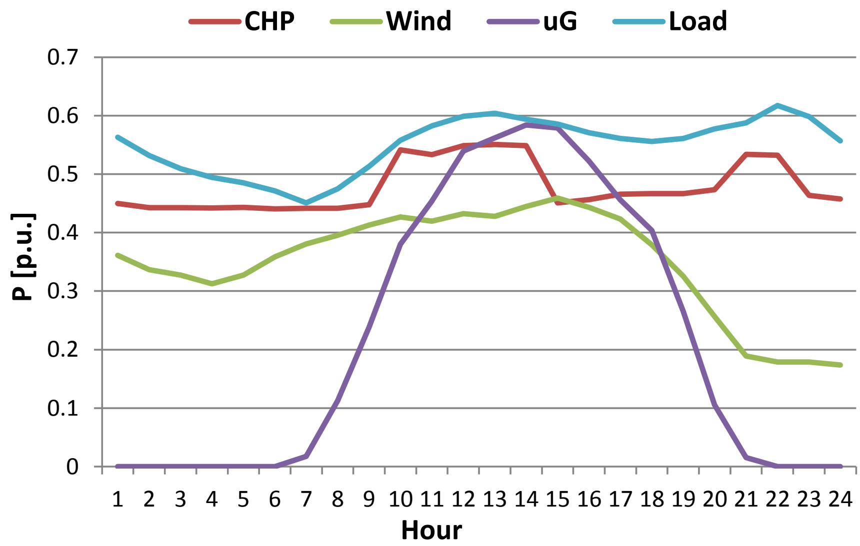

Figure 32 – Load and Generation Profiles used for Intraday Analysis

The comparison between the day-ahead analysis performed for the extreme scenario in Section 3.1.4.1.2 and intraday analysis is shown in Figure 33. It can be observed that in the intraday, more generation was available than anticipated in the day-ahead.

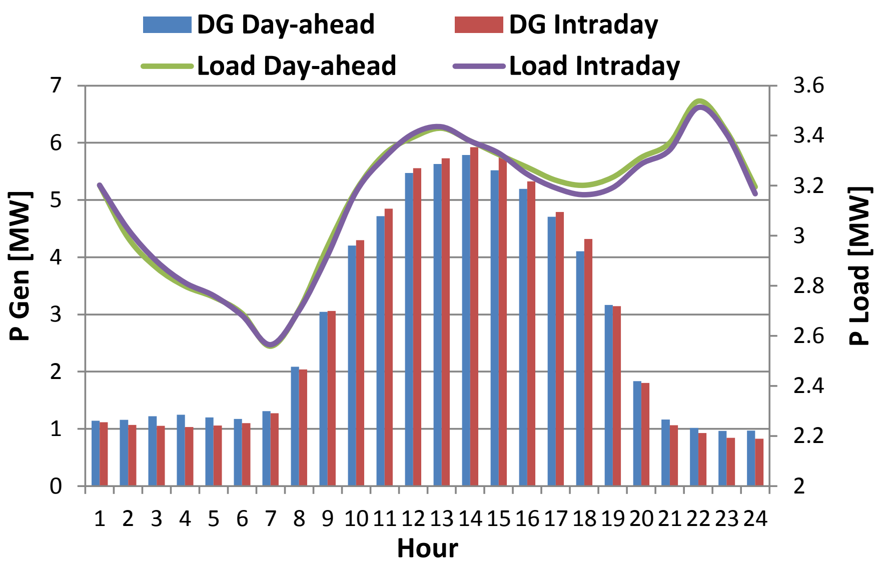

Figure 33 – Comparison of Load and Generation Scenarios for Day-ahead and Intraday Analyses

As a result, some voltage violations will occur that cannot be corrected using the plan defined in the day-ahead.

3.1.4.2.1 Sliding Window (9:00 – 14:00)

In this section, results are shown for a sliding window starting at 9:00 where the first voltage violation is identified at hour 14:00 in order to illustrate one run of the optimization process in the intraday. After running the optimization algorithm, the voltage violation at hour 14:00 was corrected as can be seen in Figure 34 (green bars).

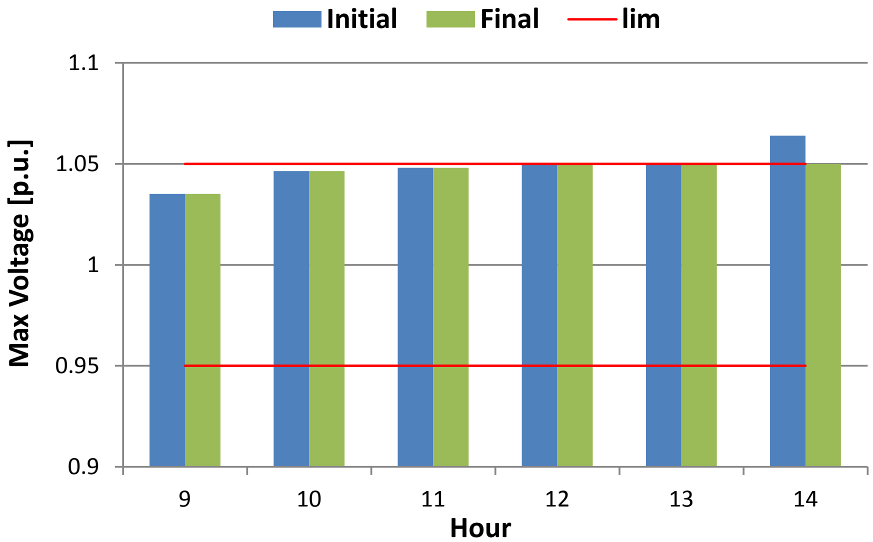

Figure 34 – Maximum Voltage Values (Sliding window from 9:00 to 14:00)

In order to ensure that the voltage values were brought inside admissible limits, the available resources such as batteries and the OLTC transformer are used while trying to minimize the deviations to the plan defined in the day-ahead. The results for these control variables are shown below. It is important to note that in this window for intraday optimization, no load shedding or DG curtailment was required in order to control the voltage profiles, unlike what happened in the day-ahead scenario for the same hours, as shown in Table 1.

Table 1 – DG Curtailment for Day-ahead and Intraday Analyses (Sliding window from 9:00 to 14:00)

Hour	DG Curtailment on Day D-1 [MW]	DG Curtailment on Day D [MW]
9:00	0.000	0.000
10:00	0.000	0.000
11:00	0.000	0.000
12:00	0.062	0.000
13:00	0.299	0.000
14:00	0.405	0.000

The contribution of the batteries for the time horizon under analysis takes into account their current SOC. Based on this consideration, the decision of the amount of energy stored at hour 13:00 and 14:00 is significantly higher in the intraday than in the day-ahead analysis, as shown in Table 2. However, this decision may suffer some slight changes when the algorithm is run around the operating hour (*i.e.*, closer to hour 13:00) since the forecasts may also change.

Table 2 – Power Absorbed by Batteries for Day-ahead and Intraday Analyses (Sliding window from 9:00 to 14:00)

Hour	Power Absorbed on Day D-1 [MW]	Power Absorbed on Day D [MW]
9:00	0.000	0.000
10:00	-0.003	-0.003
11:00	-0.001	-0.001
12:00	-0.130	-0.130
13:00	-0.003	-0.212
14:00	-0.026	-0.135

The contribution of the reactive power provided by the DG units has no major changes relatively to the day-ahead (D-1) analysis, as shown in Figure 35. As it can be seen, at hour 9:00 there is no reactive power injection / absorption, which can be explained by the fact that there is no voltage violation at this hour and the total load and generation are almost identical.

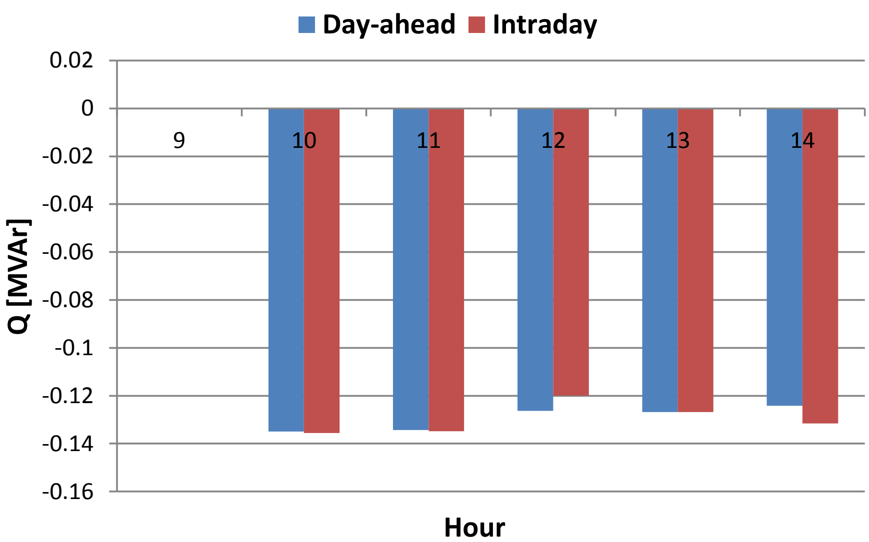

Figure 35 – Comparison of Total Reactive Power provided by DG for Day-ahead and Intraday Analyses (Sliding window from 9:00 to 14:00)

As can be observed in Figure 36, the OLTC transformer changed one tap position at hour 14:00 from the D-1, which was enough to bring voltage values back inside admissible limits.

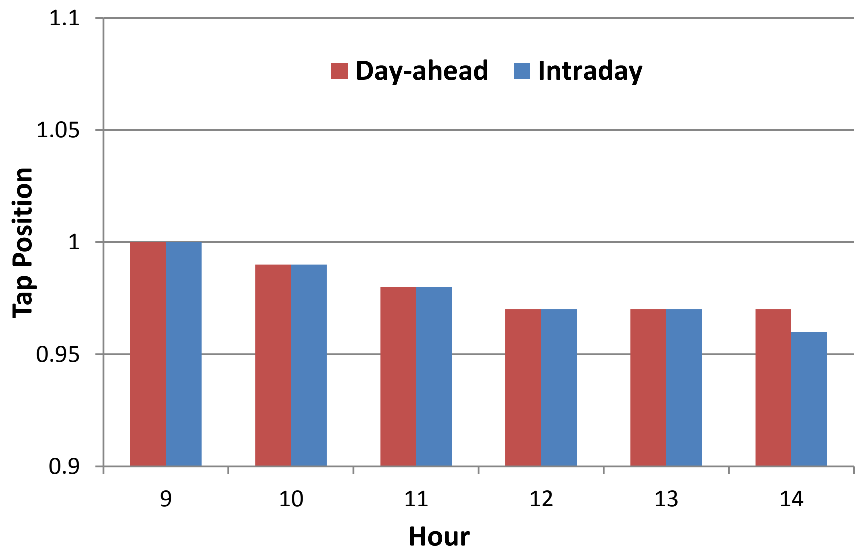

Figure 36 – Comparison of Tap Positions of the OLTC Transformer for Day-ahead and Intraday Analyses (Sliding window from 9:00 to 14:00)

3.1.4.2.2 Whole Day

This section presents the results for all operational hours, *i.e.* with the sliding window being run each hour for the whole day. The results for the most relevant optimization variables are presented below by comparing the day-ahead and intraday analyses.

As it occurred in the optimization for day-ahead scenario, no load shedding was required in order to control the voltage profiles and all voltage values were brought inside admissible limits using the control variables, namely the available DER available, batteries, CBs and the OLTC transformer. In Figure 37 it can be observed that generation curtailment is required around the hours with higher RES generation, which correspond to the most severe cases of overvoltages.

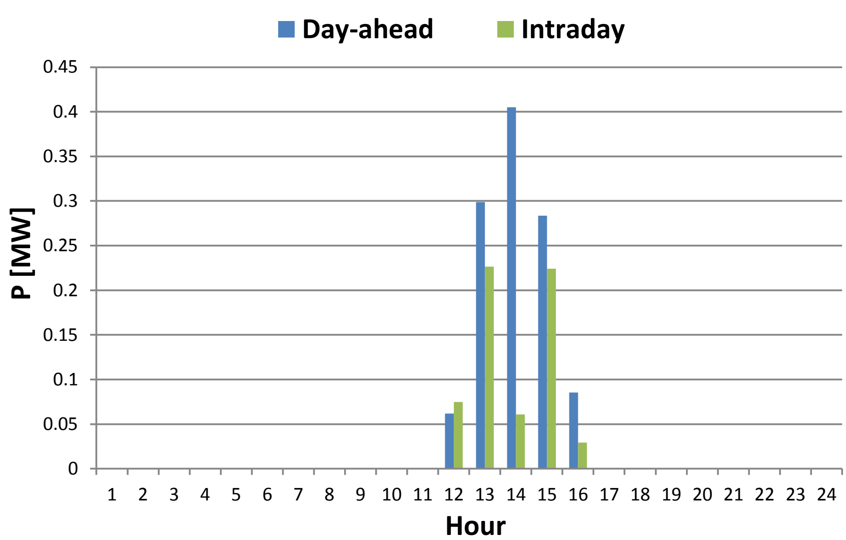

Figure 37 – Comparison of DG Curtailment for Day-ahead and Intraday Analyses (Whole day)

Compared to the day-ahead scenario, in the intraday it was possible to reduce the amount of DG to be curtailed, except for hour 12:00.

Regarding the contribution of the other control variables, such as the batteries, there are no major changes relative to the day-ahead (D-1), as shown in Figure 38.

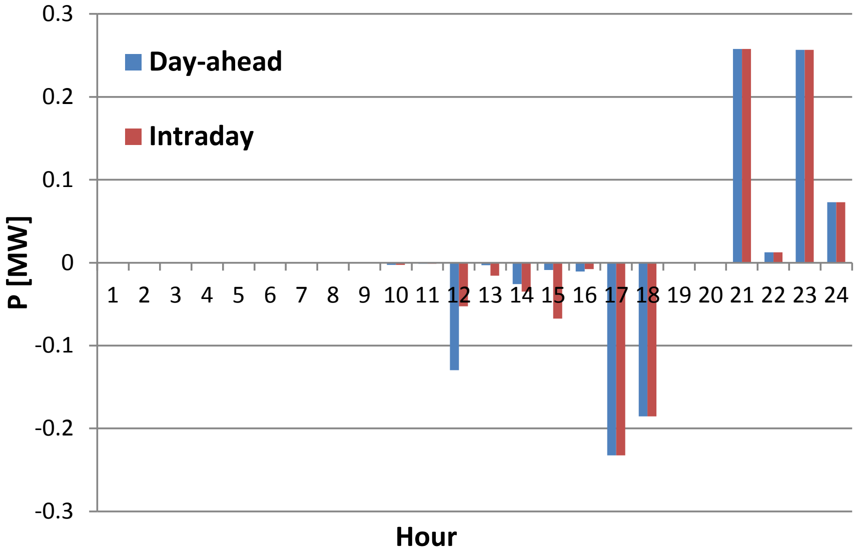

Figure 38 – Comparison of Power Absorbed by Batteries for Day-ahead and Intraday Analyses (Whole day)

The reactive power profile ensured by the DG units was also similar to the day-ahead (D-1). The main differences are the hours 1:00 and 22:00 that correspond to undervoltage situations.

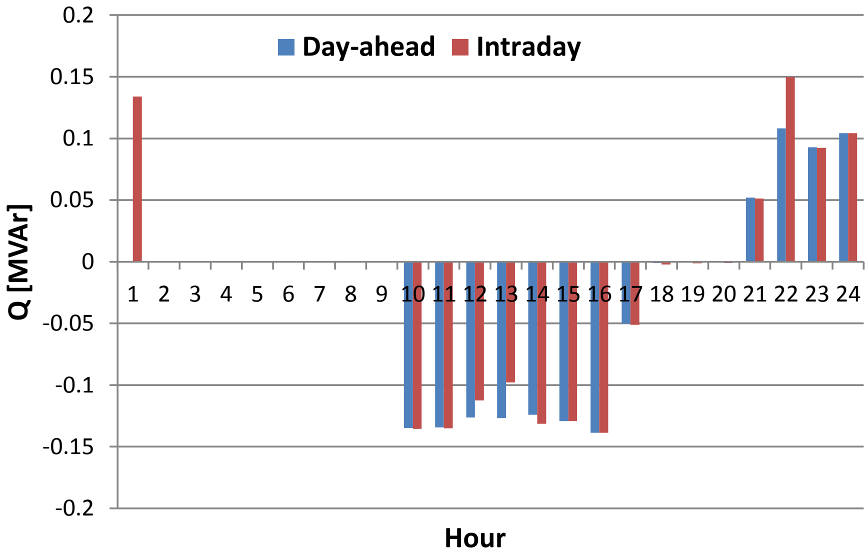

Figure 39 – Comparison of Total Reactive Power provided by DG for Day-ahead and Intraday Analyses (Whole day)

The same happens for the CBs, which contribute to increase the voltage in hour 22:00, as shown in Figure 40.

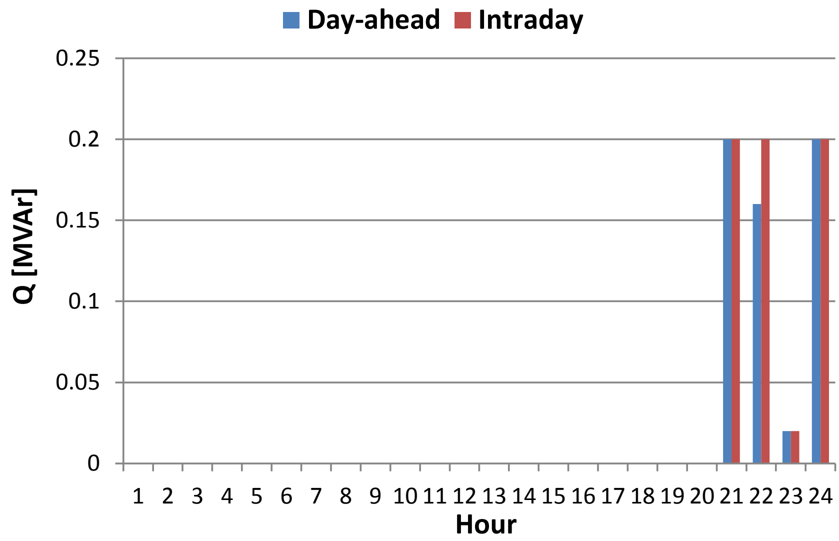

Figure 40 – Comparison of Reactive Power provided by the Capacitor Bank (in Bus 199) for Day-ahead and Intraday Analyses

The OLTC transformer has a similar behaviour to the day-ahead, with the only difference being the decrease of one position tap at hour 14:00 (comparing to the D-1), as can be observed in Figure 41, which contributes to bring voltage values back inside admissible limits at that hour and reduce the amount of DG to be curtailed (as shown in Figure 37).

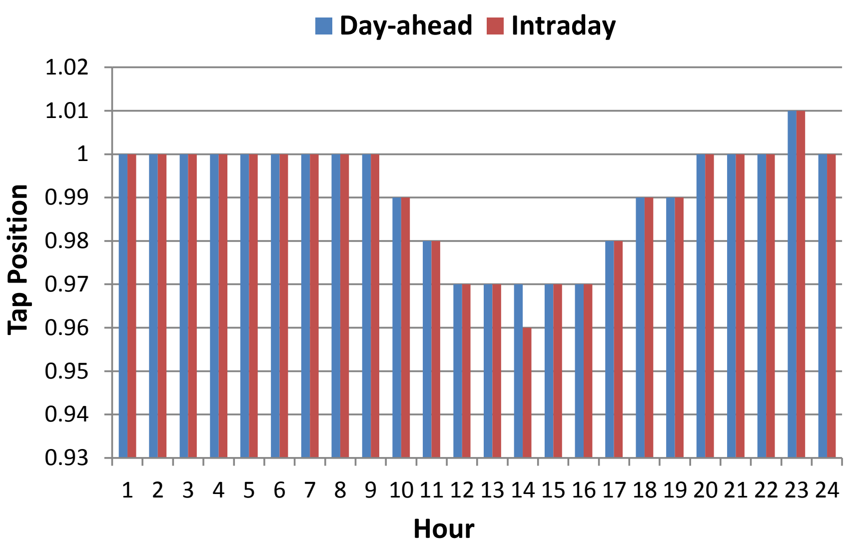

Figure 41 – Comparison of Tap Positions of the OLTC Transformer for Day-ahead and Intraday Analyses

3.2 Multi-objective Formulation

The primary objective of coordinated voltage control is to maintain the voltage at every node of a MV network within the permitted voltage limits. Since voltage is one of the most important technical constraints for the integration of RES, coordinated voltage control contributes also to increasing DER hosting capacity. Additional targets are also incorporated in the overall optimization problem, including the reduction of losses, RES energy curtailments, tap operations and wear, *etc.*

To this end, available control variables include the active and reactive output power of all DER units, the HV transformer OLTC, line voltage regulators and switchable capacitors. Storage is also incorporated in the algorithm.

The large number of variables and constraints leads to a hard optimization problem, in order to optimize the operating schedule over an adjustable look-ahead horizon, which may be either the following day (day-ahead scheduling) or the next n hours (intraday dispatch).

Application of the optimal voltage control module necessarily relies on other functionalities, such as short-term load and RES forecasting, developed within the project.

3.2.1 Analysis of the Coordinated Control Algorithm

3.2.1.1 Description of the Module

Advanced coordinated voltage control, which is one of the main functionalities to be developed within SuSTAINABLE project, plays a crucial role in controlling the MV network, taking advantage of the capabilities offered by other functionalities under development in the project. The developed tool approaches the issue of network optimal operation principally from a DSO perspective, taking however into account the impact on DG station operation.

The algorithm takes into consideration all network devices and systems that contribute to voltage regulation. The operation of certain of them (*e.g.* storage systems) is time dependent, which means that the optimization problem becomes dynamic, as operation during any hour is related to the previous and following intervals. For this purpose, the approach is to determine an optimal dispatch schedule over a suitable time period, rather than for a single dispatch period. A reasonable dispatch horizon would be one day ahead, while shorter intervals are also possible, *i.e.* intraday execution of the algorithm at a time closer to operation (*e.g.* every 6 hours within a 24h time period), using improved short-term forecasts and accounting for actual network conditions.

The module aims at minimizing a multi-objective function, incorporating different optimization targets, while constraints describe the available range of variation of control variables or the operating requirements and restrictions set by the DSO.

The algorithm uses a standard simplified distribution power flow solver, where non-linear terms (especially second order ones) are neglected. This simplifies drastically the optimization problem, avoiding the need to deal with a tough non-linear and non-convex problem. In this way, the complexity is reduced, along with the calculation burden, without sacrificing accuracy, rendering thus the algorithm suitable for more realistic distribution networks, including a multitude of controllable devices.

The whole algorithm has been written in MATLAB environment where the required data and parameters are given as inputs. In this algorithm there is a connection with the IBM CPLEX Optimizer which takes the necessary inputs as matrixes that describe the objective function, the bounds and the quadratic and linear constraints having been created within the MATLAB code. After finding the optimal solution for a-day-ahead IBM CPLEX Optimizer returns it in the MATLAB code. Then, the algorithm continues in order to find the corresponding voltages, power losses, *etc.* The method for solving the optimization problem is based exclusively on the IBM CPLEX Optimizer using some external parameters so as to make the algorithm more efficient and less time consuming.

3.2.1.2 Implementation of the Algorithm

3.2.1.2.1 Objectives of Optimal Control

The objective function is composed of technical quantities significant for network and DG operation, which are combined in a multi-objective function, using suitable normalization and weighting factors, while no direct financial cost is used in the objective function. Certain optimization objectives may be contradictory to others, making the algorithm tougher to converge. In the following, the optimization objectives are further described:

- **Voltage deviations**
  The square summation of the deviation of node voltages from nominal, at every node of the MV network and every hour of the dispatch period (24-hours).

- **Energy losses**
  The sum of active power losses on all branches of the network, including the HV/MV transformer, over the dispatch period (24-hours).

- **DG active power curtailments**
  The sum of active power curtailments of all DG units connected to the network, over the dispatch period (24-hours). Curtailing DG active power, especially in the case of small units, is a last resort means to be exploited by the DSO for voltage regulation purposes.

- **Daily OLTC and SVR operations**
  Total number of tap changes over the dispatch period (24-hours). A large number of daily operations has an impact on maintenance and wear of OLTC (*e.g.* contacts and oil carbonisation). It is not unusual for DSOs to increase the dead-band or

lower the gradient of the voltage regulator relay I-V characteristic, so as to reduce the number of daily tap operations.

- **Daily SC switchings**
  Number of bank switching operations over the dispatch period (24-hours). As for OLTCs, SC switchings also affect maintenance and life expectancy of components.

- **Reactive power injection/absorption by DG**
  Square summation of reactive output power of all DG connected to the network over the dispatch period (24-hours).
  Reactive power generation or absorption is not desirable from the viewpoint of the DG operator, as it increases losses on the DG station components and at the same time utilizes part of the units' apparent power capabilities, reducing in principle the active power generation margin or necessitating a potential oversizing of equipment. From the network viewpoint, reactive power may contribute to voltage regulation, however its circulation increases losses on the feeders and may affect negatively the overall feeder or substation power factor.

- **Reactive power through the HV/MV transformer**
  Square summation of reactive power flows through the HV/MV transformer over the dispatch time period (24-hours).
  A lower reactive power on the HV/MV transformer signifies reduced losses, less reactive power compensation needs and a higher substation power factor, with all related benefits from the viewpoint of the upstream transmission system.

3.2.1.2.2 Control Variables – Outputs

Control variables include all quantities that may be controlled by the DSO in order to achieve the optimization objectives set, as enumerated in Table 3. Every variable constitutes a vector of 24 elements, each corresponding to one dispatch period (hour of the day). Variables can be time-dependent, discrete or continuous, which strongly affects the kind of the optimization problem to be solved.

Table 3 – Controllable Devices and Control Variables

	Controllable device	Variable
1	OLTC	Tap position
2	DG	Reactive output power
		Active power curtailment
3	Storage systems	Active output power
		Reactive output power
4	SC	Capacitor status
5	SVR	Tap position

3.2.1.2.3 Constraints

The constraints included in the algorithm along with a short description are presented below.

- Load flow equations.
- Voltage limits: The voltage at every node at every hour should lie within a specific range.
- Thermal limit of the feeder: The current of every branch should not exceed the respective thermal limit.
- OLTC and SVR tap limits: Available max/min tap positions.
- DG operating capability curve: Active and reactive output power should comply with the capability curve of the unit, incorporating constraints related to its current rating, max active power, pf regulation limit and other possible restrictions (*e.g.* excitation limits in case of synchronous machines).
- Active power curtailment limits: The hourly energy curtailments should not exceed a predefined maximum.
- Capacity and SOC limits of storage: The stored energy of every storage device should remain within the respective acceptable range.
- Storage operating constraints: Boundary conditions may be included in the optimization problem through appropriate constraints for the storage systems.
- Storage operating capability curve: Similar as for DG above.

3.2.2 Mathematical Formulation

A multi-objective optimization problem can be generally formulated as:

$$\begin{aligned} &\text{minimize} && f(x) \\ &s.t. && g(x)\leq 0 \\ & && h(x)=0 \end{aligned} \qquad (3.22)$$

The optimization problem addressed here is a convex Mixed Integer Quadratically Constrained Quadratic problem (MIQCQP), which can be analytically expressed as:

$$\begin{aligned} &\text{minimize} && \frac{1}{2} * x^T * H * x + f * x \\ &s.t. && Aineq * x \leq bineq \\ & && Aeq * x = beq \\ & && x^T * Q * x + l * x \leq r \\ & && lb \leq x \leq ub \end{aligned} \qquad (3.23)$$

The objective function to be minimized is the following:

$$\text{minimize } \sum_{t=1}^{24}\left(\sum_{k=1}^{8} w_k J_k\right) \tag{3.24}$$

Where

$$J_1 = \theta_1 \sum_{i=1}^{N_b} (V_{it} - V_n)^2 \text{ : Voltage deviation from nominal} \tag{3.25}$$

$$J_2 = \theta_2 \left(\sum_{i=1}^{N_b} P_{loss\_it} + P_{loss\_HV/MV\_t}\right)\text{: Losses} \tag{3.26}$$

$$J_3 = \theta_3 \sum_{i=1}^{N_g} P_{curt\_it} \text{ : DG active power curtailment} \tag{3.27}$$

$$J_4 = \theta_4 \left|Tap_{t+1} - Tap_t\right| \text{, t<24: Daily OLTC operations} \tag{3.28}$$

$$J_5 = \theta_5 \left|Cap_{t+1} - Cap_t\right| \text{, t<24: Daily SC switchings} \tag{3.29}$$

$$J_6 = \theta_6 \sum_{i=1}^{N_g} Q_{g\_it}^2 \text{ : DG reactive output power} \tag{3.30}$$

$$J_7 = \theta_7 Q_{tr\_t}^2 \text{: HV/MV transformer reactive power flow} \tag{3.31}$$

$$J_8 = \theta_8 \left|Tap_{SVR\_t+1} - Tap_{SVR\_t}\right| \text{, t<24: Daily SVR operations} \tag{3.32}$$

$$\sum_{k=1}^{8} w_k = 1 \tag{3.33}$$

w_k ≥0 weighting coefficients
θ_k normalization factors

Vector $\mathbf{x}^T$ includes the control variables:

$$\mathbf{x}^T = \left[\text{Tap, } \text{Q}_\text{g}\text{, } \text{P}_\text{curt}\text{, } \text{P}_\text{stor}\text{, } \text{Q}_\text{stor}\text{, Cap, } \text{Tap}_{SVR}\right] \tag{3.34}$$

Where

$$\mathbf{Tap} = \left[Tap_1, \ldots, Tap_{24} \right] \quad (3.35)$$

$$\mathbf{Q_g} = \underbrace{\left[Q_{g1,1}, \ldots, Q_{g1,24}, \ldots, Q_{gN_g,1}, \ldots, Q_{gN_g,24} \right]}_{24*N_g \text{ variables}} \quad (3.36)$$

$$\mathbf{P_{curt}} = \underbrace{\left[P_{curt1,1}, \ldots, P_{curt1,24}, \ldots, P_{curtN_g,1}, \ldots, P_{curtN_g,24} \right]}_{24*N_g \text{ variables}} \quad (3.37)$$

$$\mathbf{P_{stor}} = \underbrace{\left[P_{stor1,1}, \ldots, P_{stor1,24}, \ldots, P_{storN_{stor},1}, \ldots, P_{storN_{stor},24} \right]}_{24*N_{stor} \text{ variables}} \quad (3.38)$$

$$\mathbf{Q_{stor}} = \underbrace{\left[Q_{stor1,1}, \ldots, Q_{stor1,24}, \ldots, Q_{storN_{stor},1}, \ldots, Q_{storN_{stor},24} \right]}_{24*N_{stor} \text{ variables}} \quad (3.39)$$

$$\mathbf{Cap} = \left[Cap_1, \ldots, Cap_{24} \right] \quad (3.40)$$

$$\mathbf{Tap_{SVR}} = \underbrace{\left[Tap_{SVR1,1}, \ldots, Tap_{SVR1,24}, \ldots, Tap_{SVRN_{SVR},1}, \ldots, Tap_{SVRN_{SVR},24} \right]}_{24*N_{SVR} \text{ variables}} \quad (3.41)$$

The constraints of the problem are described in the following equality and inequality constraints:

Inequality constraints

$$V_{\min} = (1-a)V_n \le V_{it} \le (1+a)V = V_{\max} \quad \forall\ i \in \{1 \ldots N_b\} : \text{Voltage limits} \quad (3.42)$$

$$Tap_{\min} \le Tap_t \le Tap_{\max} : \text{OLTC tap limits} \quad (3.43)$$

$$Tap_{SVR\_\min} \le Tap_{it} \le Tap_{SVR\_\max} \quad \forall\ i \in \{1 \ldots N_{SVR}\} : \text{SVR tap limits} \quad (3.44)$$

$$0 \le Cap_t \le 1 : \text{SC status} \quad (3.45)$$

$$I_{it} \le I_{thermal} \qquad \forall\ i \in \{1 \ldots N_b\} : \text{Thermal limit of feeder} \quad (3.46)$$

$$0 \le P_{g\_it} \le P_{g\_i}^{\max} \qquad \forall\ i \in \{1 \ldots N_g\} : \text{DG active power limits} \quad (3.47)$$

$$\sqrt{P_{g\_it}^2 + Q_{g\_it}^2} \le S_{n\_i} \quad \forall \text{ i } \in \{1 \ldots N_g\} : \text{DG apparent power limits} \tag{3.48}$$

$$Q_{g\_i}^{\min} \le Q_{g\_it} \le Q_{g\_i}^{\max} \quad \forall \text{ i } \in \{1 \ldots N_g\} : \text{DG reactive power limits} \tag{3.49}$$

$$PF_i^{\min} \le PF_{it} \le PF_i^{\max} \quad \forall \text{ i } \in \{1 \ldots N_g\} : \text{DG power factor limits} \tag{3.50}$$

$$0 \le P_{curt\_it} \le bP_{g\_it} \quad \forall \text{ i } \in \{1 \ldots N_g\} : \text{DG power curtailment limits} \tag{3.51}$$

where b is the maximum permissible DER power curtailment ratio

$$-P_{stor\_i}^n \le P_{stor\_it} \le P_{stor\_i}^n \quad \forall \text{i } \in \{1 \ldots N_{stor}\} : \text{Active power limits of storage} \tag{3.52}$$

$$Q_{stor\_i}^{\min} \le Q_{stor\_it} \le Q_{stor\_i}^{\max} \quad \forall \text{ i } \in \{1 \ldots N_{stor}\} : \text{Reactive power limits of storage} \tag{3.53}$$

$$SOC_{\text{i}}^{\min} \le SOC_{it} \le SOC_i^{\max} \quad \forall \text{ i } \in \{1 \ldots N_{stor}\} : \text{Storage capacity limits} \tag{3.54}$$

Equality constraints

$$P_{j+1} = P_j - p_{j+1}^l + p_{j+1}^g - p_{curt\_j+1}^g \pm p_{j+1}^{stor} : \text{Active power flow} \tag{3.55}$$

$$Q_{j+1} = Q_j - q_{j+1}^l \pm q_{j+1}^g \pm q_{j+1}^{stor} + q^c : \text{Reactive power flow} \tag{3.56}$$

$$SOC_{i,24} = SOC_{i,1} = SOC_i^{boundary} \quad \forall \text{ i } \in \{1 \ldots N_{stor}\} : \text{Boundary conditions of storage} \tag{3.57}$$

$$SOC_{it} = (1-\delta)SOC_{i,t-1} - n_c P_{stor\_i} \Delta t / E_{stor\_i}^{nominal} \quad \forall \text{ i } \in \{1 \ldots N_{stor}\} : \text{Charging operation constraint} \tag{3.58}$$

where δ is the self-discharge rate of storage

$$SOC_{it} = (1-\delta)SOC_{i,t-1} - P_{stor\_i} \Delta t / (n_d E_{stor\_i}^{nominal}) \quad \forall \text{ i } \in \{1 \ldots N_{stor}\} : \text{Discharging operation constraint} \tag{3.59}$$

3.2.3 Application Results

The functionality of the coordinated control algorithm was tested on a small scale demo network characterized by high DG penetration using as a reference an optimal control scenario. The full proof-of-concept validation will be performed in WP5.

The reference optimal control scenario makes use of the following indicative weighting factors for the components of the multi-objective function:

- Voltage deviation from nominal: $\omega_{dv} = 0.35$
- Power losses: $\omega_{Ploss} = 0.25$
- DG active power curtailments: $\omega_{Pcurt} = 0.2$
- Daily OLTC operations: $\omega_{tap} = 0.1$
- Daily SC switchings: $\omega_{bank\_feeder} = 0$
- Reactive power generation by DG: $\omega_{Qg} = 0.05$
- Reactive power flow through the HV/MV transformer: $\omega_{Qms} = 0.05$

In order to have a benchmark to assess the results obtained via the optimal control policy, conventional voltage regulation (current practice) was also implemented on the same network, based on OLTC operation via a Line Drop Compensation characteristic. This current regulation approach does not include any other sophisticated functionality, such as DER reactive power control, active power curtailments, nor does the network include storage. In addition, a parametric investigation concerning the formulation of the objective function was carried out, results of which are provided in this section.

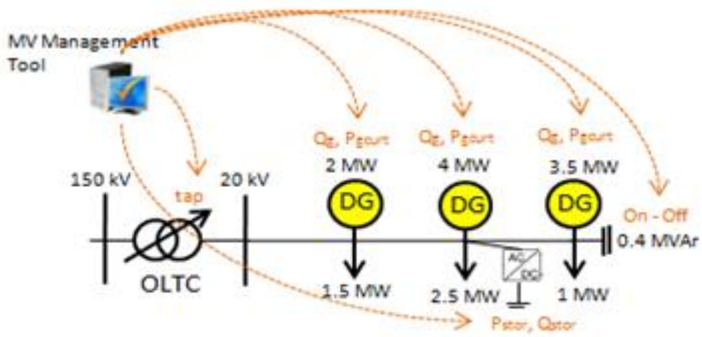

Figure 42 – Proposed Approach for the Voltage Control at the MV Level

The study-case demo network is depicted in Figure 42. Its main characteristics are the following:

- HV/MV transformer: 25MVA, u = 20% (short-circuit voltage), 150/20 kV – OLTC (17 available tap positions)
- Feeder 20 kV: 30 km, ACSR 95mm^2 (R = 0.215 Ω/km, X = 0.334 Ω/km)
- 3 nodes (one per 10 km)
    - Loads per node: 1.5 - 2.5 - 1 MW
    - PV plants per node: 2 - 4 - 3.5 MWp
- Shunt capacitors 400 kVAr installed at 3rd node
- Centralized storage system at node 2: 1 MW, 5 MWh

Typical load and PV daily profiles are used, as presented in Figure 43.

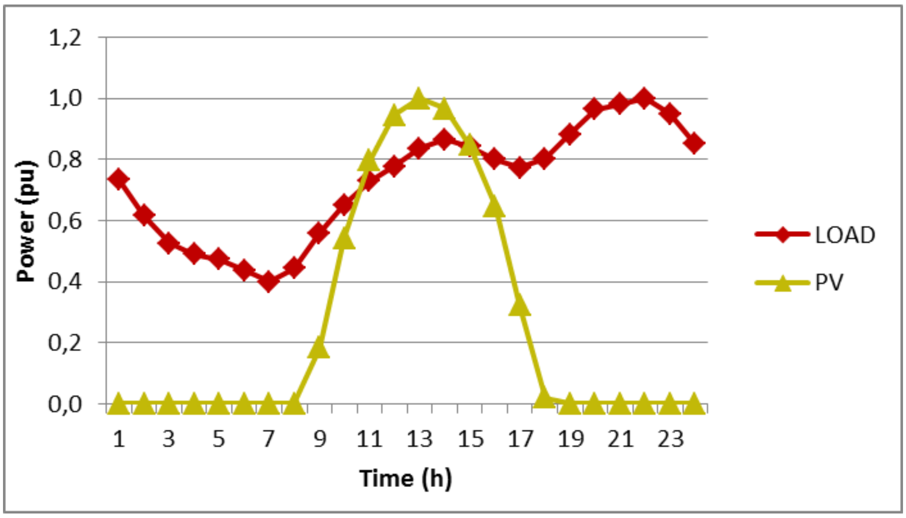

Figure 43 – Hourly Load and PV Generation Curves

A demonstration of the potential benefits is presented comparing the results of optimal control with current practice.

3.2.3.1 Improvement in Voltage Regulation

The coordinated voltage control leads to significantly better voltage profile than the conventional voltage regulation policy both along the feeder and over a whole day (Figure 44, Figure 45 – a and b). In Figure 44 the voltage profile along the length of the feeder is shown, at different hours of the day (lines with different colours), adopting either the standard regulation practice or optimal control with two different weights on voltage deviations. In Figure 45 the same results are plotted against the time in the day for each of the 4 network nodes (different coloured lines for the MV bus bars and the 3 nodes along the feeder). With the current practice, there are hours when the voltage remains very close to the upper permitted voltage limit (red dashed horizontal line) especially at the end of the feeder, but also at the beginning due to the OLTC action. Implementing optimal control, the voltage remains much closer to nominal, while voltage variation at any given node at different hours of the day is also considerably reduced, facilitating thus the selection of the fixed tap ratio for the MV/LV distribution transformers and voltage regulation in the subordinate LV networks. Voltage deviation along the length of the feeder at any given hour is also reduced. Such improvements regarding voltage control become more prominent as a higher weighting factor is applied for voltage deviation in the objective function, albeit at the expense of other optimization objectives.

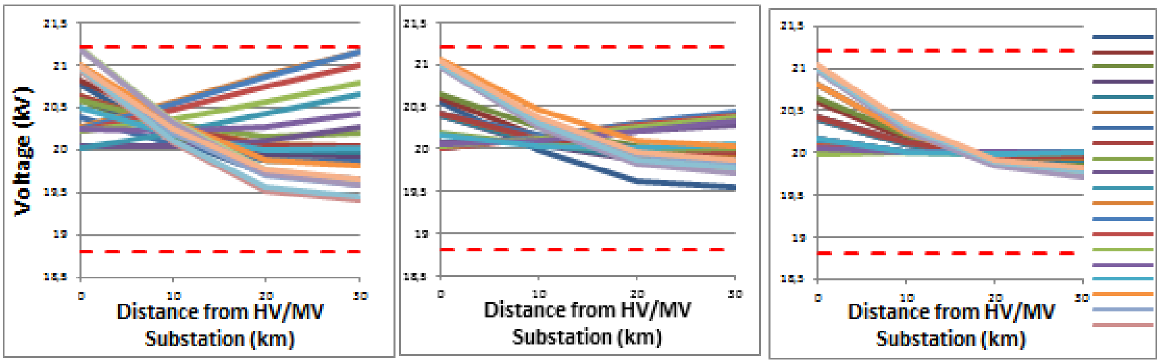

a. Current Practice **b. Optimal control (w_{dv} = 0.35)** **c. Optimal control (w_{dv} = 1)**

Figure 44 – Voltage Profile along the Feeder for each Hour of a Day

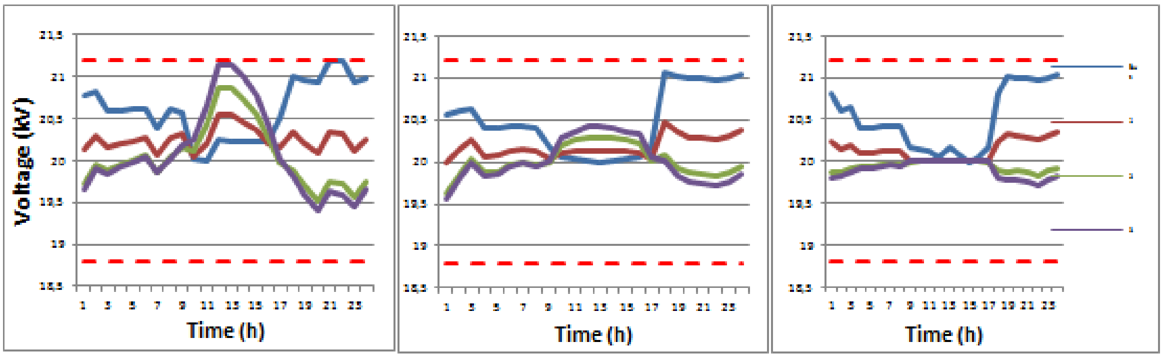

a. Current Practice **b. Optimal control (w_{dv} = 0.35)** **c. Optimal control (w_{dv} = 1)**

Figure 45 – Daily Voltage Variation for each of the 3 Nodes of the Feeder

3.2.3.2 Improvement in Energy Losses

In optimal control scenario, a reduction of losses by 34% is achieved compared to current operation. This can be further improved if losses are more heavily weighted in the objective function (Figure 46), although at the expense of higher operating voltages.

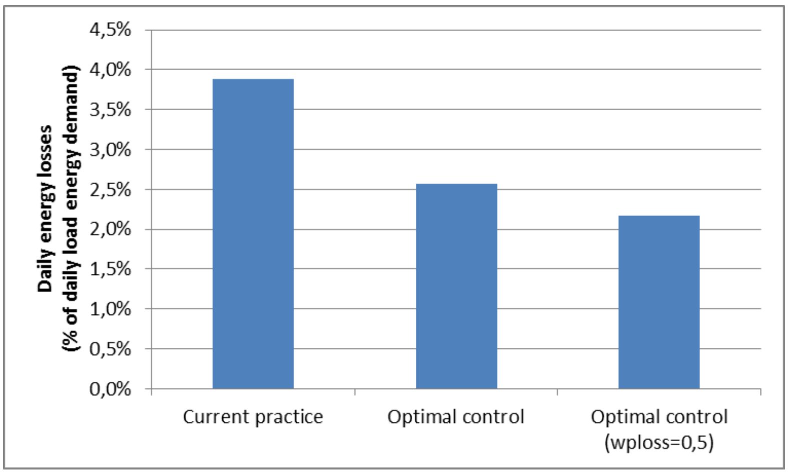

Figure 46 – Daily Losses, in % of the Daily Load Energy Demand

3.2.3.3 Improvement in Curtailed Distributed Generation Energy

DG curtailments may be imposed by the algorithm in order to manage congestion or improve voltage regulation, eventually leading to increased DG hosting capacity. Since the assumed current operating practice scenario does not impose such curtailments, a comparison is presented below adopting different weighting factors in the objective function It is clear that the higher the weight, the lower the curtailed energy (Figure 47).

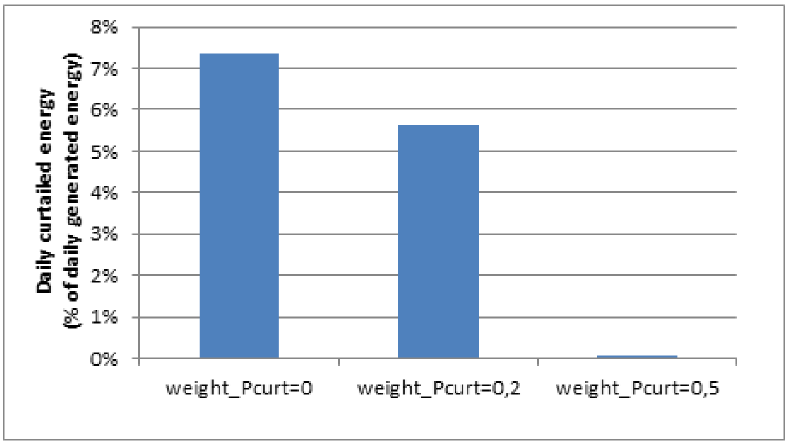

Figure 47 – Curtailed DG Energy, in % of Available Energy

3.2.3.4 Improvement in Daily On-Load Tap Changer Operations

Coordinated voltage control may decrease substantially the number of tap operations, by more than 60%, as shown in Figure 48, managing at the same time to improve voltage regulation over the entire network.

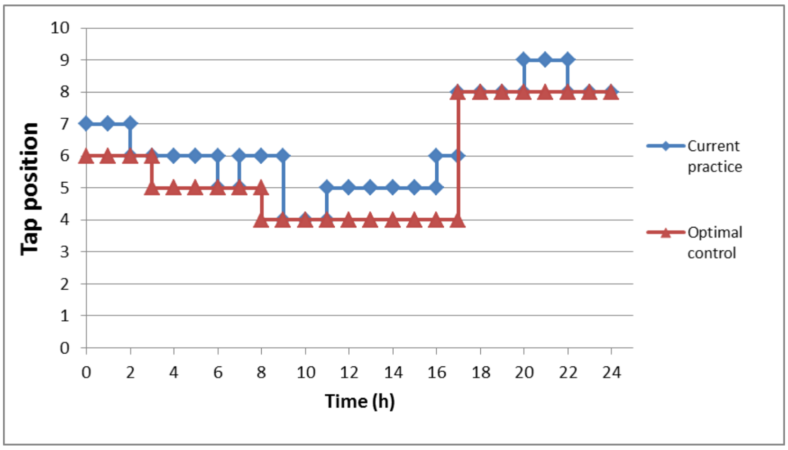

Figure 48 – Tap Position Variations over a Day

3.2.3.5 Reactive Power from Distributed Generation

The amount of generated or absorbed reactive energy by all DGs over the scheduling period can be controlled using different weighting factors (for relatively low factors there can be a differentiation higher than 50%), leading thus the DG units to contribute to network regulation at different degrees. Of course, reducing the exploitation of the reactive power regulation capabilities of DG units affects the overall effectiveness of the control.

3.2.3.6 Reactive Power Flow through the HV/MV Transformer

Applying optimal control, the reactive power flowing through the HV/MV transformer to and from the upstream transmission network may decrease by more than 30% in comparison to the current operating policy (Figure 49).

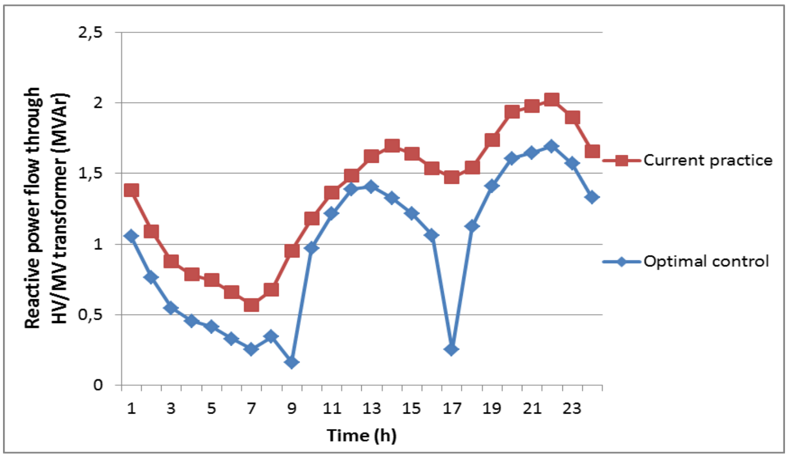

Figure 49 – Hourly Reactive Power Flow through the HV/MV Transformer (positive when absorbed from the upstream system)

3.2.3.7 Effectiveness of Available Control Means

Figure 50 and Figure 51 show how the gradual application of available control means leads to improvement in voltage regulation. It is observed that practically optimal results can be obtained from the application of optimal OLTC control and DG reactive power regulation, while additional control means (capacitors, active power curtailments and storage) contribute only marginally, although this is not a conclusion to generalize.

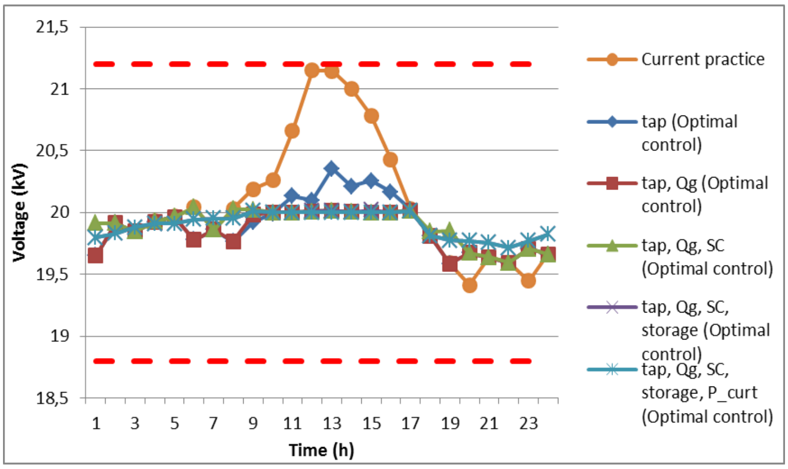

Figure 50 – Voltage Variation at the 3rd Node over a Day (24 hours)

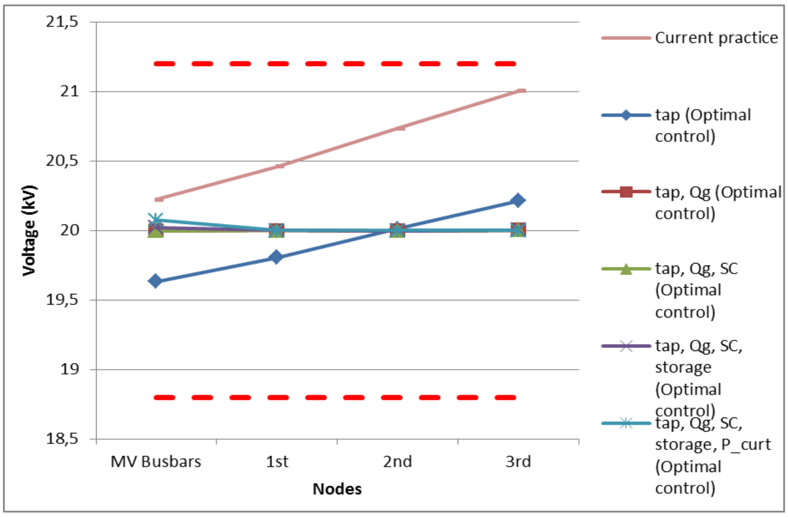

Figure 51 – Voltage Profile along the Feeder at 14:00

4 Voltage Control Scheme for LV Grids

The work presented in this chapter corresponds to the developments on voltage control specifically for LV distribution networks. As previously explained, the proposed approach can be divided in two levels as follows:

- **A local control scheme** based on droops operating at the inverter level of some DER in order to quickly react to sudden voltage drop/rise phenomena (for instance, to locally act on a PV µG unit that has high voltage values at its terminals due to a change in the primary resource – sun, in order to avoid technical violations).
- **A centralized control scheme** based on a set of rules that will aim at sending set-points to DER located at the LV level, *i.e.* controllable loads, µG and storage devices exploiting data collected from smart meters (for instance, sending a set-point to a storage unit that is electrically (or at least geographically) close and on the same phase as a client with a high voltage value);

The local control scheme will be embedded in the power electronic interface of the DER, particularly for RES-based µG units and will operate based on local measurements of voltage magnitude. In case the voltage is outside of the admissible band, the local control is able to adjust the active power (by reducing or increasing the injection) in order to mitigate the voltage violation.

The centralized control scheme will operate at the functional level of the MV/LV secondary substation (*i.e.* at the DTC level) and will be physically embedded in the DTC. This centralized control scheme may run periodically by polling some specific smart meters or may be triggered by the detection of a voltage violation in order to mobilize the most adequate resource(s) at the LV level in order to solve the voltage problem.

Although these two types of action rely on different philosophies, they can coexist. In case there is no local control, the centralized control scheme is able to ensure that voltages in the LV grid remain within admissible limits. If, on the other hand, inverters with droop characteristics exist in the network, they can be managed by the centralized algorithm that is able to enable or disable their droop functionality and/or remotely adjust the droop parameters.

Concerning the coordination between the two control levels (at the MV and LV), this is ensured as the multi-temporal OPF may define the “desired” power injection at the MV/LV transformer level that is then incorporated in the rules of the LV centralized control scheme for the corresponding DTC. In this case, the centralized voltage control algorithm will coordinate the available DER in order to ensure a specific power flow value in the MV/LV transformer, thus complying with the request from the upstream controller while ensuring that voltage profiles remain within an admissible band.

The following sections describe the approach developed by INESC for voltage control in LV grids. In Section 4.1 the local control scheme based on droops implemented at the level of the power electronic interfaces is presented and in Section 4.2 the centralized control scheme based on a set of rules implemented at the DTC level is described.

4.1 Local Control Scheme

The voltage rise effect in LV distribution grids is mostly related to the low X/R (reactance over resistance) ratio of the power lines in this type of grids, as well as with the reduced simultaneity between load and renewable generation profiles, namely solar PV. Under certain conditions, significantly high voltage profiles in LV distribution grids may lead to overvoltage tripping of µG units, thus limiting the possibility of increasing the amount of µG that can be integrated in the system. In order to overcome this situation, it is necessary to develop efficient control mechanisms at the µG power electronic interfaces for conditioning the power that is injected into the LV grid.

During normal operating conditions, the main objective is to accommodate the power generation from RES-based µG units, while ensuring adequate voltage profiles. Reactive power control strategies can produce effective results in LV feeders with high X/R ratio. However, as the resistance of the feeders increase (for example in the end of the feeder), the higher will be the amount of reactive power required to regulate voltage, thus limiting the inverters' capacity to inject active power [13].

In order to deal with the voltage rise effect in weak LV distribution grids in situations characterized by a high penetration of µG, innovative control strategies need to be adopted. Therefore, a droop control strategy – active power / voltage droop (P-V) functionality – will be exploited. This functionality will be implemented at the power electronic interfaces of the µG units connected to the LV grid. The control parameters of the local regulation functionality will be remotely adjusted through the DTC in accordance to the grid operating conditions or other requirements defined by the grid operator.

4.1.1 Proposed Approach

Active power injection can be determined by a droop characteristic such as the one represented in Figure 52, which includes the possibility of specifying a power set-point for the operation of the µG unit (P_{ref}) within a certain voltage dead-band. When the voltage exceeds the pre-defined dead-band, the output power is reduced in order to limit the voltage rise effect. On the contrary, if the µG unit was operating below its maximum capacity and the voltage drops below the dead-band, the unit may increase its power output. The active power control strategy depends on the µG technology. In the case of PV µG, active power variations can be achieved by modifying the maximum power point tracking algorithm, although this will affect the efficiency of the PV panels. In the case of the micro-wind inverters, a dump load can be used to dissipate the power surplus that cannot be accommodated by the LV grid. The proposed strategies are then able to provide additional flexibility to the DSO in comparison with more conservative approaches based on the strict limitation of the injected power by curtailing the µG units altogether.

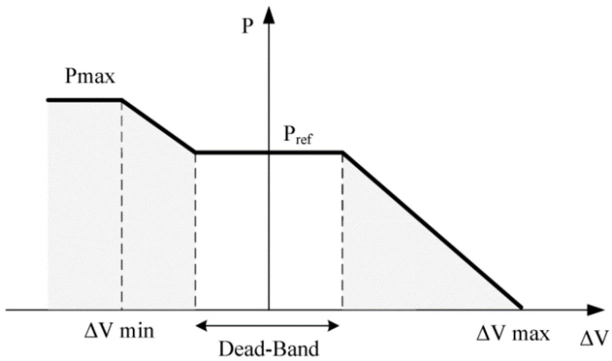

Figure 52 – PV Active Power Droop Control Strategy

4.1.2 Implementation

The possibility of conditioning the power injected by power electronic converters used in µG units in an LV distribution grid is to be organized in a hierarchical structure, as represented in Figure 53. In the local control level (power electronic converter of a µG unit), the injected power is controlled through a droop control functionality relating the node voltage deviations with active power injections. The higher hierarchical control level (*i.e.* the DTC), as a supervision and control unit responsible for the operation and management of the LV grid, has the responsibility of periodically defining the most adequate parameters of the droop function operating at each µG unit.

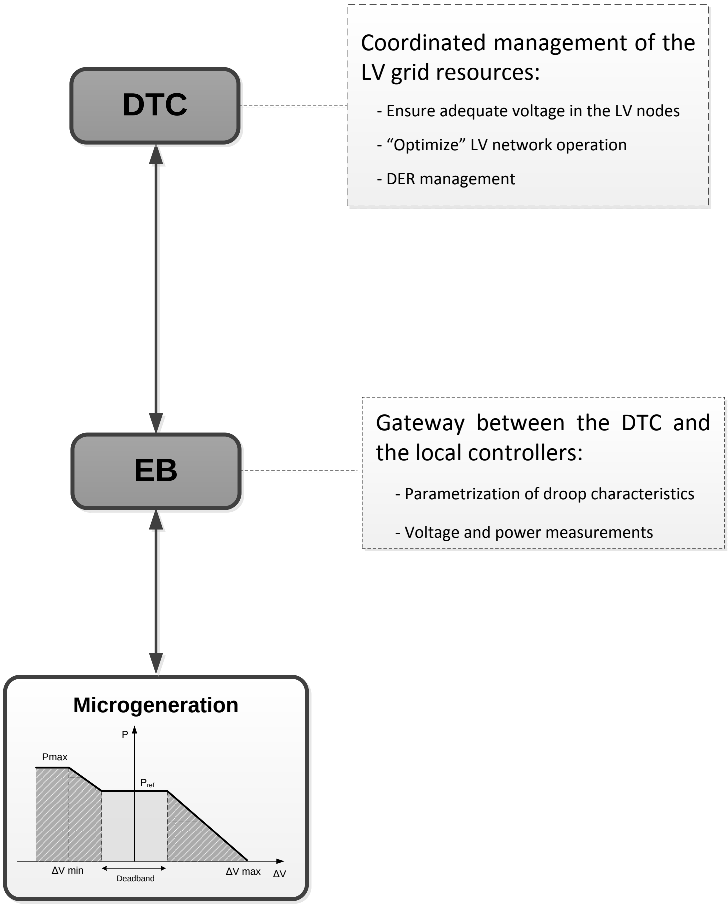

Figure 53 – General Overview of the LV Grid Control

4.1.3 Application Results

The LV grid control architecture represented in Figure 53 was implemented in the Smart Grid and Electric Vehicles Laboratory at INESC, in order to validate the local voltage control strategies presented previously.

The main building block of the laboratory includes µG technologies, energy storage devices, controllable loads as well as the LV grid cable simulators. The electric infrastructure is overlaid by a communication, information and measuring layer in order to enable the laboratory automation and the implementation of the LV network controllers (*i.e.* the DTC and the EB). A description of the laboratory electric infrastructure and communication and information system can be found in [9].

Figure 54 shows the microgrid topology adopted for the experimental testing of the local voltage control strategies adopted. Regarding µG, the system includes RES based µG consisting of PV panels with a maximum installed power of 15.5 kWp and a micro-Wind Turbine (WT) emulated through a 3 kW permanent magnet synchronous generator (300 V, 330 rpm) coupled to variable speed motor drive. Both PV and the emulated micro-WT are connected to the electric network through single-phase inverter prototypes developed in-house and incorporating the local voltage control strategy based on droop strategy represented in Figure 14. A detailed description of PV and WT inverter design can be found in [15] and [16] respectively.

A state of the art three-phase 20 kW / 400 V four quadrant (4Q) back-to-back inverter is connected to node 4. The inverter can be remotely controlled in terms of its active power output in order to emulate a fully controlled µG unit, which can also respond to local voltage measurement according to a droop function as in Figure 54.

Regarding loads a single-phase 3 kW load is connected to phase A of node 3, which corresponds to the same phase where the PV and micro-WT are connected.

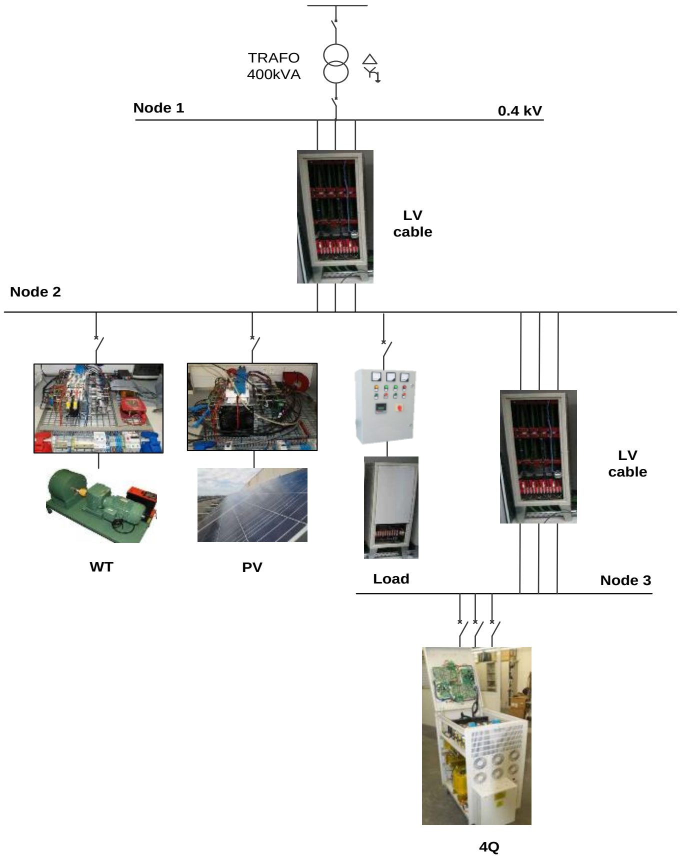

Figure 54 – Microgrid Laboratorial Test System

The tests performed represent the LV network operation considering a large scale integration of µG in periods of off-peak load. In the beginning of the first experiment (no load condition) the 4Q inverter was injecting about 6 kW of active power in node 4. The test sequence was then performed as follows:

- Step 1 – At t = 30 s the PV inverter starts to inject about 2.5 kW of active power.
- Step 2 – At t = 55 s the PV inverter active power-voltage droop is remotely activated by the MicroGrid Central Controller (MGCC) which is located at the MV/LV secondary substation level (similar to the DTC) and is in charge of the LV microgrid.

- Step 3 – At t = 75 s the micro-WT inverter is connected to the MG and is set to inject also 2.5 kW.
- Step 4 – At t = 110 s the micro-WT inverter power-voltage droop is remotely activated by the MGCC.
- Step 5 – At t = 135 s the 4Q inverter active power-voltage droop is also activated.
- Step 6 – At t = 165 s a single-phase load is connected in node 3 with a 1.5kW power consumption

Figure 55 and Figure 56 present the obtained results in terms of total active power (negative power refers to power injection into the microgrid) and phase A voltages, respectively. Each event of the experiment is numbered in the figure.

In the beginning of the experiment (no load condition) the 4Q inverter was injecting about 6 kW of active power in node 3, consequently increasing voltages in node 3 to 245V and to 240V in node 2. When the PV starts to inject about 2.5 kW of active power at t = 30 s (step 1) the voltage at node 2 increases to 252 V as shown in Figure 56, being close to the 10% voltage limit impose by voltage quality standards [15]. In order to reduce voltage to more admissible values, at t = 55 s (step 2), the PV inverter active power-voltage droop is remotely activated by the MGCC. Since node 2 voltage was higher than the dead-band maximum value (set at 240 V), the PV inverter reduces its active power output, consequently reducing voltage at node 3 to 245 V.

At t = 75 s (step 3), the micro-WT inverter is connected to the microgrid injecting 2.5 kW, consequently increasing the voltage magnitude which leads to an additional reduction of the PV power injected in the grid, since its droop control functionality remained in operation. At t = 110 s (step 4), the micro-WT inverter power-voltage droop is remotely activated by the MGCC. As shown in Figure 55 both micro-WT and PV inverters share the active power reduction and voltage stabilizes around 248 V. At t = 135 s (step 5), the 4Q inverter active power-voltage droop is also activated and leads to a 3 kW reduction of its injected active power as well as a reduction of the node voltages.

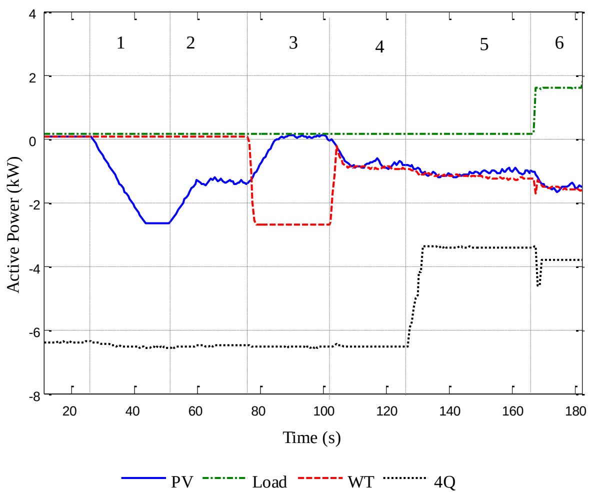

Figure 55 – Microgrid interconnected Operation Mode: Active Power Consumption and Generation (No Load Condition)

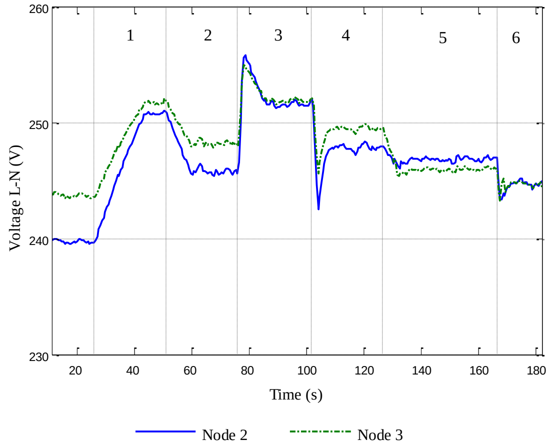

Figure 56 – Microgrid interconnected Operation Mode: Voltage Profiles (No Load Condition)

In order to further demonstrate the local response of µG to changes in the LV network operating conditions, at t = 165 s (step 6), a single-phase load is connected with a 1.5 kW power consumption. The increase of power consumption causes a small voltage decrease, allowing a small increase of the droop controlled µG units. The results obtained reinforce the importance of coordinating the operation of the µG units with other flexible resources, such as storage or flexible loads. This coordination will be further exploited in future work.

A second test was performed in order to study the impact of different communications delays and losses in packed data in the communication between the MGCC and local controllers. The experimental procedure followed in this experiment is similar to the first test performed. In the beginning of the experiment, the PV unit was injecting about 1.8 kW of active power. At t = 55 s a signal is sent from the MGCC to the PV controller in order to activate the P-V droop. At t = 75 s the micro-WT inverter connects to the network and starts to produce about 1.5 kW of active power. At t = 85 s the micro-WT P-V droop is activated through the MGCC.

Figure 57 shows the impact of a 4 s delays in the activation of the PV inverter droop with 10% to 50% probabilities of occurring data losses. With 50% of data losses only the PV responds at t = 130 s. Figure 58 shows the impact of a 2 s and 4 s delay when enabling the micro-WT inverter P-V droop. As shown in Figure 59, the delay caused by the communication system consequently delays the response of the micro-WT and PV inverters and the voltage compensation effect.

When considering data losses, the inverters may not respond until a new signal is sent. LV networks with long feeders having high penetration of µG may experience high voltages along the feeder. When voltages are close to the admissible inverter limits the communication delays and losses leading to unresponsive or delayed control may cause the disconnection of a large amount of generation, which would have a significant impact in terms of the MG operation.

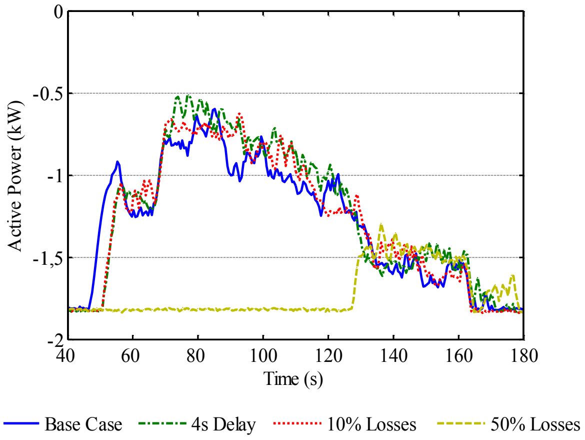

Figure 57 – PV Active Power Response (considering a 4 s delay with losses on the data sent by the MGCC to the local controllers)

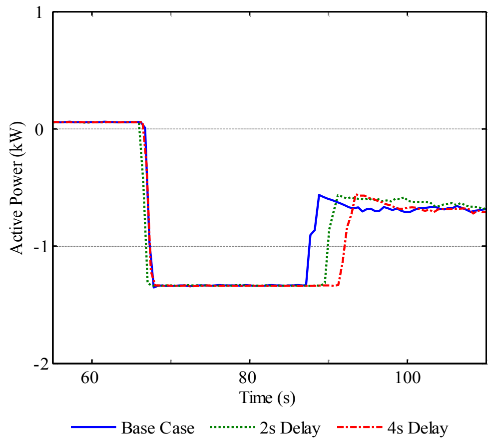

Figure 58 – Micro-WT Inverter Active Power (considering 2 s and 4 s delays on the data sent by the MGCC to the local controllers)

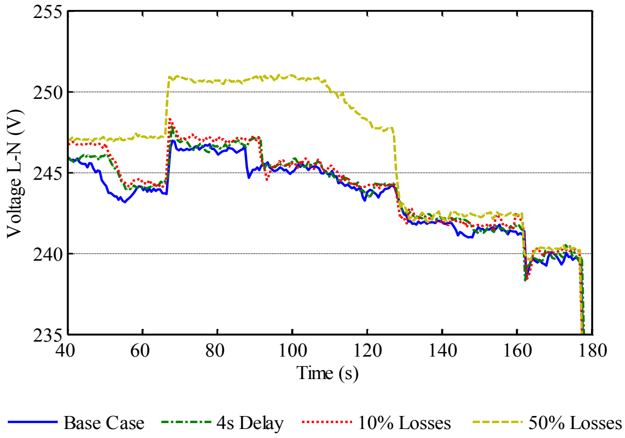

Figure 59 – PV Terminal Voltage (considering a 4 s delay with losses on the data sent by the MGCC to the local controllers)

More results of laboratorial tests on the performance of the local control strategy, including the coordination between storage and µG, in will be presented in Deliverable D5.2 "Evaluation of the Operation Methodologies".

4.2 Centralized Control Scheme

As previously mentioned, LV distribution systems often include resistive networks (*i.e.* with low X/R ratio), which means traditional regulation through reactive power control may not be sufficient. In this case, the most effective means of mitigating overvoltages (from the point of view of control) that may result from excess generation from RES is through local control actions, namely by curtailing excess power. This can be done by simply disconnecting µG units (before the actuation of protection systems), by reducing the injected power through the control of the power electronic interface (inverter) using a droop characteristic [17, 18] or by sending a new power set-point to the inverter in order to change its output (which is a solution already available by some inverter manufacturers such as SMA[3]). However, this strategy can be very penalizing to the RES-based µG owners especially those who are located in critical areas of the network such as at the end of long resistive feeders, since these may result in frequent curtailment actions in case of excess generation.

Here a new voltage control strategy for LV grids is proposed, leveraging the information from the AMI, which will enable a coordinated operation of the available DER in order to solve voltage violations that may occur, especially in situations with high RES integration. This methodology aims at providing a close to real time solution in order to control voltage deviations in LV grids based on a set of rules that is able to manage all the controllable grid assets according to a merit order. The proposed approach has the capability of handling three-phase unbalanced grid operation and is not fully dependent on the observability of the LV grid.

Moreover, the communication requirements for the Centralized Control Scheme have been identified in order to evaluate the suitability of communication technologies to support the proposed control approach.

Therefore, the main simulation platform for the electrical network developed by INESC has been coupled to a communications simulation platform developed by COMILLAS to be able to assess the impact of communication in the performance of the voltage control algorithm at the LV level. It should be stressed that the communications simulation platform will also be used for the development of Task T7.1 "Cost-Benefit Analysis" within WP7. Consequently, more details on the performance of the centralized control scheme for LV will be included in Deliverable D7.1 "Cost and Benefit Analysis in the SuSTAINABLE Demos" to be delivered in Month 36.

[3] For more information see:
http://www.sma.de/en/partners/knowledgebase/sma-inverters-as-grid-managers.html

4.2.1 Proposed Approach

The proposed methodology is based on a set of rules and measures that follows a merit order of the grid's controllable resources in order to fulfil the macro objectives of the DSO of maximizing RES generation (*i.e.* use all other control alternatives before resorting to RES power curtailments) and minimizing costs (*i.e.* use control actions with less impact in terms of financial compensations to the affected consumers/producers).

The selected control actions are prioritized regarding the type of controllable resources that are available in the grid and the macro objectives previously stated. The priority of grid resource's actuation is as follows:

- Energy storage devices (in case they are property of DSO);
- MV/LV secondary substation transformers with OLTC;
- µG units;
- Controllable loads under DSM actions.

The first two control actions to be undertaken are directed to the assets that are property of the DSO since their actuation represents little or no cost. Power curtailments in µG units and controllable loads are the second set of actions since they are expected to represent higher costs for the DSO and might affect reliability and customers' satisfaction. In this last case, it is assumed that the flexibility of the customer (either for generation or load) must be secured through some type of special type of bilateral contract between the client and the DSO or through a market mechanism for ancillary services provision by means of an aggregator agent. It must be stressed that although it is possible that storage devices may also belong to private promoters, in this case it is assumed that these devices belong to the DSO and that are managed according to its own needs.

For each type of controllable grid asset, the control action is determined taking into account a set of decision factors that prioritize which is the unit best suited to solve a specific voltage violation. Some of the most relevant decision factors are:

- Proximity to overvoltage location;
- Flexibility of operation;
- Cost of operation;
- Impact in mitigating the voltage deviation.

As previously mentioned, two modes of operation are envisioned for this functionality:

- <u>Following a voltage problem in the LV grid</u> → In case a voltage violation is detected in the LV grid, the centralized voltage control module is triggered in order to solve the voltage violation by managing the available DER at the LV level.
- <u>Following a request from an upstream controller</u> → the DTC may be required to respond to a request from a high level controller such as the SSC in order to ensure

a given active power flow in the corresponding MV/LV distribution transformer, determined by the voltage control algorithm for MV (*i.e.* the multi-temporal OPF).

4.2.2 Implementation

Each LV grid is managed by a DTC that is responsible for managing the different DER downstream of the corresponding MV/LV secondary substation. Each DTC may incorporate its own set of rules depending on the characteristics and degree of knowledge of the LV grid, amount and type of DER present, *etc.* The smart meters installed at the customer's level can be used as a gateway to monitor and control these local resources, either load or generation. The proposed voltage control algorithm is assumed to be installed in the DTC in order to manage the downstream LV grid.

However, the main obstacle to an efficient operation of the LV distribution system has to do with the fact that these grids are often poorly characterized both in terms of topology and electrical characteristics of the lines or cables. In some cases, the only information available is the knowledge of which loads connect to which MV/LV distribution transformer, without data regarding the lines, type and length.

Therefore, the proposed methodology (shown in Figure 60) is adaptive since it is capable of solving voltage problems taking advantage of the available distributed resources in two distinct situations:

- **Full knowledge of the LV grid**: Topology and access to smart metering devices and possibility of running a power flow routine.
- **Limited knowledge of the LV grid**: Unknown topology; access only to smart meter readings and geographic coordinates of customers.

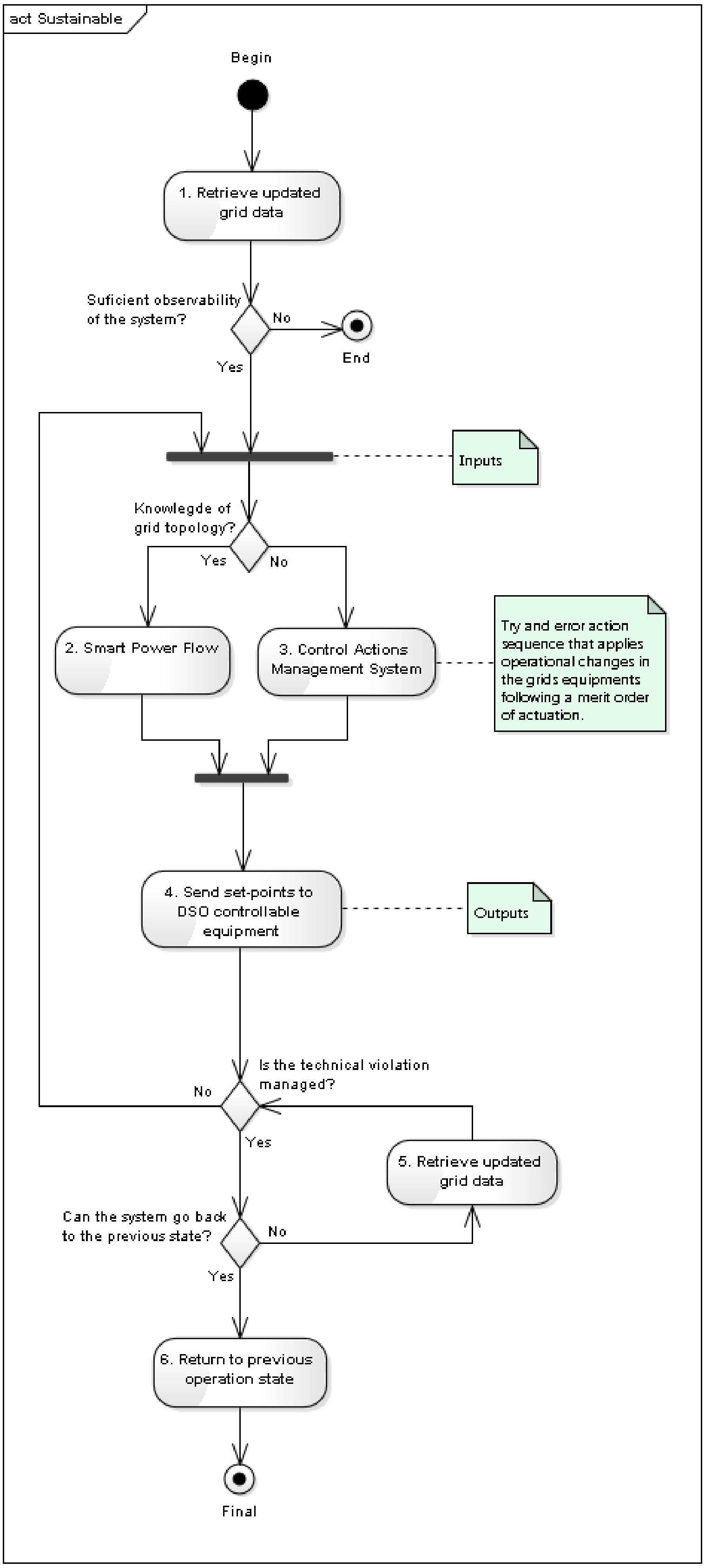

Figure 60 – Flowchart of the Centralized Control Scheme

The figure clearly shows the two alternative approaches depending on the degree of knowledge of the LV network, which are described in more detail in Sections 4.2.2.1 and 4.2.2.2.

4.2.2.1 Full Knowledge of the LV Grid

If there is full knowledge of the LV grid (including topology, characteristics of lines/transformers), there is sufficient information to run a three-phase unbalanced power flow. This power flow routine may be embedded in the corresponding DTC's software as a local function to be used primarily for voltage control purposes.

The algorithm for the centralized control scheme was developed in MATLAB and includes power flow routine used for three-phase, four-wire radial distribution networks, where the neutral wire and the ground are explicitly represented [19]. It uses a general power flow algorithm based on backward-forward technique, which is extremely fast to reach convergence. It must be noted that this method was designed for radial distribution networks, although it may adapted for weakly meshed networks [19]. Also, the proposed power flow method enables the investigation of the effects of neutrals and system grounding on the operation of real distribution networks.

This information is complemented by the most recent data available of power injections in the different network nodes, historical data collected by the DTC, which provides an approximate view of the state of the grid in quasi-real time, *i.e.* a snapshot of the LV system.

As previously explained the voltage control algorithm may run periodically after polling some specific smart meters or after identifying a voltage violation. Whenever a violation is detected, with the possibility of running a "smart" power flow, a suitable solution for controlling voltage profiles is determined by testing several possible solutions iteratively and then identifying which resources need to be actuated in order to solve the voltage violation.

The results of the voltage control algorithm will be set-points to µG units, storage devices and controllable loads as well as tap positions for MV/LV transformers with OLTC capability.

4.2.2.2 Limited Knowledge of the LV Grid

With limited information and without the possibility of running a power flow, the algorithm used is based on a recursive approach. In this case, apart from the availability of smart meter readings, the minimum information required is the geographical position of each unit (load, µG unit or storage device) as well as the phase to which it is connected.

In this case, a voltage violation is identified and its location is determined. Then, the proposed control actions management system is used and successive control actions are applied to the controllable assets until the voltage deviation is corrected, according to the priority rules previously established. These control actions correlate the severity of the voltage violation with the distance to the controllable asset to be actuated, therefore working as a type of sensitivity analysis. The flowchart of the control actions management system is presented in Figure 61.

The main difference between this case and the one presented in Section 4.2.2.1 is that here there is no possibility of evaluating the actual effects of the control actions determined through simulation. This has obvious implications on the level of accuracy of the control procedure as well as on the total time of response required to solve the voltage problem.

As in the previous case, the results of the voltage control algorithm will be set-points to the grid's assets.

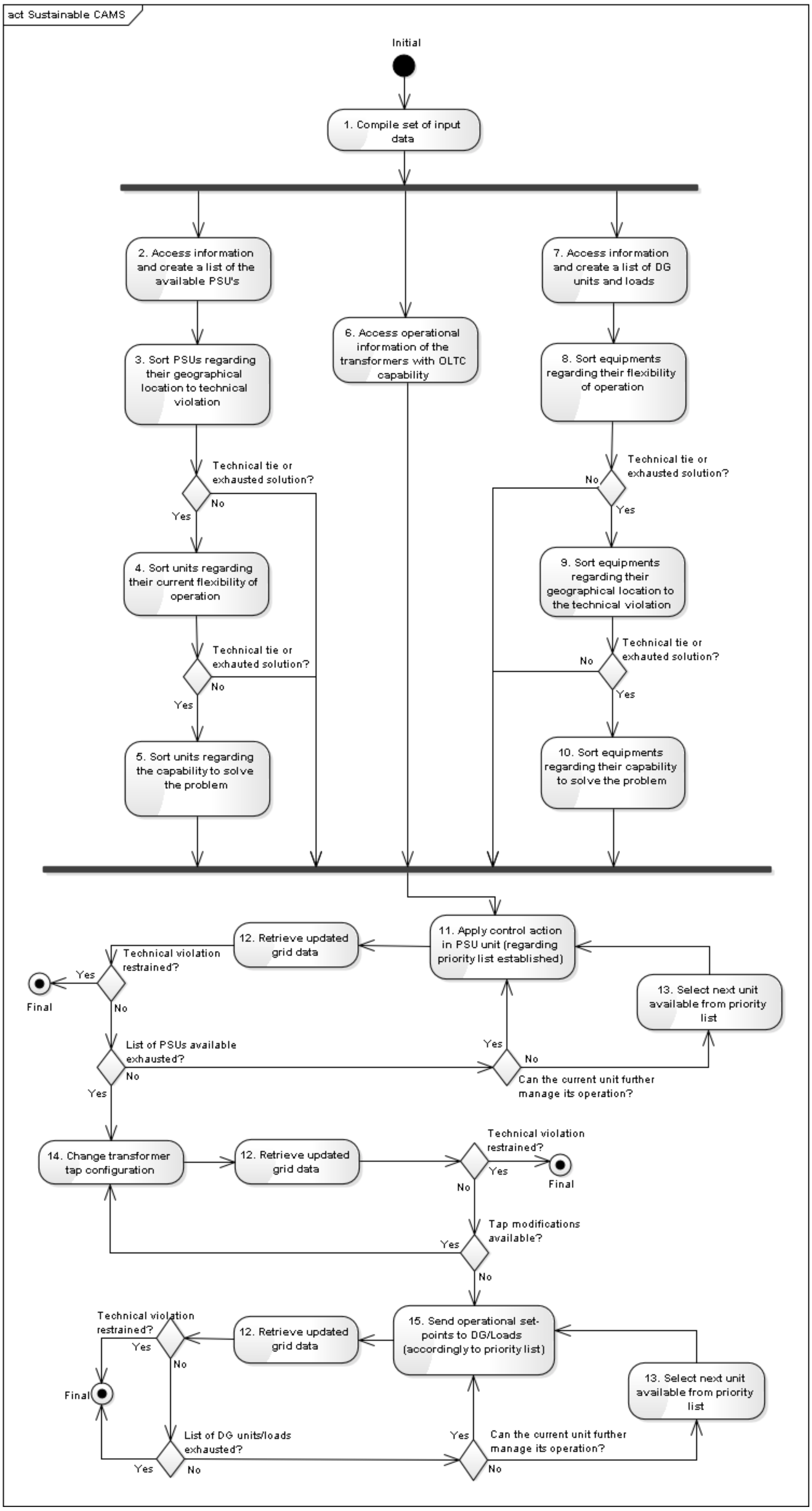

Figure 61 – Flowchart of the Control Actions Management System

4.2.3 Application Results

This section presents some of the simulation results that were obtained using the centralized control algorithm developed by INESC. A real test network shown in Figure 62 was used in order to test the algorithm developed. This is a real LV Portuguese network with a 100 kVA distribution transformer feeding three main feeders.

A future scenario with large integration of DER was created in order to assess the performance of the centralized voltage control algorithm. Therefore, several energy storage units based on batteries, µG units using PV technology and controllable loads were introduced. In addition, a MV/LV transformer with OLTC has also been included. The controllable resources are identified in **green** in Figure 62.

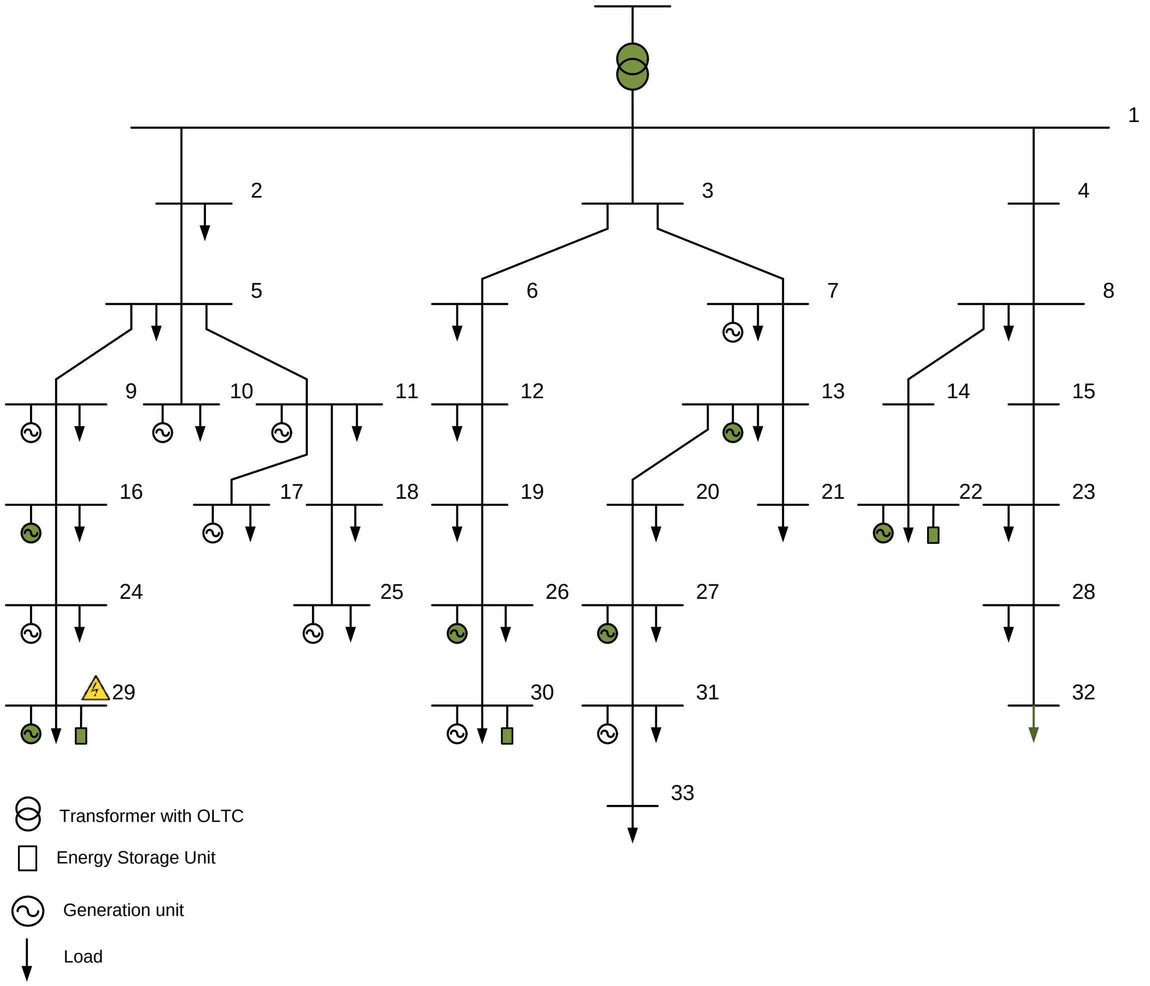

Figure 62 – LV Test Network

4.2.3.1 Voltage Violation in the LV Network

A voltage violation was simulated in the LV test network shown in Figure 62. An overvoltage was detected at bus 29 where the voltage magnitude reached 1.11 p.u. (the threshold value for the voltage considered here is 1.05 p.u.). In this case, it is assumed that there is full knowledge of the grid and therefore the centralized control scheme using the smart power flow is used in order to mitigate the voltage problem.

As previously explained, the first step of the algorithm is to identify the available resources that can be mobilized to solve the voltage problem. Then, a merit order of actuation is identified as shown in Table 4. This means that the first to be actuated is the storage unit at bus 29, then the transformer with OLTC, then the µG unit at bus 29 and finally the µG unit at bus 16.

Table 4 – Merit Order of Actuation

Merit Order	Controllable Resource
1	STOR29
2	OLTC
3	µG29
4	µG16

The algorithm of control then follows a set of guidelines to determine new set-points of operation for the controllable resources following the merit order of actuation in order to solve the voltage violation. The control actions identified for the controllable grid resources for this voltage violation scenario are presented in Table 5.

Table 5 – Control Actions for Overvoltage at Bus 29

	Current State	Set-Point	Set-Point (%)
STOR29	0.00 kW	-6.69 kW	98.00
OLTC	1.00 p.u.	0.98 p.u.	-2.00
µG29	10.97 kW	10.13 kW	-7.62

In the simulation stage of the control actions, the set-point of operation for each equipment is chosen taking into account the magnitude of the voltage deviation, as well as the proximity between the selected controllable equipment and the location of the voltage violation. After a new set-point is determined for a specific device, the simulation (three-phase power flow) is run and the results are obtained. If the overvoltage situation is not corrected, another set-point is calculated for that equipment. If the selected resource is not capable of mitigating the problem the following equipment from the merit order of actuation is selected and a new set-point is determined and then tested and so on.

For the specific case of the transformer with OLTC, the set-point is considered to be a change in one position of the winding tap. The procedure is done until the problem is corrected or the winding's tap reaches the limit position.

In the current example, the storage device located at bus 29 is the first equipment to be managed and the resulting set-point shows that the storage device is absorbing power almost at the nominal rated power of the unit.

Concerning the OLTC transformer, one tap position is considered to be the limit. As the voltage is still beyond the limit, the next equipment in the merit order is selected. The DG unit located at bus 29, being a controllable equipment, can have its power output curtailed following a request by the DSO. A final set-point of operation, curtailing nearly 8% of the unit's nominal power is applied to that unit, which enables returning the grid voltage to the operational limits.

The voltage variations resulting from the control actions undertaken in order to manage the overvoltage is represented in Figure 63.

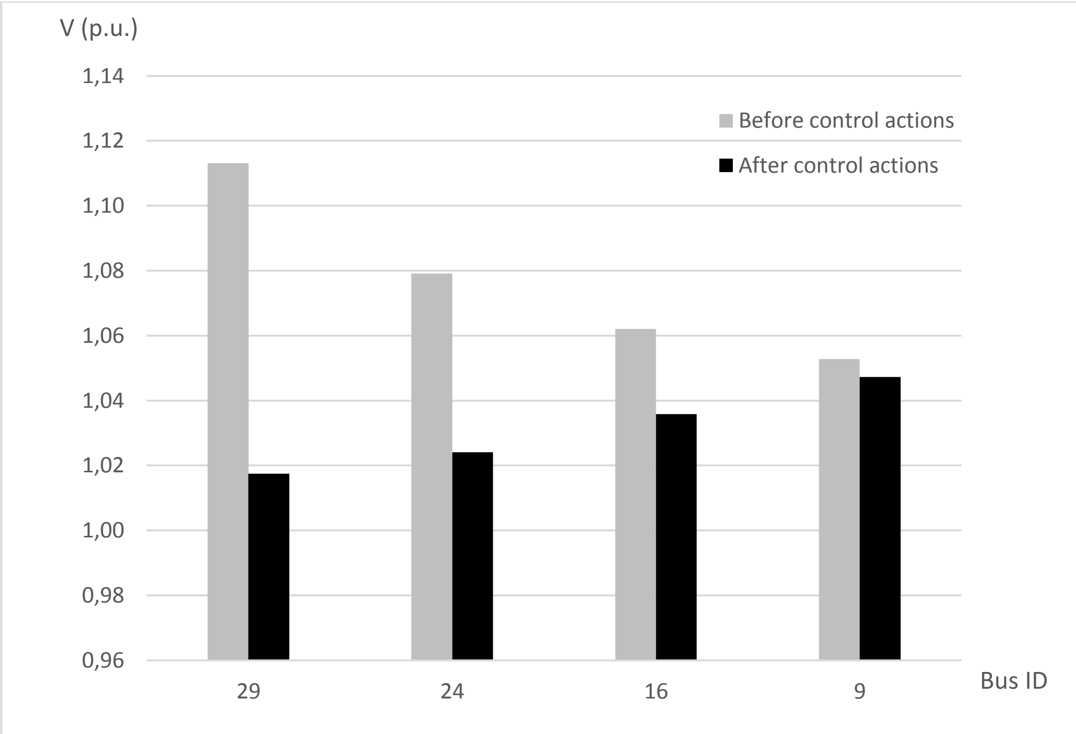

Figure 63 – Voltage Values in some Buses before and after Control Actions for Overvoltage at Bus 29

4.2.3.2 Request from the Smart Substation Controller

In order to ensure coordination between the two voltage control levels (MV and LV), it is foreseen that the DTC may receive a request from an upstream controller (*i.e.*, the SSC) as a form of set-point in order to change the power flow in the MV/LV distribution transformer.

In this case, it is assumed that an excess of generation at the level of the MV network occurs. As a result, the SSC sends a request to the DTCs downstream in order to change their active power injection and consume more power so as to absorb the available generation. As a result, the resources located at the LV level are used in order to comply with the request from above and make the LV network that was exporting power import power instead.

Therefore, the control algorithm is based on an analysis per phase of the flow at the MV/LV distribution transformer aimed at maintaining the power flow values within specific limits without causing problems in the LV network.

In this simulation, power flow limits are imposed for the active power from the substation level to the LV grid (*i.e.* $P_{substation,1}$). In this scenario, as previously explained, for technical reasons, there is the need to restrict the reverse power flow from the MV network point of view and ensure that the LV network consumes more power. Therefore, in this case, only storage devices should be managed to comply with the limitation imposed.

The network used is the one shown in Figure 62 however it is assumed that two large storage units are available (one located at bus 2 and the other at bus 3) in order to maintain the imposed limits.

The main results obtained for this operation scenario are shown in the table below with the power flow limitations imposed at the distribution transformer level. In this case, four storage units are used to increase the load and turn an exporting LV network into an importing LV network.

Table 6 – Control Actions for limiting the Power Flow in the MV/LV Distribution Transformer

	Current State (kW)	Set-Point (kW)	Set-Point (%)
PSU30	0.00	-8.00	100.00
PSU2,2	0.00	-16.00	96.00
PSU29	0.00	-8.00	100.00
PSU2,3	0.00	-14.70	88.00

In Table 7, it is possible to observe the initial and final values of the power flow for each feeder and each phase and the resulting value at the MV/LV distribution transformer level.

As can be observed in Figure 64, the reverse power flow is avoided (previously, the LV network was exporting power to the MV network) and the LV network is now importing around 1.5 kW following the request from the SSC.

In Figure 65, it is possible to see that voltage values are kept within admissible limits.

Table 7 – Active Power Flow in the MV/LV Distribution Transformer

	P1,2 (kW)		P1,3 (kW)		P1,4 (kW)		P substation,1 (kW)	
	Initial	Final	Initial	Final	Initial	Final	Initial	Final
Phase R	0.028	0.375	-0.034	0.192	-0.021	-0.047	-0.027	0.519
Phase S	0.028	0.463	0.045	-0.006	0.089	0.087	0.162	0.544
Phase T	-0.737	0.163	0.038	0.273	0.072	0.070	-0.626	0.505

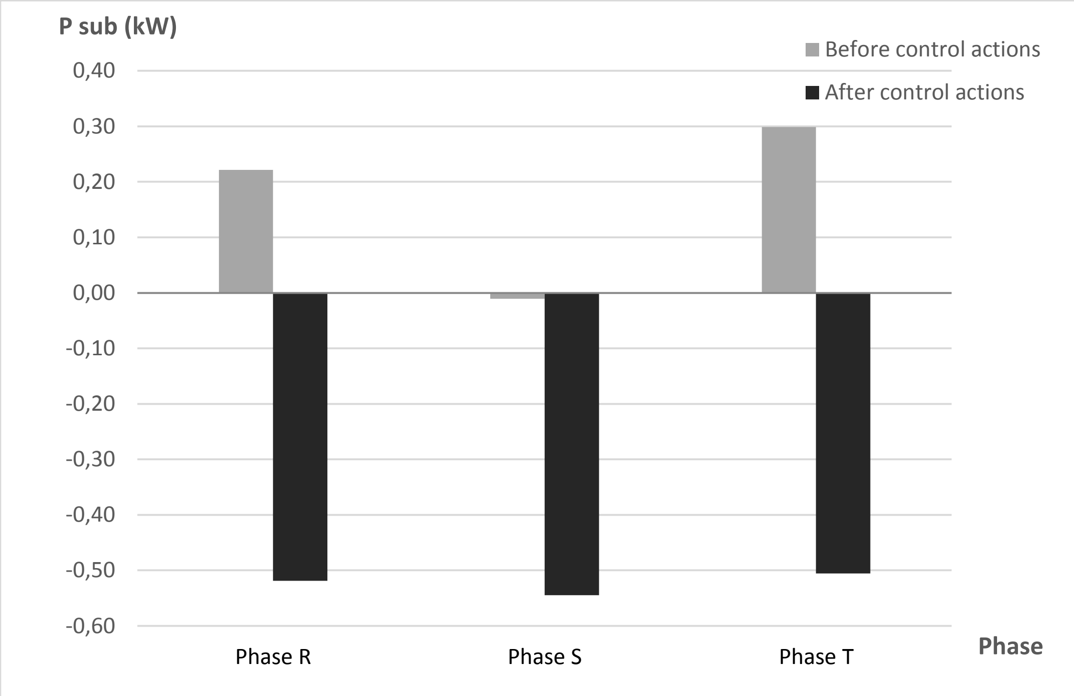

Figure 64 – Resulting Active Power Flow in the MV/LV Distribution Transformer

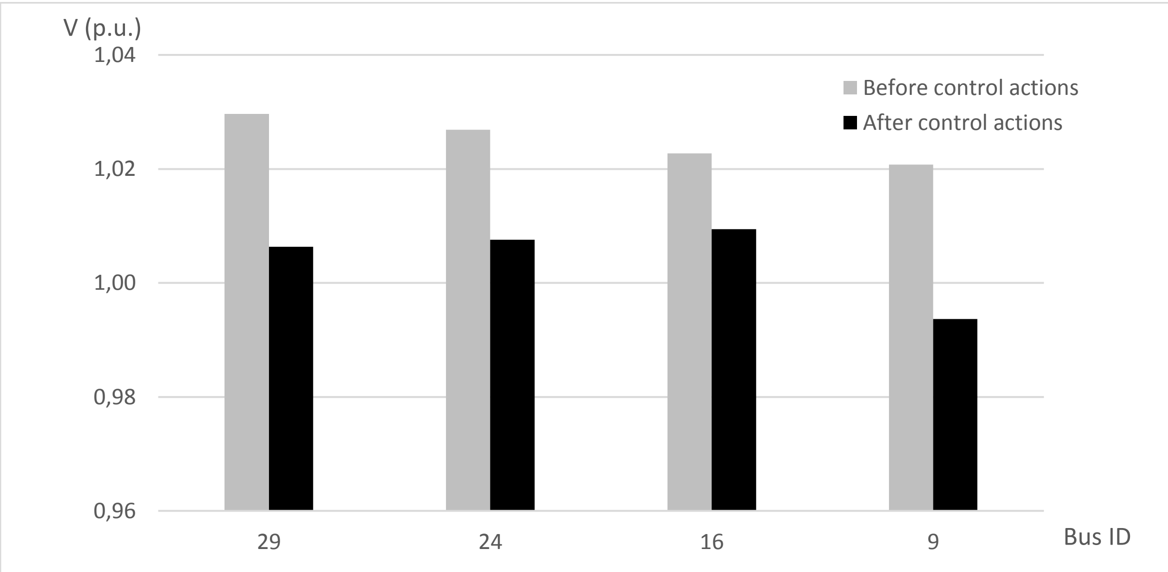

Figure 65 – Voltage Values in some Buses before and after Control Actions following a Request by the SSC

4.2.3.3 Communication Requirements

The performance of the required communication infrastructure has been validated using a simulator for communication networks developed by COMILLAS. This tool has been built on the OMNeT++ simulation framework, where the PRIME protocol has been implemented to perform the communications via PLC. The assessment methodology is the following:

First, the characteristics of the physical channel are assessed according to the transmission line theory based on the electrical parameters of the network. To simplify the simulation, it has been assumed that all nodes have communication capabilities and that there is just one control device per node. As result, the attenuation between each pair of nodes is obtained. Figure 66 shows the representation of the attenuation matrix obtained for the LV test network presented in Figure 62.

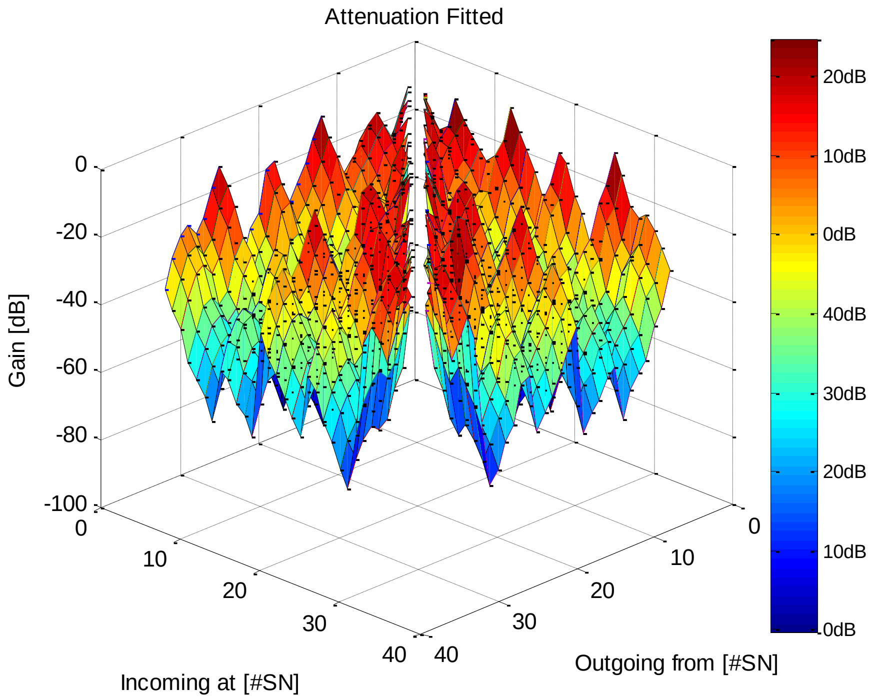

Figure 66 – Attenuation Matrix obtained for the LV Test Network

The attenuation obtained in the previous stage is used to assess the Bit Error Rate (BER), which defines the communication mode to transmit the data in a way that the higher the BER, the more robustness is required. However, higher robustness is traded off by slower transmission speed. Table 8 summarizes the main options used by PRIME, where it can be noticed for instance that the use of Forward Error Correction (FEC) reduces the bit rate by half. The BER is assessed from the Signal to Noise Ratio (SNR) between each pair of nodes, obtained with the attenuation matrix. The relationship between BER and SNR for each communication mode is shown in Figure 67 [20].

Table 8 – Communication Modes used by PRIME

Mode	FEC-ON	FEC-OFF
DBPSK	21.4 kbps	42.9 kbps
DQPSK	42.9 kbps	85.7 kbps
D8PSK	64.3 kbps	128.6 kbps

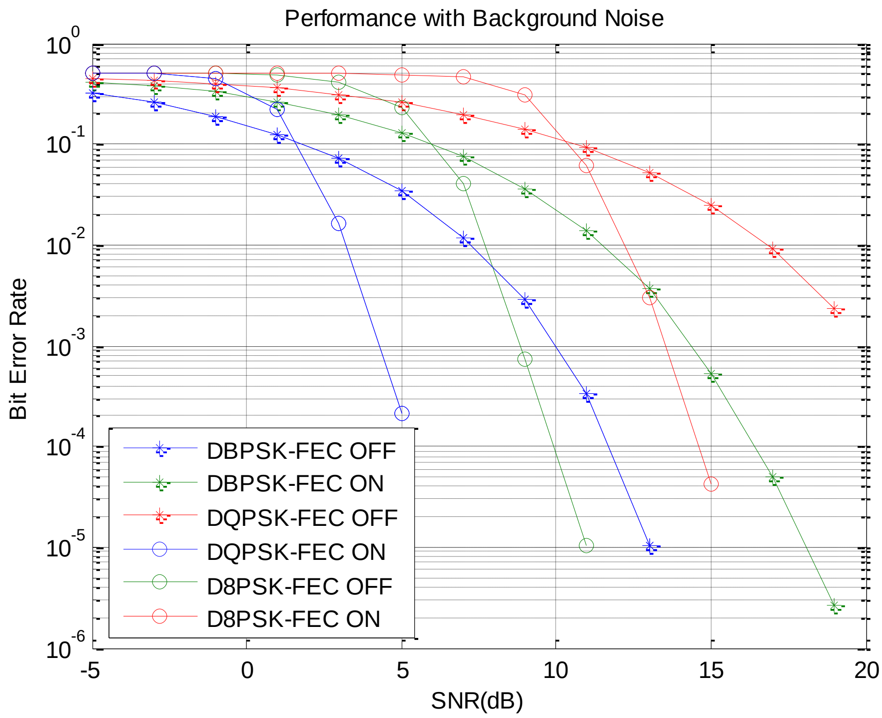

Figure 67 – Relationship between BER and SNR for each Communication Mode

Then, the PLC network is analysed in OMNeT++ based on the PRIME standard, which defines a protocol for the Logical Link Control (LLC), the Media Access Control (MAC), and the Physical layer (PHY). The analysed scenario represents 5.000 seconds of simulation, where the first 3.000 seconds are exclusively dedicated to register all the Service Nodes (SN) by the Base Node (BN) located in the secondary substation, and the next 2.000 to send messages of 200 Bytes to all the nodes in a sequential manner, repeating this process until the simulation finishes.

For the voltage control functionality, the One-Way Latency (OWL) has been analysed to check how long the set-points take to reach the control devices. The process of sending a set-point is illustrated in Figure 68. Basically, the OWL is made up of two main components: the first one is due to the Carrier Sense Multiple Access (CSMA) mechanism, which is needed to ensure that the access to the channel can be performed minimizing the collisions, referred as macSCPRBO in the figure; and the second one represents the time to transmit all the data through the physical channel, called Tx time.

Finally, the box plot of the obtained OWL for all nodes of the network is presented in Figure 69, where the order corresponds to a Depth First Search of all the nodes of the network. In this case, the propagation delay is very low for all the nodes, so the differences in the topology are not very well appreciated. This is mainly due to the fact that the attenuation is so low that no switches are needed to send the messages, which is usually related to larger delays. However, it can be noticed in the figure that the largest delays are obtained for the nodes 22 and 23, which, precisely, were the ones that exhibit a higher attenuation. Thanks to these results it can be concluded that PLC can be a good choice to implement this functionality in this type of network.

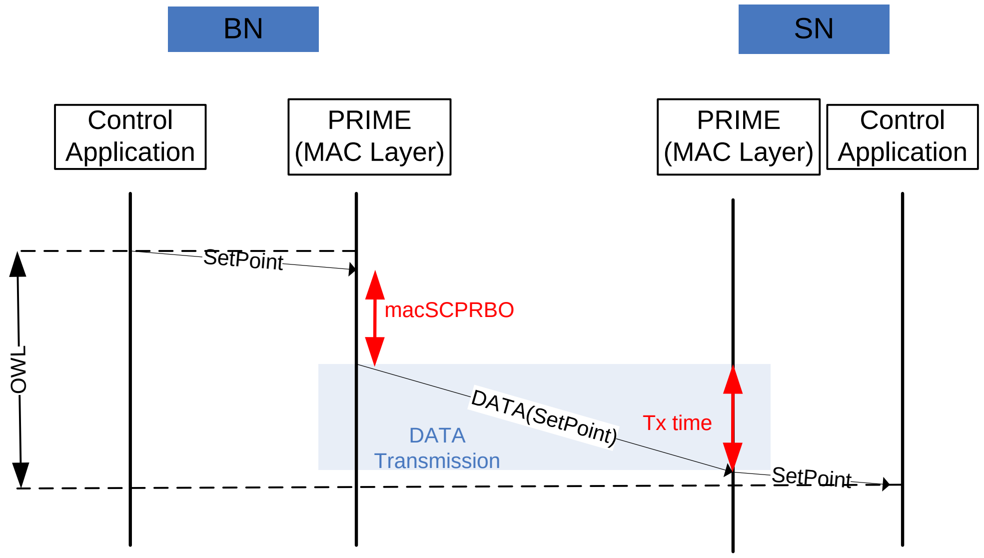

Figure 68 – Scheme of the Communication Process

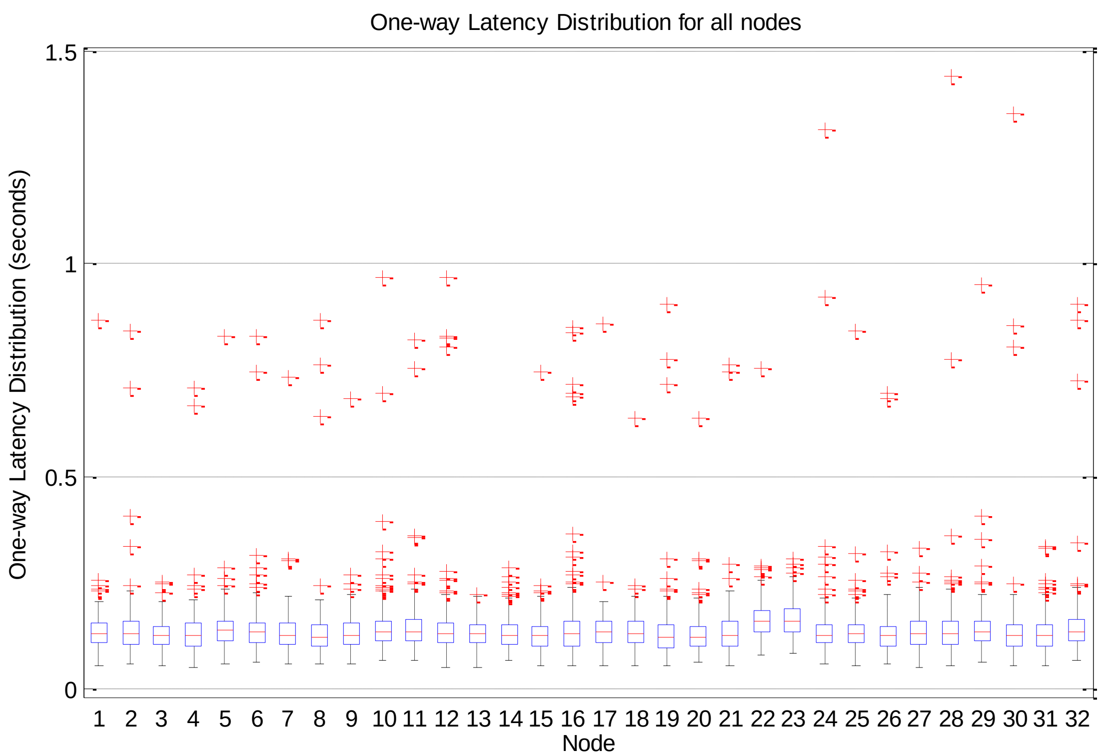

Figure 69 – One-way Latency Distribution for all Nodes

5 Implementation Details

In this chapter, EFACEC provides an insight to the implementation of the voltage control algorithms for MV and LV at the SSC level (Section 5.1) and at the DTC level (Section 5.2), respectively.

5.1 Smart Substation Controller Platform

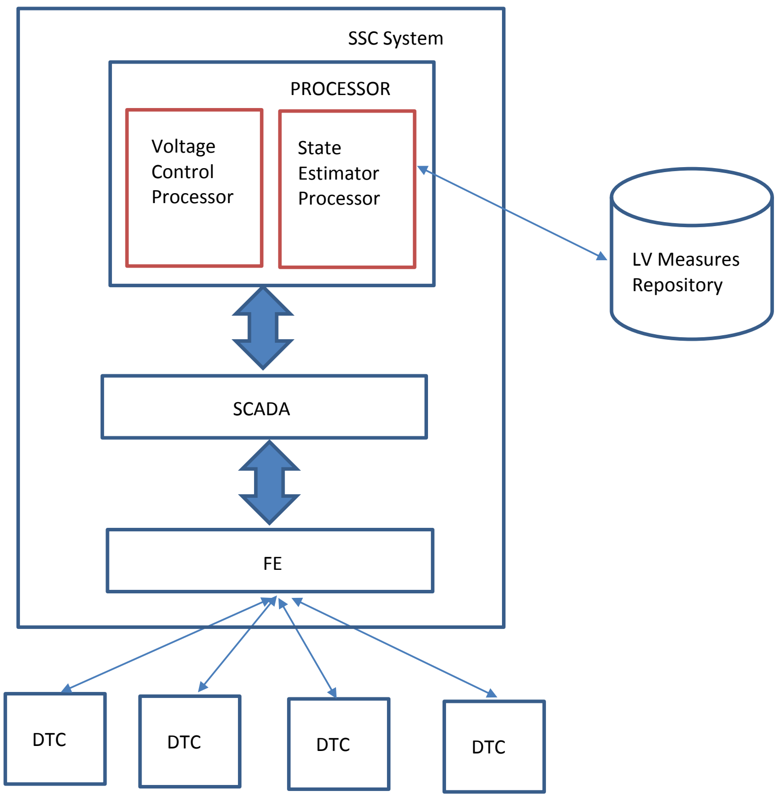

Figure 70 – The SSC System

The SSC System is composed by the following structural parts:

- Frontend (FE) – Real time communication frontend
- SCADA Server – SCADA core server
- Processor Server – High level processor server
- Workstation – User interface device (not present in Figure 70)

The FE communicates with the DTCs through IEC60870-5-104 real time communication protocol. Whenever the system starts, FE will do a general interrogation to all DTCs that are connected. After that, the DTCs will send measurement updates by exception to the FE.

The SCADA Server maintains the state and values of all entities that are acquired in real time from the DTCs through the FE. The configuration of the network under control by the SSC, including its electrical characteristics, is maintained in the SCADA Server database.

The Processor Server runs two processor components: the Voltage Control Processor and the State Estimator Processor. Both processors load the network configuration from the database and react to state and values updates processed by the SCADA Server.

In order to control voltage at the MV level, the Voltage Control Processor produces a set of set-points that will be sent to DTCs through the SCADA Server and FE.

The SSC Workstation should present to the user a diagram of the secondary substation and LV network with all the relevant real time and calculated data. In addition, the user will be able to:

- Consult the measured values;
- Consult the estimated data;
- Consult the data associated to the voltage control set-points;
- Consult Key Performance Indicator (KPI) calculation for voltage control.

5.2 Distribution Transformer Controller Platform

The DTC, by integrating multiple automation functions with the downstream LV smart meter data collection and management through multiple standard communication interfaces, enables the implementation of real smart grid solutions from MV and LV network automation.

The DTC can include a built-in Web server, I/O, data storage, fault detection, communications, condition monitoring, local energy metering and power quality analysis, as well as extensive self-monitoring. The LV Voltage Control will be included as an advanced built-in application.

5.2.1 Physical Interfaces

5.2.1.1 Metering Interfaces

The DTC metering capabilities can be used to acquire power transformer's instantaneous voltage and current for remote monitoring and control of all the assets downstream, typically using a smart meter as an information gateway through the Local Area Network (LAN). Also, these interfaces will be used to supply data to upstream control layers (*i.e.*, the SSC) to feed in with aggregated information for the functionalities inherent to that control level. Furthermore, the DTC can run typical functions required by the utilities such as load diagram analysis and reports, billing, reliability and fault alarms, fraud detection and energy balancing.

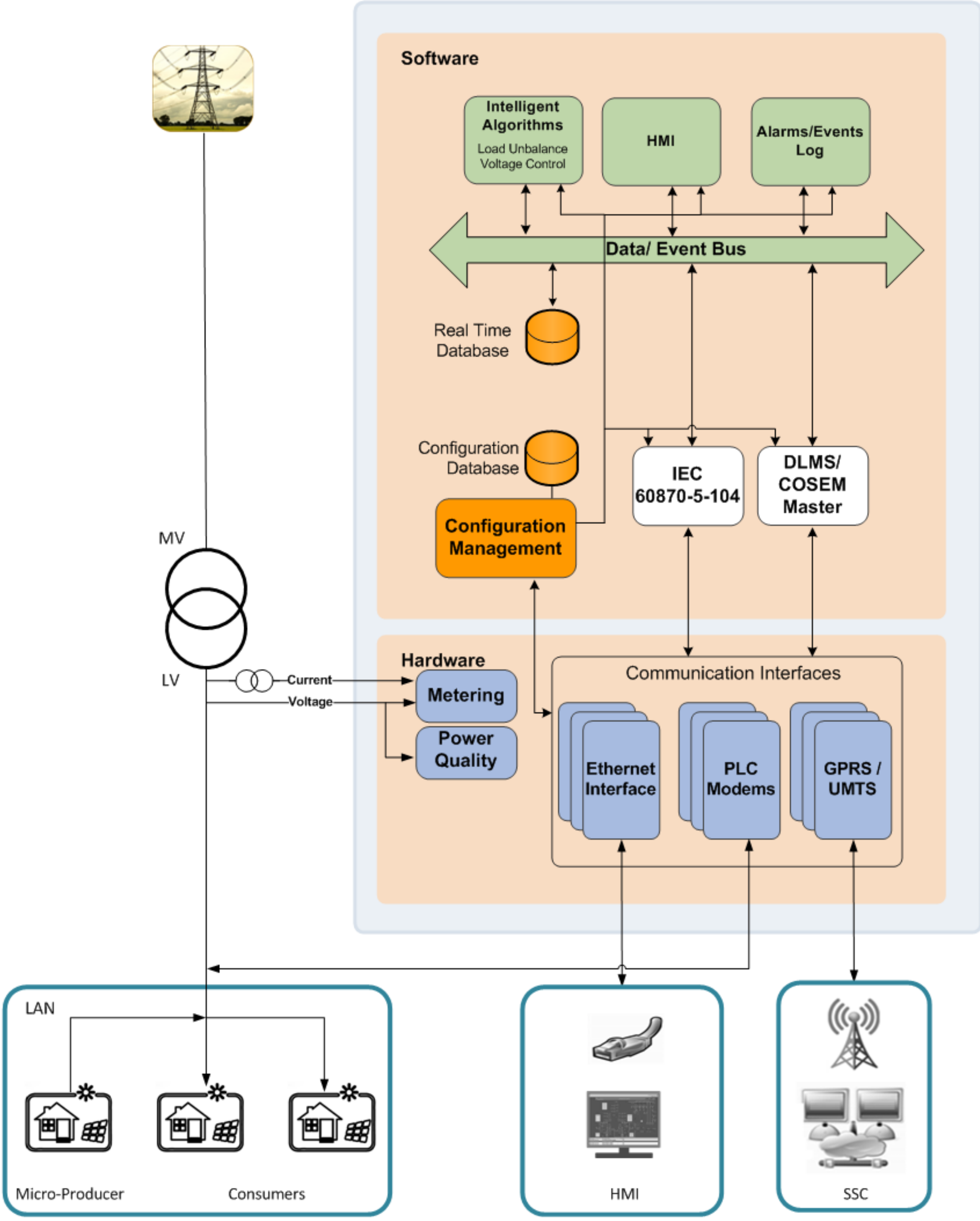

Figure 71 – DTC Architecture

5.2.1.2 Communication Interfaces

A wide range of communications protocols is possible, enabling multiple system architectures. The serial interfaces are commonly used for connectivity between devices on the TAN (Transformer Area Network), locally at the MV/LV secondary substation. PLC, Radio-Frequency (RF) Mesh or General Packet Radio Service (GPRS) are used for interfacing with the LV meters. GPRS/UMTS modem or Ethernet ports are used to integrate the system in the WAN, which is used as the SSC communication interface. These interfaces give the DTC the necessary interoperability to enable communication and operation in real-time, with the LAN, TAN and Wide Area Network (WAN) networks devices. This assures the requirements to maintain the necessary information exchange to feed in the other hierarchical control layers.

5.2.2 Communications Protocols

The common setup includes IEC 60870-5-104 (TCP/IP) or Web Services for remote control, DLMS/COSEM for LV network communications and MODBUS protocol for local station communication. Such protocols can be used through several interfaces such as Ethernet, GPRS/UMTS, RS485, PLC or RF Mesh. These are well proven protocols (in use within industry and utilities) and give the DTC the necessary capabilities to efficiently communicate and interact with other devices, assuring the information and data formats required for the deployment of the coordinated voltage control.

5.2.3 Data and Event Logging

The DTC provides a range of organized logs and alarms. Through an analysis of this information, it is possible to check relevant alarms and with the corresponding timestamp, corresponding to operational constraints, out of range values, and equipment, metering and power quality events. The device event log stores all DTC related events for offline analysis.

The DTC internal database must be capable to store several months of measured data which is relevant for the deployment and execution of the LV Voltage Control functionality, such as:

- Voltage;
- Currents;
- Active energy (four quadrants);
- Reactive energy (four quadrants);
- Active power (four quadrants);
- Reactive power (four quadrants).

Internally, it optimizes its organization through complex structures (load diagrams, billings and logs) so that communications protocols and local processing by built-in algorithms (such as the LV Voltage Control) and others are used reducing response times and facilitate the data provision to up- and down-stream control layers.

5.2.4 Web-Based Interface

LV Network monitorization and statistical information can be displayed, providing information such as:

- Information collection and report for KPI analysis ;
- Load diagrams visualization (voltage, current, powers, *etc.*);
- Event logs (actions over the network, alarms, *etc.*).

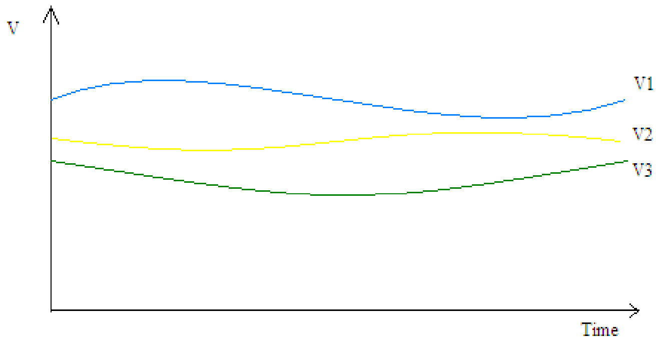

Figure 72 – Example of a Three-phase Voltage Diagram

5.2.5 LV Voltage Control

The DTC will be work as a smart Remote Terminal Unit (RTU) and MV/LV station automation unit providing built-in functions, such as LV Voltage Control, MV fault detection, transformer monitoring and control, MV circuit breaker control, and several measurements (RMS values, power factor and others).

The LV Voltage Control algorithm is an intrinsic functionality which runs on a near real-time basis using information received from the devices at the LV level, from the SSC and from local metering and local databases as depicted in Figure 73.

DLMS/COSEM protocol will be used to communicate with the LV devices. The LV Voltage Control module uses as input the data received from the LV devices and generates the adequate set-point controls as outputs, thus changing the settings of the LV devices. The DTC may also receive set-points from the SSC, through IEC 60870-5-104 to change the settings of its internal module. The real time data received from LV network and acquired from MV/LV power transformer will be sent to the SCC via the same protocol.

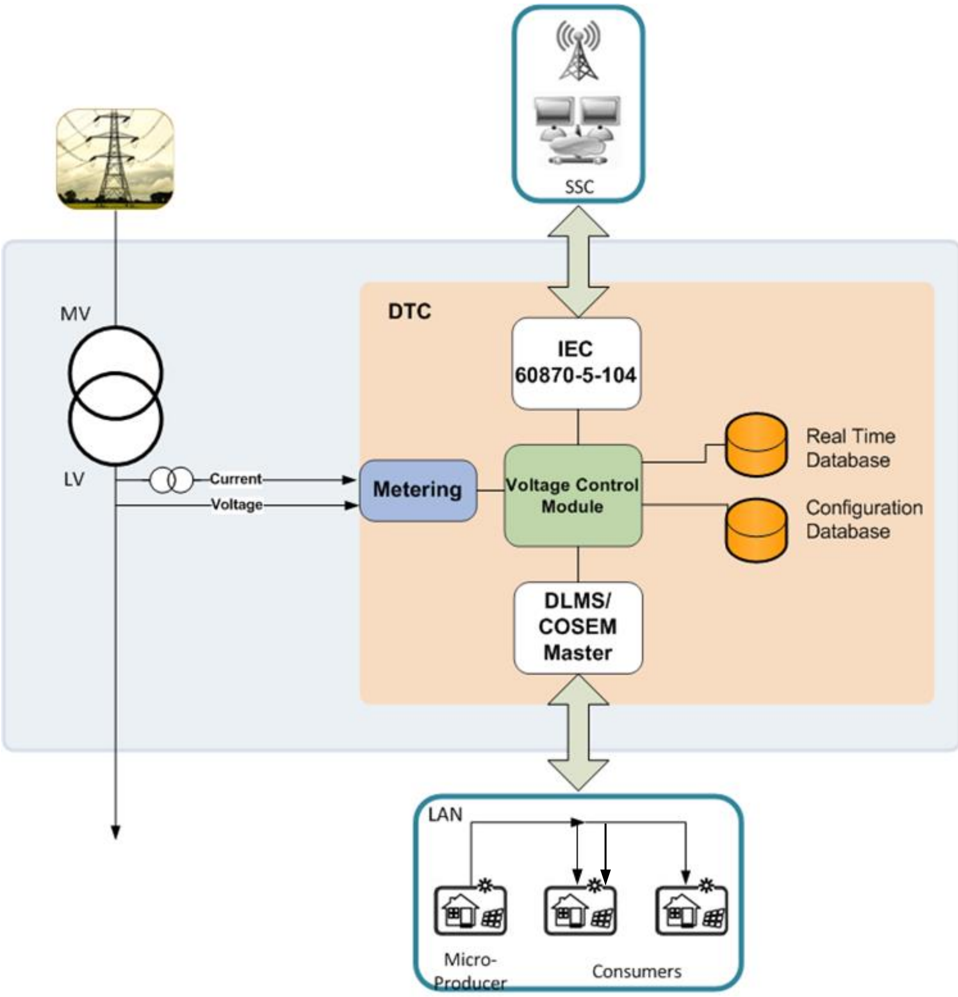

Figure 73 – Voltage Control Module

6 Conclusions

This deliverable presents the approach for advanced coordinated voltage control that was developed according to the SuSTAINABLE concept. The proposed framework aims at exploiting the available DER in order to improve grid operation at both the MV and LV levels.

At the MV level, the approach proposed works a in two time-frames: day-ahead analysis where an optimal dispatch schedule is sought for the next day to coordinate the several DER available in the MV network in order to avoid technical problems in terms of voltage profiles; and intraday analysis where a new optimal dispatch schedule will be redefined closer to operation (in a sliding window of 6 hours-ahead) with improved forecasts and actual unforeseen conditions.

INESC developed a multi-temporal OPF that is able to coordinate the available DER connected at the MV level such as OLTC transformers, DG units, controllable loads or storage devices in order to keep voltage profiles within admissible limits. The problem is formulated as an optimization problem and is solved by a meta-heuristic (DEEPSO) that is able to tackle large dimension systems such as real MV grids with several control variables, both continuous and discrete. In this case, the main objective is to minimize the required control actions, namely DG curtailment and shedding of controllable loads subject to a set of technical and operational constraints including admissible voltage limits and physical limits of devices. The proposed algorithm revealed a good performance using a real test network with multiple control variables even in extreme scenarios with large-scale integration of RES, which proved the effectiveness of the proposed approach for both the day-ahead and intraday analyses. Furthermore, the algorithm will be tested within WP6 through simulation using real data from the main test site of Évora, including real prediction data for PV generation for that location using the forecasting tools developed in Task T3.2.

ICCS also developed a multi-temporal optimization algorithm, which enables coordinated voltage control over the MV network, taking advantage of load and RES power forecasts. At the same time, additional optimization objectives, such as energy losses, RES curtailments, wear of network devices, *etc.* were also incorporated in the algorithm. The developed tool addresses a hard multi-objective decision problem with a large number of variables and constraints. The DSO can set operational targets regarding the voltage profile, energy losses and other quantities for a day-ahead and the algorithm is capable of determining the optimal hourly operating schedule for all controllable devices. As a first demonstration of the algorithm’s potential, it was implemented for a small MV demo network, along with conventional voltage regulation (current practice), in order to comparatively assess their performance. Simulation results presented show that proper formulation of the optimization problem can lead to a substantial improvement in network operation. Further exploration and validation of the algorithm’s potential will be undertaken in Sub-task 5.2.2 within WP5, using the real MV test network from the island of Rhodes.

At the LV level, a two-stage approach is also foreseen where a centralized control scheme based on a set of rules defines set-points for DER located at the LV level exploiting data collected from smart meters and a local control scheme based on droops operating at the inverter level of the DER in order to quickly react to sudden voltage drop/rise phenomena.

First, a strategy for local voltage control was proposed by INESC based on the inclusion of voltage / active power droops embedded in the power electronic interfaces of RES, namely in PV microgenerators. This local control action enables adjusting the output power of the inverter in face of the voltage values at its terminals in order to locally prevent overvoltages. The differentiating features of these inverters regarding the commercial ones is its interaction with the LV control system (including the DTC and the smart meter) and the possibility of providing voltage support through the active-power droop strategy. The preliminary results obtained show the effectiveness of the proposed strategy in maintaining voltage within admissible limits. Also, the droop strategy enables the autonomous coordination between different µG units without depending on the LV network communication infrastructure and allows the LV system to react even when the uncertainty introduced by communications systems is considered. However, the droop strategy proposed also limits the dispatchable capacity of microsources, particularly those connected at the end of the feeders. Coordinating the µG units with other flexible resources such as loads and distributed storage may produce effective results and increase the efficiency of the system. Further simulation studies and experimental tests are required in order to test such coordinated control.

In order to overcome the limitations of local control, INESC also developed an algorithm for a centralized control scheme aimed at managing DER at the LV level taking into account two distinct realities: full knowledge of the grid and limited knowledge of the grid. The proposed approach uses a merit order to define the most suitable resource to be used in order to solve a voltage problem. This functionality will be installed at the secondary substation level, *i.e.* in the DTC. The resulting algorithm was tested in a real LV test network with several DER and showed a good performance by being able to mitigate the voltage violations while avoiding the spillage of energy from RES. Two situations were analysed: first a case of an overvoltage in the LV grid and then a case with a request from an upstream controller in order to change the power flow in the MV/LV distribution transformer. Furthermore, the impact of communications on the performance of the LV control algorithm was evaluated by simulating the behaviour of the communication infrastructure. In this case, a simulation platform for communications developed by COMILLAS was used in coordination with the simulation platform for the electrical network. This allowed concluding that communication solutions based on PLC are adequate to implement the proposed control scheme.

EFACEC provided details on the actual implementation of the voltage control modules developed for MV and LV and their integration in the SSC and DTC, respectively, with emphasis on the corresponding interfaces and communication protocols used. The implementation described proves to be adequate for the correct execution of the coordinated voltage control functionality (both at the MV and LV levels), respecting the required performance as specified by the control algorithms.

The proposed approaches for voltage control in LV grids will be tested in a controlled environment exploiting the laboratorial infrastructure available at INESC in Sub-task 5.2.2 within the framework of WP5, which includes evaluating the effect of local droop voltage control installed in the µG devices (for which the some preliminary results are presented here) as well as the performance of the LV centralized scheme. The final validation of the centralized control scheme for LV will be performed through field tests within WP6 on a feeder of the Évora network to be selected.

The successful completion of Task 3.4 and corresponding deliverable enables partially fulfilling Milestone MS12 “Prototypes and Tools Developed”, as defined in the DoW, according to schedule.

References

1. Grant Agreement, Collaborative Project *Smart distribution System operaTion for mAximizing the INtegration of renewable Generation*, Annex I – "Description of Work", October 2012.
2. N. Jenkins, J.B. Ekanayake and G. Strbac, "Distributed Generation", London, *The Institution of Engineering and Technology*, 2010.
3. C. L. Masters, "Voltage rise - the big issue when connecting embedded generation to long 11 kV overhead lines", *Power Engineering Journal*, vol. 16, no.1, pp. 5-12, February 2002.
4. A. Madureira, "Coordinated and Optimized Voltage Management of Distribution Networks with Multi-Microgrids", PhD Thesis, *Faculty of Engineering*, *University of Porto*, November July 2010. Available at: http://repositorio-aberto.up.pt/bitstream/10216/58358/1/000143265.pdf
5. S. N. Liew and G. Strbac, "Maximising penetration of wind generation in existing distribution networks", *IEE Generation Transmission and Distribution*, vol. 149, no. 3, pp. 256-262, May 2002.
6. P. N. Vovos, *et al.*, "Centralized and distributed voltage control: Impact on distributed generation penetration", *IEEE Transactions on Power Systems*, vol. 22, no. 1, pp. 476-483, February 2007.
7. A. Kulmala, *et al.*, "Active voltage level management of distribution networks with distributed generation using on load tap changing transformers", in *IEEE Powertech 2007*, pp. 455-460, July 2007.
8. A. G. Madureira and J. A. P. Lopes, "Coordinated Voltage Support in Distribution Networks with Distributed Generation and Microgrids", *IET Renewable Power Generation*, vol. 3, no. 4, pp. 439-454, December 2009.
9. R. Shivarudraswamy and D. N. Gaonkar, "Coordinated Voltage Regulation of Distribution Network with Distributed Generators and Multiple Voltage-control Devices", *Electric Power Components and Systems*, vol. 40, no. 9, pp. 1072-1088, June 2012.
10. Project Deliverable D2.3 "Definition of Overall System Architecture", Collaborative Project *Smart distribution System operaTion for mAximizing the INtegration of renewable Generation*, February 2014.
11. V. Miranda and R. Alves, "Differential Evolutionary Particle Swarm Optimization (DEEPSO): A Successful Hybrid", in *2013 BRICS Congress on Computational Intelligence and 11th Brazilian Congress on Computational Intelligence (BRICS-CCI & CBIC)*, pp. 368-374, September 2013.
12. REN (Portuguese TSO), Centre of Information, Daily Statistics – Diagrams. Available at: http://www.centrodeinformacao.ren.pt/EN/InformacaoExploracao/Pages/EstatisticaDiariaDiagrama.aspx
13. T. Stetz, F. Marten and M. Braun, "Improved Low Voltage Grid-Integration of Photovoltaic Systems in Germany", *IEEE Transactions on Sustainable Energy*, vol. 4, no. 2, pp. 534,542, April 2013.
14. C. Gouveia, *et al.*, "Development and Implementation of Portuguese Smart Distribution System", *Electric Power Systems Research*, vol. 120, pp. 150-162, March 2015.
15. CENELEC EN 50160, "Voltage characteristics of electricity supplied by public distribution systems", 1999.
16. J. M. Rodrigues and F. Resende, "Using Photovoltaic Systems to Improve Voltage Control in Low Voltage Networks", in *IEEE PES Conference On Innovative Smart Grid Technologies Europe*, pp- 1-7, October 2012.
17. A. Madureira, *et al.*, "Coordinated Management of Distributed Energy Resources in Electrical Distribution Systems", in *IEEE PES Conference On Innovative Smart Grid Technologies Latin America (ISGT LA)*, pp. 1-8, April 2013.

18. R. Tonkoski, *et al.*, "Coordinated Active Power Curtailment of Grid Connected PV Inverters for Overvoltage Prevention", *IEEE Transactions on Sustainable Energy*, vol. 2, no. 2, pp. 139-147, April 2011.
19. R. M. Ciric, *et al.*, "Power flow in four-wire distribution networks - General approach", *IEEE Transactions on Power Systems*, vol. 18, no. 4, pp. 1283-1290, November 2003.
20. J. Matanza, S. Alexandres, C. Rodríguez-Morcillo, "Advanced metering infrastructure performance using European low-voltage power line communication networks", *IET Communications*, vol. 8, no. 7, pp. 1041-1047, May 2014.

Appendix A. Test Network Data

In this appendix, the full data concerning the test networks used in Sections 3.1 and 4.2 is provided. In particular, transformer and branch data, as well as load and generation data are provided for the MV and LV networks presented previously.

As seen in Section 3.1.4, MV Network 1 is a real Portuguese distribution network from a typical rural area. The scheme of this network is presented in Figure 74.

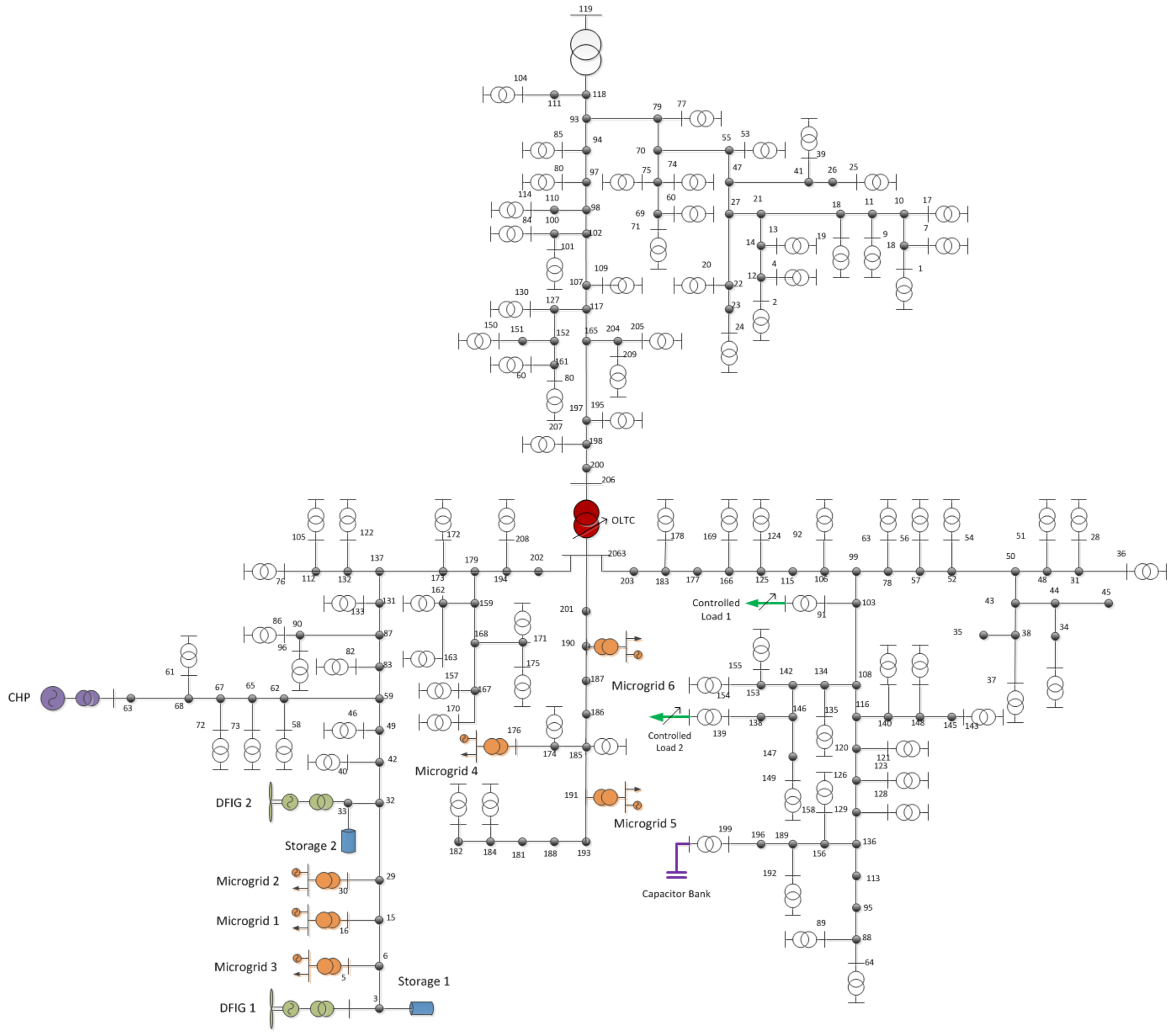

Figure 74 – MV Test Network One-Line Diagram

The line data for this network is presented in Table 9.

Table 9 – Line Data for MV Test Network

Branch Number	From Bus	To Bus	Resistance [Ω]	Reactance [Ω]	Shunt Susceptance [Ω]
1	1	8	0.2047	0.1103	7.0E-05
2	2	12	0.1268	0.0683	4.0E-05
3	3	6	0.1415	0.0763	0.0E+00
4	4	12	0.1814	0.0978	6.0E-05
5	5	6	0.2068	0.0699	0.0E+00
6	6	15	0.2170	0.1984	1.0E-05
7	7	8	0.0055	0.0019	0.0E+00
8	8	10	0.0676	0.0228	1.0E-05
9	9	11	0.0553	0.0298	2.0E-05
10	10	11	0.0396	0.0134	1.0E-05
11	10	17	0.0518	0.0279	2.0E-05
12	11	18	0.1462	0.0494	3.0E-05
13	12	14	0.0268	0.0145	1.0E-05
14	13	14	0.0013	0.0004	0.0E+00
15	14	21	0.0794	0.0428	3.0E-05
16	15	16	0.0068	0.0037	0.0E+00
17	15	29	0.4408	0.4030	2.0E-05
18	18	19	0.0750	0.0405	2.0E-05
19	18	21	0.0780	0.0263	2.0E-05
20	20	22	0.0416	0.0177	1.0E-05
21	21	27	0.1462	0.0494	3.0E-05
22	22	23	0.1090	0.0277	2.0E-05
23	22	27	0.1424	0.0606	4.0E-05
24	23	24	0.0963	0.0245	1.0E-05
25	25	26	0.0001	0.0000	0.0E+00
26	26	41	0.2183	0.1177	7.0E-05
27	27	47	0.3495	0.1487	9.0E-05
28	28	31	0.1930	0.1040	0.0E+00

Branch Number	From Bus	To Bus	Resistance [Ω]	Reactance [Ω]	Shunt Susceptance [Ω]
29	29	30	0.1049	0.0566	0.0E+00
30	29	32	0.0948	0.0866	0.0E+00
31	31	36	0.3823	0.2061	1.0E-05
32	31	48	1.1241	0.6059	2.0E-05
33	32	33	0.0835	0.0450	0.0E+00
34	32	42	0.1740	0.1591	1.0E-05
35	34	44	0.2061	0.1111	0.0E+00
36	35	38	0.0448	0.0242	0.0E+00
37	37	38	0.1453	0.0362	0.0E+00
38	38	43	0.1039	0.0560	0.0E+00
39	39	41	0.0314	0.0080	0.0E+00
40	40	42	0.0039	0.0021	0.0E+00
41	41	47	0.2609	0.0664	4.0E-05
42	42	49	0.4222	0.3860	2.0E-05
43	43	44	0.3860	0.1304	0.0E+00
44	43	50	0.4990	0.2690	1.0E-05
45	44	45	0.3469	0.1172	0.0E+00
46	46	49	0.2259	0.1218	0.0E+00
47	47	55	0.2067	0.0880	5.0E-05
48	48	50	0.5840	0.3148	1.0E-05
49	48	51	0.2461	0.1327	0.0E+00
50	49	59	0.3764	0.3441	1.0E-05
51	50	52	0.0663	0.0357	0.0E+00
52	52	54	0.1428	0.0482	0.0E+00
53	52	57	0.2855	0.1539	1.0E-05
54	53	55	0.0988	0.0533	3.0E-05
55	55	70	0.1623	0.0691	4.0E-05
56	56	57	0.2525	0.0853	0.0E+00
57	57	78	0.4794	0.2584	1.0E-05

Branch Number	From Bus	To Bus	Resistance [Ω]	Reactance [Ω]	Shunt Susceptance [Ω]
58	58	62	0.1962	0.1058	0.0E+00
59	59	62	0.1475	0.0795	0.0E+00
60	59	83	0.2648	0.2421	1.0E-05
61	60	69	0.0997	0.0537	3.0E-05
62	61	68	0.1803	0.0972	0.0E+00
63	62	65	0.1788	0.0964	0.0E+00
64	63	78	1.0034	0.2554	1.0E-05
65	64	88	0.5042	0.2718	1.0E-05
66	65	67	0.1230	0.0663	0.0E+00
67	65	73	0.2771	0.0936	0.0E+00
68	66	68	0.2173	0.1171	0.0E+00
69	67	68	0.0570	0.0307	0.0E+00
70	67	72	0.0789	0.0426	0.0E+00
71	69	71	0.0067	0.0036	0.0E+00
72	69	75	0.0688	0.0371	2.0E-05
73	70	75	0.0379	0.0204	1.0E-05
74	70	79	0.0618	0.0263	2.0E-05
75	74	75	0.0176	0.0095	1.0E-05
76	75	81	0.0324	0.0175	1.0E-05
77	76	112	1.6337	0.4159	1.0E-05
78	77	79	0.0037	0.0020	0.0E+00
79	78	99	0.4483	0.2416	1.0E-05
80	79	93	0.1407	0.0599	4.0E-05
81	80	97	0.0866	0.0467	3.0E-05
82	82	83	0.5953	0.3209	1.0E-05
83	83	87	0.0980	0.0896	0.0E+00
84	84	100	0.0817	0.0440	3.0E-05
85	85	94	0.0577	0.0311	2.0E-05
86	86	90	0.0528	0.0285	0.0E+00

Branch Number	From Bus	To Bus	Resistance [Ω]	Reactance [Ω]	Shunt Susceptance [Ω]
87	87	90	0.1284	0.0692	0.0E+00
88	87	131	0.6507	0.5949	2.0E-05
89	88	89	0.0041	0.0022	0.0E+00
90	88	95	0.1258	0.0678	0.0E+00
91	90	96	0.2214	0.1194	0.0E+00
92	91	103	0.4638	0.1181	0.0E+00
93	92	106	0.5553	0.1876	1.0E-05
94	93	94	0.0681	0.0501	3.0E-05
95	93	118	0.2905	0.2138	1.3E-04
96	94	97	0.0637	0.0469	3.0E-05
97	95	113	0.3209	0.1730	1.0E-05
98	97	98	0.0035	0.0026	0.0E+00
99	98	102	0.1530	0.1126	7.0E-05
100	98	110	0.0891	0.0379	2.0E-05
101	99	103	0.4853	0.2616	1.0E-05
102	99	106	0.2313	0.1247	0.0E+00
103	100	101	0.0014	0.0005	0.0E+00
104	100	102	0.0083	0.0045	0.0E+00
105	102	107	0.0486	0.0357	2.0E-05
106	103	108	0.3099	0.1671	1.0E-05
107	104	111	0.0171	0.0062	2.3E-04
108	105	112	0.2902	0.0739	0.0E+00
109	106	115	0.3037	0.1637	1.0E-05
110	107	109	0.0013	0.0004	0.0E+00
111	107	117	0.0880	0.0648	4.0E-05
112	108	116	0.8409	0.4533	2.0E-05
113	108	134	1.2249	0.3118	1.0E-05
114	110	114	0.0001	0.0001	0.0E+00
115	111	118	0.0754	0.0321	2.0E-05

Branch Number	From Bus	To Bus	Resistance [Ω]	Reactance [Ω]	Shunt Susceptance [Ω]
116	112	132	1.3514	0.3440	1.0E-05
117	113	136	1.0006	0.5394	2.0E-05
118	115	125	0.4096	0.2208	1.0E-05
119	116	120	0.5514	0.2972	1.0E-05
120	116	140	0.8183	0.2764	1.0E-05
121	117	127	0.0978	0.0330	2.0E-05
122	117	165	0.2989	0.2200	1.4E-04
123	118	119	0.0487	0.0359	2.0E-05
124	120	121	0.0064	0.0016	0.0E+00
125	120	126	0.2964	0.1598	1.0E-05
126	122	132	0.2456	0.1324	0.0E+00
127	123	126	0.0543	0.0292	0.0E+00
128	124	125	0.0158	0.0053	0.0E+00
129	125	166	0.7455	0.4019	1.0E-05
130	126	129	0.3266	0.0831	0.0E+00
131	127	130	0.0226	0.0076	0.0E+00
132	127	152	0.1983	0.0670	4.0E-05
133	128	129	0.1443	0.0488	0.0E+00
134	129	136	0.1918	0.0488	0.0E+00
135	131	133	0.0088	0.0048	0.0E+00
136	131	137	0.1223	0.1119	0.0E+00
137	132	137	0.3695	0.0941	0.0E+00
138	134	135	0.0625	0.0211	0.0E+00
139	134	142	0.3531	0.0899	0.0E+00
140	136	156	0.9744	0.2480	1.0E-05
141	137	173	0.6280	0.5741	2.0E-05
142	138	139	0.0088	0.0017	1.0E-05
143	138	146	0.2060	0.1110	0.0E+00
144	140	148	0.2126	0.0718	0.0E+00

Branch Number	From Bus	To Bus	Resistance [Ω]	Reactance [Ω]	Shunt Susceptance [Ω]
145	140	154	0.4309	0.1456	1.0E-05
146	141	148	0.1800	0.0608	0.0E+00
147	142	146	0.1286	0.0328	0.0E+00
148	142	153	0.3278	0.1767	1.0E-05
149	143	145	0.0333	0.0112	0.0E+00
150	144	162	0.7668	0.1952	1.0E-05
151	145	148	0.0318	0.0108	0.0E+00
152	146	147	0.0486	0.0124	0.0E+00
153	147	149	0.0065	0.0037	0.0E+00
154	150	151	0.0040	0.0009	3.0E-05
155	151	152	0.0303	0.0102	1.0E-05
156	152	161	0.0703	0.0238	1.0E-05
157	153	155	0.1286	0.0434	0.0E+00
158	153	164	0.2271	0.1224	0.0E+00
159	156	158	0.4256	0.2294	1.0E-05
160	156	189	1.1513	0.2931	1.0E-05
161	157	167	0.2284	0.1231	0.0E+00
162	159	162	0.0523	0.0282	0.0E+00
163	159	168	0.2601	0.0662	0.0E+00
164	159	179	0.3629	0.1956	1.0E-05
165	160	161	0.0013	0.0004	0.0E+00
166	161	180	0.1066	0.0360	2.0E-05
167	162	163	0.0341	0.0184	0.0E+00
168	165	197	0.1210	0.0891	6.0E-05
169	165	204	0.1680	0.0906	5.0E-05
170	166	169	0.0200	0.0067	0.0E+00
171	166	177	0.1472	0.0793	0.0E+00
172	167	168	0.2711	0.0916	0.0E+00
173	167	170	0.0296	0.0100	0.0E+00

Branch Number	From Bus	To Bus	Resistance [Ω]	Reactance [Ω]	Shunt Susceptance [Ω]
174	168	171	0.2323	0.0591	0.0E+00
175	171	175	0.0585	0.0103	4.0E-05
176	172	173	0.0714	0.0241	0.0E+00
177	173	179	0.0665	0.0608	0.0E+00
178	174	176	0.0706	0.0221	9.0E-05
179	174	185	0.1267	0.0262	8.0E-05
180	175	176	0.0130	0.0041	2.0E-05
181	176	182	0.0730	0.0128	5.0E-05
182	177	183	0.0634	0.0342	0.0E+00
183	178	183	0.0336	0.0114	0.0E+00
184	179	194	0.1142	0.1044	0.0E+00
185	181	184	0.0222	0.0070	3.0E-05
186	181	188	0.0931	0.0083	2.0E-05
187	182	184	0.0341	0.0107	4.0E-05
188	183	203	0.6081	0.3278	1.0E-05
189	185	186	0.0193	0.0043	2.0E-05
190	185	191	0.0631	0.0123	4.0E-05
191	186	187	0.0032	0.0007	0.0E+00
192	187	190	0.0377	0.0084	4.0E-05
193	188	193	0.1864	0.0242	8.0E-05
194	189	192	0.0715	0.0182	0.0E+00
195	189	196	0.2876	0.0972	0.0E+00
196	190	201	0.4383	0.2363	1.0E-05
197	191	193	0.0111	0.0025	1.0E-05
198	194	202	0.2091	0.1911	1.0E-05
199	194	208	0.9957	0.2481	1.0E-05
200	195	197	0.0008	0.0004	0.0E+00
201	196	199	0.1212	0.0235	7.0E-05
202	197	198	0.0056	0.0041	0.0E+00

Branch Number	From Bus	To Bus	Resistance [Ω]	Reactance [Ω]	Shunt Susceptance [Ω]
203	198	200	0.0473	0.0348	2.0E-05
204	198	207	0.0989	0.0533	3.0E-05
205	200	2063	0.0386	0.0284	2.0E-05
206	201	206	0.0102	0.0032	1.0E-05
207	202	206	0.0098	0.0031	1.0E-05
208	203	206	0.0072	0.0023	1.0E-05
209	204	205	0.0033	0.0018	0.0E+00
210	204	209	0.0498	0.0268	2.0E-05

The transformer data for this network is presented in Table 10.

Table 10 – Transformer Data for MV Test Network

Branch Number	From Bus	To Bus	Rated Power [MVA]	Primary Voltage [kV]	Secondary Voltage [kV]	Reactance [%]
1	206	2063	5	30	15	5.79

The load data for this network is presented in Table 11.

Table 11 – Load Data for MV Test Network

Bus Number	Load Installed Capacity [kVA]
1	100
2	100
3	160
4	100
5	160
7	100
9	100
13	100
16	100
17	50
19	100

Bus Number	Load Installed Capacity [kVA]
20	1200
24	100
25	630
28	50
30	100
33	100
34	100
36	100
37	15
39	25
40	50
45	25
46	100
51	160
53	160
54	250
56	250
58	100
60	100
61	160
63	160
64	50
66	200
71	160
72	50
73	100
74	160
76	100
77	50

Bus Number	Load Installed Capacity [kVA]
80	100
81	250
82	100
84	50
85	100
86	25
89	100
91	100
92	250
96	75
101	50
104	0
105	100
109	100
114	1335
121	100
122	50
123	160
124	100
128	100
130	100
133	100
135	50
139	1000
141	50
143	500
144	100
149	500
150	630

Bus Number	Load Installed Capacity [kVA]
154	100
155	0
157	100
158	100
160	100
163	100
164	100
169	50
170	200
171	100
172	100
174	400
175	160
176	630
178	50
180	100
182	125
184	400
185	250
190	630
191	630
192	100
195	25
199	160
205	250
207	100
208	30
209	100

The generation data for this network is presented in Table 12.

Table 12 – Generation Data for MV Test Network

Bus Number	Type	Installed Capacity [MVA]	
		Scenario 1	Scenario 2
5	µG	0.90	1.30
16	µG	0.90	1.30
30	µG	0.90	1.30
176	µG	0.80	1.20
191	µG	0.80	1.20
190	µG	0.70	1.10
66	CHP	1.50	1.00
3	Wind	1.00	0.80
33	Wind	1.00	0.80

As seen in Section 4.2.3, the LV network used is a real Portuguese distribution network from a rural area fed by a 100 kVA distribution transformer that comprises three feeders. The scheme of this network is presented in Figure 75.

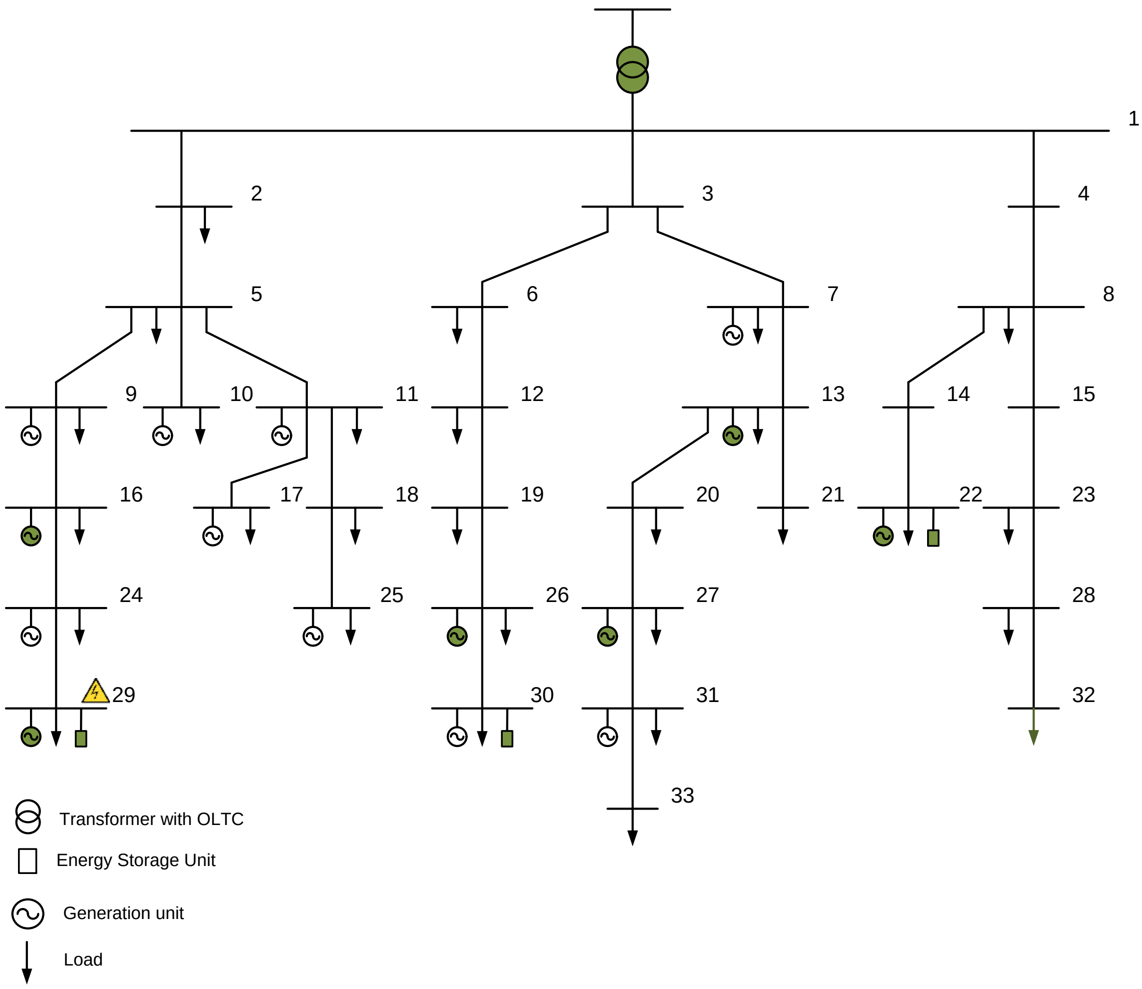

Figure 75 – LV Network One-Line Diagram

The line data for this network is presented in Table 13.

Table 13 – Line Data for LV Test Network

Branch Number	From Bus	To Bus	Phase Resistance [Ω]	Phase Reactance [Ω]	Neutral Resistance [Ω]
1	1	2	0.0567	5.7E-06	5.7E-06
2	1	3	0.0190	1.9E-06	1.9E-06
3	1	4	0.0367	3.7E-06	3.7E-06
4	2	5	0.0310	3.1E-06	3.1E-06
5	3	6	0.0769	1.2E-05	1.2E-05
6	3	7	0.0700	7.0E-06	7.0E-06
7	4	8	0.0667	6.7E-06	6.7E-06

Branch Number	From Bus	To Bus	Phase Resistance [Ω]	Phase Reactance [Ω]	Neutral Resistance [Ω]
8	5	9	0.0467	4.7E-06	4.7E-06
9	5	10	0.1040	1.6E-05	1.6E-05
10	5	11	0.2187	2.2E-05	2.2E-05
11	6	12	0.2917	2.9E-05	2.9E-05
12	7	13	0.0233	2.3E-06	2.3E-06
13	8	14	0.1989	3.0E-05	3.0E-05
14	8	15	0.1242	1.9E-05	1.9E-05
15	9	16	0.0233	2.3E-06	2.3E-06
16	11	17	0.2496	3.7E-05	3.7E-05
17	11	18	0.0955	1.4E-05	1.4E-05
18	12	19	0.0381	3.8E-06	3.8E-06
19	13	20	0.1528	2.3E-05	2.3E-05
20	13	21	0.4841	7.3E-05	7.3E-05
21	14	22	1.2121	1.8E-04	1.8E-04
22	15	23	0.2674	4.0E-05	4.0E-05
23	16	24	0.0467	4.7E-06	4.7E-06
24	18	25	0.1614	2.4E-05	2.4E-05
25	19	26	0.0238	2.4E-06	2.4E-06
26	20	27	0.1875	1.9E-05	1.9E-05
27	23	28	0.9345	9.3E-05	9.3E-05
28	24	29	0.1844	2.8E-05	2.8E-05
29	26	30	0.0533	5.3E-06	5.3E-06
30	27	31	0.2142	3.2E-05	3.2E-05
31	28	32	0.3227	4.8E-05	4.8E-05
32	31	33	0.1614	2.4E-05	2.4E-05

The load data for this network is presented in Table 14. In order to compute active and reactive powers, a value of $\tan \varphi = 0.4$ was used.

Table 14 – Load Data for LV Test Network

Bus Number	Load Installed Capacity [kVA]		
	Phase A	Phase B	Phase C
2	3.45	3.45	0
5	0	0	3.45
6	1.15	0	0
7	10.35	0	0
8	3.45	3.45	3.45
9	6.9	3.45	3.45
10	3.45	13.8	0
11	3.45	0	6.9
12	3.45	3.45	0
13	6.9	3.45	3.45
16	0	6.9	0
17	13.8	0	0
18	0	3.45	3.45
19	3.45	3.45	0
20	0	3.45	3.45
22	10.35	3.45	3.45
23	0	0	3.45
24	20.7	17.25	20.7
25	0	3.45	13.8
26	0	13.8	0
27	6.9	3.45	3.45
29	3.45	3.45	10.35
30	0	0	13.8
31	0	6.9	0
32	0	3.45	3.45
33	0	0	3.45

The generation data for this network is presented in Table 15.

Table 15 – Generation Data for LV Test Network

Bus Number	Generation Installed Capacity [kVA]		
	Phase A	Phase B	Phase C
7	5.175	0	0
9	3.45	0	0
10	0	5.75	0
11	0	0	3.45
13	3.45	0	0
16	0	3.45	0
17	5.75	0	0
22	5.175	0	0
24	5.75	5.75	5.75
25	0	0	5.75
26	0	5.75	0
27	3.45	0	0
29	0	0	5.175
30	0	0	5.75
31	0	3.45	0

Appendix B. Database Specification and Data Communication Requirements

In this appendix a specification of the database and data communication requirements for the software pre-prototypes developed for voltage control are established and will serve to feed the operational phase.

Multi-Temporal Optimal Power Flow for MV Grids

Required data as input	• Network topology • Feeder branch data (*e.g.* impedance, length, thermal limits) and node data (loads, DER connected *etc.*) • HV/MV transformer data (*e.g.* nominal power, short-circuit voltage, *etc.*) • OLTC transformer data (*e.g.* tap step, number of available tap positions, *etc.*) • DER data: connection node, nominal power, type of DG, reactive power capability characteristics, power curtailment possibilities, *etc.* • Storage systems: connection node, capacity limits (min/max), charging and discharging efficiency, active and reactive power constraints, *etc.* • CBs: connection node, bank steps, capacity per step, *etc.* • SVRs: node and branch, tap step, number of available taps, regulation mode, *etc.*
Data obtained by other functionalities	• Forecasted active and reactive power demand per MV network node. • Forecasted active power generation capability for each DG station. • Current network topology and parameters (including status of switches, OLTC transformers tap position, status of CBs, SOC of storage systems, *etc.*) from the state estimator

Communication requirements	Dispatch set-points to controllable devices and DER: • OLTC transformers • Step Voltage Regulators • CBs • DG • Controllable loads • Storage systems
	Connection with the following functionalities (receiving inputs from): • Load forecasting • RES forecasting • State estimation • Network SCADA (topology)
	Communication time intervals: • Controllable devices: set-points using an hourly time resolution • Required functionalities: data available before the following day (day-ahead forecast) with hourly steps

Voltage Control Scheme for LV Grids

Required data as input	• Grid topology data (optional) • Technical data of grid assets: technical parameters of the equipment installed in the LV-network; complete geographical coordinates information of all grid's equipment per phase • Installed capacity in the grid: loads, storage, generation, *etc.* • Grid current status: voltage magnitude and active power injections (from the State Estimation Algorithm – LV Network) • Estimated costs of control actions for each grid asset (optional) • Technical constraints of the DSO (voltage limits, line ratings, etc.) • Contract data: available flexibility; Relevant details of contract between network operator and customer for network operation for each contract type (optional)
Data obtained by other functionalities	• Events associated to voltage profiles (measured or estimated)

Communication requirements	Dispatch set-points to controllable devices and DER: • MV/LV transformers with OLTC • Storage devices • Microgeneration with non-firm contracts (for instance, subject to limitation in case of technical problems in the grid) • Flexible loads
	Connection with the following functionalities (receiving inputs from): • Multi-Temporal Optimal Power Flow for MV Grids
	Communication time intervals: • Controllable devices: set-points on a periodic basis (*e.g.* each 30 minutes) • Required functionalities: phase indication and geographical coordinated for each DER